Final Report | *Covering the Period 30 September to 31 December 1962 in Detail, with a Summary from 1 January 1961 to 31 December 1962*

MICROWAVE FILTERS AND COUPLING STRUCTURES

Prepared for:

U.S. ARMY ELECTRONICS RESEARCH AND DEVELOPMENT LABORATORY
FORT MONMOUTH, NEW JERSEY

CONTRACT DA 36-039 SC 87398
DA PROJECT 3A99-15-002-02-06

By: *G. L. Matthaei* *B. M. Schiffman* *E. G. Cristal*
L. A. Robinson

STANFORD RESEARCH INSTITUTE

MENLO PARK, CALIFORNIA

STANFORD RESEARCH INSTITUTE
MENLO PARK, CALIFORNIA

February 1963

Final Report | *Covering the Period 30 September to 31 December 1962 in Detail, with a Summary from 1 January 1961 to 31 December 1962*

MICROWAVE FILTERS AND COUPLING STRUCTURES

Prepared for:

U.S. ARMY ELECTRONICS RESEARCH AND DEVELOPMENT LABORATORY
FORT MONMOUTH, NEW JERSEY

CONTRACT DA 36-039 SC 87398
FILE NO. 40553-PM-61-93-93
DA PROJECT 3A99-15-002-02-06
SCL-2101N (14 JULY 1961)

By: *G. L. Matthaei* *B. M. Schiffman* *E. G. Cristal*
L. A. Robinson

SRI Project No. 3527

Objective: To advance the state of the art in the field of microwave filters and coupling structures through applied research and development.

Approved:

G. L. Matthaei

G. L. MATTHAEI, MANAGER ELECTROMAGNETIC TECHNIQUES LABORATORY

D. R. SCHEUCH, DIRECTOR ELECTRONICS AND RADIO SCIENCES DIVISION

Copy No. 12

CONTENTS

CONTENTS

ILLUSTRATIONS

ILLUSTRATIONS

ILLUSTRATIONS

TABLES

PURPOSE OF THE CONTRACT

This contract continues the work of Contracts DA 36-039 SC-64625, DA 36-039 SC-63232, and DA 36-039 SC-74862 to develop new design techniques for waveguide, strip-line, and coaxial-line microwave components, and to prepare a book on techniques for microwave filter design.

ABSTRACT

Section II of this report briefly summarizes the work of the two-year course of this contract. In Sec. III a two-resonator waveguide magnetically tunable filter and a two-resonator strip-line magnetically tunable filter are described. These filters utilize ferrimagnetic resonance in single-crystal yttrium-iron-garnet (YIG) to achieve tuning which is controlled by a biasing dc magnetic field. The waveguide filter is for *X*-band and uses a novel coupling structure which increases the coupling between the external circuit and the YIG resonators. This makes it possible to use unusually small resonators (0.025-inch diameter), which helps to reduce spurious response activity in the stop bands. The strip-line filter is for *S*-band and is an advanced version of a design discussed in Quarterly Progress Report 7. In Sec. IV of this report our previous work on the exact design of band-stop filters is extended to cover additional strip-line (or coaxial) configurations which have practical advantages. These include a configuration where the resonator lines are parallel to, but separate from, the main transmission line, and a configuration where the resonators are parallel to the main transmission line and attached to it. The first form is advantageous for narrow-stop-band filters, while the latter form is advantageous for wide-stop-band filters. Design equations and the computed and experimental results of trial designs are given. In Sec. V the experimental results of a trial, three-channel multiplexer using comb-line filters are discussed. The results are found to be in good agreement with the theory previously discussed in Quarterly Progress Report 6. This particular multiplexer has contiguous pass-bands, and a mathematical analysis is presented for the corresponding case where guard-bands are desired between channels. In Sec. VI design equations are presented for wideband, interdigital band-pass filters having capacitive loading at one end of each resonator line, and a short circuit at the other. The use of capacitive loading is seen to permit even more compact filter structures, and causes the first spurious response to be unusually far removed from the main pass-band.

CONFERENCES AND TECHNICAL PAPERS DURING LAST QUARTER

Conferences

None

Technical Papers

Leo Young, "The Practical Realization of Series-Capacitance Couplings for Microwave Filters," *The Microwave Journal*, Vol. 5, pp. 79-81 (December 1962).

Leo Young, "Stepped-Impedance Transformers and Filter Prototypes," *IRE Trans. PGMTT*-**10**, pp. 339-359 (September 1962).

G. L. Matthaei, "Interdigital Band-Pass Filters," *IRE Trans. PGMTT*-**10**, pp. 479-491 (November 1962).

Leo Young, G. L. Matthaei, and E. M. T. Jones, "Microwave Band-Stop Filters with Narrow Stop Bands," *IRE Trans. PGMTT*-**10**, pp. 416-427 (November 1962).

Y. Sato and P. S. Carter, "A Device for Rapidly Aligning and Mounting Ferromagnetic Single Crystals Along Any Desired Axis," *IRE Trans. PGMTT*-**10**, pp. 611-612 (November 1962).

I INTRODUCTION

Section II gives a brief summary of the previous work done on this contract, while the remainder of this report describes results obtained during the last quarter.

Various means for electronic tuning have been studied on this project, including tuning by use of electronically tunable up-converters, and by use of filters having ferrimagnetic resonators which are tuned by varying a biasing magnetic field. Our latest results on magnetically tunable filters will be found in Sec. III of this report. Our previous work on band-stop filters is extended in Sec. IV, where some new configurations for band-stop filters are described, and the results of some trial designs are presented. In Quarterly Progress Report 7 on this contract an analysis of a method for multiplexer design was made, and the performance of some trial designs was computed. In Sec. V. of this report the results obtained from a three-channel multiplexer which was constructed, are given. This multiplexer has contiguous pass-bands. Analysis of the case where there are guard bands between the pass-bands is also presented. In Sec. VI of this report our previous work on interdigital filters is extended to cover the case of interdigital filters with capacitively loaded resonators. The addition of capacitive loading makes possible a much broader upper stop-band, and yields an even more compact structure.

II A BRIEF REVIEW OF PRIOR WORK ON THIS CONTRACT

A. GENERAL

In this section the contents of the previous reports on this contract, and of a book prepared on this contract, are described. Also, since numerous technical papers have resulted from this contract, other references are given in which some of the results of the contract are discussed.

B. BOOK ON MICROWAVE FILTERS, IMPEDANCE-MATCHING NETWORKS, AND COUPLING STRUCTURES

One of the major activities on this contract has been to prepare an extensive book dealing with practical design techniques for microwave filters, impedance-matching networks, and coupling structures.[1*] This book is largely an outgrowth of our research activities for the Signal Corps under Contracts DA 36-039 SC-63232, DA 36-039 SC-64625, DA 36-039 SC-74862, and DA 36-039 SC-87398. The preparation of this book has been mainly supported by this contract (DA 36-039 SC-87398), though its preparation has been partly supported by Stanford Research Institute and by off-work time contributed by the authors. The book will be issued for the Signal Corps at about the same time as this report. An abstract is given below.

Abstract

The book prepared on this contract presents design techniques for a wide variety of low-pass, band-pass, and band-stop microwave filters; for multiplexers; and for certain kinds of directional couplers. The material is organized to be used by the designer who wants to work out a specific design quickly, with a minimum of reading, as well as by the engineer who wants a deeper understanding of the design techniques used to be able to apply them to new and unusual situations.

Most of the design procedures described make use of either a lumped-element low-pass prototype filter or a step-transformer prototype as a basis for design. Using these prototypes, microwave filters can be obtained which derive response

* References are listed at the end of each major section of the report.

characteristics (such as a Tchebyscheff attenuation ripples in the pass-band) from their prototype. Tabulated prototype filter designs are given as well as data relevant to the use of prototype filters as a basis for the design of impedance-matching networks and time-delay networks. Data for step-transformer prototypes are also given.

The design of microwave filter structures to serve as impedance-matching networks is discussed, and examples are presented. The techniques described should find application in the design of impedance-matching networks for use in microwave devices such as tubes, parametric devices, antennas, etc., to achieve efficient broad-band operation. The design of microwave filters to achieve various time-delay (or slow-wave) properties is also discussed.

Various equations, graphs, and tables are collected together relevant to the design of coaxial lines, strip-lines, waveguides, parallel-coupled lines between common ground planes, arrays of lines between ground planes, coupling and junction discontinuities, and resonators. Techniques for measuring the Q's of resonators and the coupling coefficients between resonators are also discussed, along with procedures for tuning filters. Equations and principles useful in the analysis of filters are collected together for easy reference and to aid the reader whose background for the subject matter of this book may contain some gaps.

Directional filters with special properties valuable for certain applications are treated in detail in a separate chapter, as are high-power filters. Tunable filters of the kind that might be desired for preselector applications are also treated. Both mechanically tunable filters and filters using ferrimagnetic resonators, which can be tuned by varying a biasing magnetic field, are discussed.

C. DESIGN DATA FOR RECTANGULAR CONDUCTORS BETWEEN GROUND PLANES

In many structures such as directional couplers and filters which use parallel-coupled line elements as resonators, it is often desirable to fabricate the line elements as rectangular bars between ground planes. A mathematical solution for the even- and odd-mode fringing capacitance associated with rectangular bars between ground planes was obtained on this project. Data was computed from these equations by use of a digital computer, and extensive curves of data were plotted to give easy-to-use design charts. These charts make the design of rectangular bars between ground planes, arrays of bars between ground planes, or rectangular bars within rectangular housings, quite simple.

The results of this research were described in Sec. II of Quarterly Progress Report 2 on this contract.[2] They have also been published in the *IRE Transactions on Microwave Theory and Techniques*;[3] and the design charts also appear in Sec. 5.05 of the book prepared on this contract.[1]

D. ANALYSIS OF THE PHASE AND FILTER PROPERTIES OF ARRAYS OF CONDUCTORS BETWEEN GROUND PLANES

A number of structures were analyzed which consisted of arrays of parallel conductors between ground planes or above a single ground plane. These included: interdigital line, meander line, a form of helix, "hairpin line," and reactively loaded comb line. Equations were derived for determining the phase function ψ per section of line in terms of voltage coupling factors K_{1n} which are obtained from the static capacitances per unit length of the conductors. Equations for the midband image impedance of finite arrays of conductors were obtained for three of the five cases considered. Data for computing coupling factors were presented for the case of arrays using small wires between ground planes, and for arrays having conductor dimensions such that fringing capacitance beyond nearest neighbors can be neglected. The phase characteristics for given coupling factors were presented for examples of the various types of structures considered. The results of the examples indicated that interdigital lines and comb lines look especially attractive as potential filter structures, or as slow-wave structures. This is because of the relatively efficient coupling between the resonant elements of structures of these types, for given spacings between the elements.

A trial interdigital structure was fabricated to check out the predicted cutoff frequency and midband image impedance. Good agreement between theory and experiment was obtained. By modifying the end elements on the structure it became a well matched filter having about an octave pass-band width.

This work is reported in Quarterly Progress Report 1[4] on this contract and also in the *Proceedings of the IRE*.[5]

E. INTERDIGITAL BAND-PASS FILTERS

The study of arrays of conductors between ground planes, discussed above, showed that interdigital-line structures are of considerable

potential interest for use as band-pass filter structures. The study described in Sec. II-D above was largely a performance *analysis* study, and further research was conducted to find a practical *synthesis* procedure for interdigital filters. By use of certain approximations, easy-to-use and reasonably accurate synthesis procedures were obtained.

In Sec. III of Quarterly Progress Report 4 on this contract,[6] the design of band-pass filters using interdigital arrays of resonator line elements between parallel ground planes is discussed. Two approximate design procedures are described, both of which permit design directly from lumped-element, low-pass, prototype filters. Both design procedures will work for either narrow- or wide-band filters, but one procedure gives more practical dimensions for filters having wide bandwidths (such as an octave), while the other gives more practical dimensions for filters having narrow or moderate bandwidths. The dimensions and measured performance curves are presented for a 10-percent-bandwidth design and an octave-bandwidth design.

Interdigital band-pass filters were demonstrated to have a number of very attractive features, including the following:

(1) They are very compact.

(2) The tolerances required in their manufacture are unusually relaxed as a result of the relatively large spacings between resonator elements.

(3) The second pass-band is centered at three times the center frequency of the first pass-band, and there is no possibility of spurious responses in between. (Note that for filters with half-wavelength, parallel-coupled resonators, and for many stub filters, even the slightest mistuning will result in narrow spurious pass-bands at twice the frequency of the first pass-band center.)

(4) The rates of cutoff and the strength of the stop-bands are enhanced by multiple-order poles of attenuation at dc and at even multiples of the center frequency of the first pass-band.

(5) Interdigital filters can be fabricated in structural forms which are self-supporting so that dielectric material need not be used. Thus, dielectric loss can be eliminated.

Besides being discussed in Quarterly Progress Report 4,[6] interdigital filters were discussed in a paper presented at the 1962 PGMTT National

Symposium at Boulder, Colorado,[7] and in a written version published in the *IRE Transactions on Microwave Theory and Techniques*.[8] Interdigital filters are also discussed in Secs. 10.06, 10.07 and 10.09 of the book prepared on this contract.[1] The design of interdigital filters with capacitive loading is discussed in Sec. VI of this report.

F. COMB-LINE FILTERS OF NARROW OR MODERATE BANDWIDTH

The study discussed in Sec. II-D above also indicated that comb-line structures should be of special interest as potential band-pass filter structures. That study showed that comb-line filters *must* use capacitive* loading on the resonators if a pass-band is to be achieved, and if sufficiently heavy capacitive loading is used, relatively large coupling can be obtained between resonator lines for given spacing between the resonator line elements. A study of the design of comb-line filter structures was made, and a design procedure was obtained which is suitable for the design of comb-line filters of narrow to moderate bandwidth.

The design of comb-line band-pass filters is discussed in Sec. II of Quarterly Progress Report 5.[9] The resonators in such a filter consist of TEM-mode lines between parallel ground planes; each resonator line is short-circuited to ground at one end, and capacitively loaded to ground at the other. Coupling between resonators is achieved by way of the fringing fields between the lines. To couple into the structure, nonresonant short-circuited lines are used at each end. The design equations given make use of a lumped-element low-pass prototype and are suitable for use in designs of narrow to moderate bandwidths (*i.e.*, probably up to around 15-percent bandwidth, although this point has not yet been fully checked). A trial filter design for 10-percent bandwidth was constructed and tested with good results.

Comb-line filters were demonstrated to have the following attractive features:

(1) They are compact (even more so than interdigital filters).

(2) They have strong stop-bands and the stop-band above the primary pass-band can be made to be very broad (in our experimental model the first spurious pass-band was at 4.2 times the frequency of the primary pass-band).

(3) If desired, they can be designed to have an unusually steep rate of cutoff on the high side of the pass-band.

* Or inductive loading.

(4) Adequate coupling can be maintained between resonator elements with sizeable spacings between resonator lines. (This feature means that the proper couplings can be maintained in manufactured filters without unreasonable tolerance requirements.)

(5) Filters of this type can usually be fabricated without the use of dielectric support materials so that, if desired, dielectric losses can be eliminated.

Besides the discussion of comb-line filter design in Quarterly Progress Report 5 on this contract,[9] their use in multiplexers is analyzed in Sec. III of Quarterly Progress Report 6,[10] and the results of a trial, three-channel multiplexer design using comb-line filters are discussed in Sec. V of this report. Comb-line filters are also discussed in Secs. 8.13, 8.14, and 16.04 of the book prepared on this contract.[1]

G. STEPPED-IMPEDANCE TRANSFORMERS AND FILTER PROTOTYPES

In Sec. IV of Quarterly Progress Report 4[6] the theory of the quarter-wave transformer is reviewed and extended, and the major results are presented. The distinctions between ideal and non-ideal junctions, homogeneous and inhomogeneous transformers, synchronous and nonsynchronous tuning, are brought out explicitly. Design formulas are presented, numerical tables are given, methods of numerical calculation are explained, and their use is illustrated by many examples. Where exact solutions are not available, two approximate design procedures are given: one is applicable where R is relatively small, and one where R is relatively large (where R is the ratio of the terminations). To help in obtaining accurate numerical solutions, the connection between antenna arrays and "small-R" transformers is utilized, as is the connection between lumped-constant, low-pass filters and "large-R" transformers.

The concept of half-wave filters (derived from quarter-wave transformers) is explained, and is later applied in Quarterly Progress Report 5[9] to the design of reactance-coupled filters.

Design formulas for inhomogeneous transformers are presented. A nonsynchronous transformer which is sometimes useful, is also described.

The last section shows how to calculate the dissipation loss and the group delay at center frequency in terms of the transmission-line filter parameters. A formula connecting dissipation loss and group delay in the pass-band is given.

In addition to the discussion of the above topics in Quarterly Progress Report 4,[6] a similar discussion will also be found in Chapter 6 of Ref. 1. Some of this material has also been published in the *IRE Trans. PGMTT*,[11] the *Journal of the Optical Society of America*,[12] and *The Microwave Journal*.[13]

H. WIDE-BAND (AND NARROW-BAND) FILTERS CONSISTING OF CASCADED TRANSMISSION LINES WITH LUMPED-REACTANCE COUPLINGS

Design procedures for reactance-coupling filters with half-wave and quarter-wave transmission-line resonators are given in Sec. III of Quarterly Progress Report 5.[9] The resonator transmission lines are coupled either by series capacitances or shunt inductances. Over narrow frequency bands, such filters show characteristics similar to those of lumped-constant filters, and their design is straightforward. The design of direct-coupled resonator filters over wide (as well as narrow) frequency bands is presented using quarter-wave transformers as prototype circuits.

Each filter has the same number of discontinuities spaced along a transmission line as has its step-transformer prototype, with corresponding discontinuities of the filter and step transformer having the same VSWR. Both the filter and its prototype are synchronously tuned circuits, which means that adjacent discontinuities have out-of-phase reflection coefficients giving the maximum cancellation. This condition determines the spacing between discontinuities. It is also shown how the line impedances of a reactance-coupled filter may be chosen to obtain a nearly equal-ripple response.

Design data and graphs are given to facilitate the prediction of filter performance when the filter is based on a selected prototype transformer. The method of design is first to select a prototype transformer and then to see if the predicted filter performance matches the specifications. If necessary, another prototype transformer has to be selected to yield another filter meeting the specifications more closely. This is illustrated by several numerical examples having fractional bandwidths from 10 to 85 percent.

The effect of repeating the central elements of an eight-resonator filter is shown for a pseudo-high-pass filter. Formulas for calculating the gap capacitance in a circular coaxial line for this type of filter are also given.

Besides being discussed in Quarterly Progress Report 5, a discussion of the above subjects will also be found in Chapter 9 of Ref. 1. Several items from the above material have appeared or are about to appear in *The Microwave Journal*.[14,15]

I. BAND-STOP FILTERS

A study was made on this contract to determine ways of designing band-stop filters in strip line or in waveguide. This work is discussed in several reports.

In Sec. III of Quarterly Progress Report 3[16] an approximate design procedure is presented for use in the design of strip-line or waveguide band-stop filters having narrow stop-bands. In order to obtain the desired narrow stop-band, the band-stop resonators in strip line are constructed from a short-circuited length of line which is capacitively coupled to the main transmission line. For waveguide, an analogous structure is used where the resonators are inductively coupled to the main waveguide by use of inductive irises. Equations are presented for estimating the effects of dissipation loss in the circuit, and procedures are outlined for experimentally adjusting the resonator couplings by use of laboratory tests. A trial, three-resonator strip-line band-stop filter was constructed, and good measured performance was obtained.

The measured characteristics of a three-resonator, waveguide, band-stop filter are discussed in Sec. II of Quarterly Progress Report 4.[6] The design of this filter had been discussed in Quarterly Progress Report 3.[16] It was found necessary to use three-quarter-wavelength spacings between resonators (instead of quarter-wavelength spacings) in order to avoid undesirable interaction between resonators. Using this larger resonator spacing, excellent agreement was obtained between the computed and measured response for the filter, although both responses had somewhat larger pass-band attenuation ripple than was called for by the prototype. This was found to be due to the selectivity effect of the coupling lines between resonators.

In Sec. II of Quarterly Progress Report 7[17] an exact method is presented for the design of band-stop filters consisting of stubs and quarter-wavelength connecting lines. Using this method, a low-pass prototype circuit is chosen, and the transmission-line band-stop filter derived from the prototype will have a response that is an exact mapping of the prototype response. In theory the stop-band can have any width, but if the stop-band is very narrow the stub impedances become unreasonable. In such cases it is found to be desirable to replace the stubs by capacitively or inductively coupled resonators of reasonable impedance. This introduces an approximation but gives very good results. The design of filters having three-quarter-wavelength spacings between resonators is also discussed. This latter case is of interest for the design of waveguide band-stop filters where it has been found desirable to separate the resonators by three quarter-wavelengths in order to avoid interactions between the fringing fields at the coupling irises.

The exact design methods discussed above are further extended to cover the design of band-stop filters in additional novel forms, in Sec. IV of this report.

Besides the discussions in Quarterly Progress Reports 3, 4, and 6, and in this report, some of the above material was discussed in a paper presented at the 1962 PGMTT National Symposium in Boulder, Colorado,[18] and also in a version published in the *IRE Transactions on Microwave Theory and Techniques*.[19] Most of the material on band-stop filters in Quarterly Progress Reports 3, 4, and 6 also appears in modified form in Chapter 12 of the book prepared on this contract.[1]

J. MULTIPLEXERS

A technique for the precision design of multiplexers was investigated on this contract.

In Sec. III of Quarterly Progress Report 6[10] a study of the design of multiplexers having contiguous pass-bands is presented. In the design procedure discussed, the individual filters are designed from Tchebyscheff low-pass prototype filters having a resistor termination at one end only. This approach can be used for the design of either series-connected or shunt-connected multiplexers. In either case an additional reactance- or susceptance-annulling network is required in order to obtain optimum

performance. A four-channel, lumped-element design is worked out, and its response is computed. Also, a three-channel design using comb-line filters is worked out, and its response computed. In both cases very low-loss performance is achieved.

In Sec. V of this report the measured performance of a three-channel diplexer with contiguous pass-bands, designed by the methods described above, is presented. Also, the use of this same technique for the design of multiplexers having guard-bands between the channel bands is evaluated. Trial designs are worked out and their responses computed. It is found that these same techniques can be applied to the design of multiplexers with guard-bands between the channel bands, but a different type of susceptance- or reactance-annulling network is then required.

Most of this work on multiplexers will be found in somewhat different form in Chapter 16 of the book prepared on this contract.[1]

K. MAGNETICALLY TUNABLE FILTERS USING FERRIMAGNETIC RESONATORS

On this contract, work on magnetically tunable filters begun on Contract DA 36-039 SC-74862[20] was continued. These filters make use of ferrimagnetic resonators consisting of spheres of single-crystal yttrium-iron-garnet (YIG) or gallium-substituted YIG (Ga-YIG). The resonant frequency of such resonators can be controlled by varying a biasing dc magnetic field.

In Sec. II of Quarterly Progress Report 3[16] on this contract, design techniques are discussed for use in the 2.0-to-4.2-Gc tuning range. A filter was designed, constructed, and tested which used overlapping sections of strip transmission line to couple to the resonators. The resonators were coupled together by an iris, preferably a slot because it gives the highest attenuation at frequencies far from the center frequency.

Design formulas and curves for this type of tunable filter are given in Quarterly Progress Report 3.[16] Test results on the experimental filter, mentioned above, are presented, including the following:

(1) Response curves for various center frequencies from 2.0 Gc to 4.8 Gc

(2) A comparison of responses using circular and slot irises to couple between resonators

(3) Curves showing center frequency as a function of dc magnetic bias field

(4) The saturation power at center frequency as a function of center frequency

(5) The effects of the conducting boundaries on the resonant frequency and unloaded Q of the resonators.

The methods of carrying out calculations of the effects of temperature are outlined. The feasibility of using gallium-substituted yttrium-iron-garnet as a resonator material for the 1.0-to-2.0-Gc range is discussed, and the results of measurements of the unloaded Q of this material in the 1.0-to-4.0-Gc range are given.

In Quarterly Progress Report 5 on this contract,[9] the design, construction, and testing of a magnetically tunable filter that uses an arrangement of spherical YIG resonators lying in a plane perpendicular to the direction of the dc magnetic biasing field is described. A minimum dc magnetic air-gap spacing is required for this type of filter. Measurements of attenuation loss, bandwidth, and tuning fields of the two-resonator prototype are discussed. The attenuation loss varies from 4.0 db at a center frequency of 2.1 Gc, to 1.65 db at 3.9 Gc. The 3-db bandwidth is about 32 Mc and is nearly constant over this tuning range. Tuning requirements for the filters with three or more resonators are discussed. A new device by means of which ferrimagnetic crystals can be quickly aligned along any desired axis is described. The results of anisotropy measurements made on crystals of YIG and Ga-YIG using this device are presented.

In Sec. III of Quarterly Progress Report 7 on this contract[17] a review of the procedure employed in the establishment of the parameters and dimensions of magnetically tunable filters is given. Charts and graphs are presented which enable a designer to arrive at the dimensions of the circuit elements, including the ferrimagnetic resonators, in order to give a specified band-pass frequency response. Circuit structures are presented which appear or have proved to be very promising for practical applications. Two typical examples are given of the design of two-resonator band-pass filters, one of which employs a waveguide and the other a strip-transmission-line coupling circuit. Finally, the performances of two side-wall-coupled strip-transmission-line filters, one containing two resonators and the other containing three, are discussed.

The results are compared with a previous version of the two-resonator side-wall-coupled filter and with a previously developed overlapping line version. As expected, the three-resonator design was found to give a steeper rate of cutoff, and very high off-resonance attenuation.

Some of this work was also discussed in a technical paper[21] and in a letter to the editor[22] in the *IRE Transactions on Microwave Theory and Techniques*. An extensive discussion on this subject also appears in Chapter 17 of the book prepared on this contract.[1]

L. UP-CONVERTERS FOR USE AS ELECTRONICALLY TUNABLE FILTERS

Another technique for electronic tuning studied on this contract (as well as on the preceding Contract DA 36-039 SC-74862)[23] is the use of variable-capacitance diode up-converters as electronically tunable filters. These devices achieve a wide tuning range (though they are narrow-band at any given tuning frequency) by use of a wide-band input-impedance-matching filter, a narrow-band sideband output-impedance-matching filter, and a voltage-tunable pump oscillator such as a backward-wave oscillator.

Defining f as the input frequency, f' as the sideband output frequency, and f^p as the pump frequency, for a *lower-sideband up-converter* the output is at the lower-sideband frequency

$$f' = f^p - f \quad . \tag{II L-1}$$

For an *upper-sideband up-converter*, the output is at the upper-sideband frequency

$$f' = f^p + f \quad . \tag{II L-2}$$

For either type of up-converter, tuning action can be achieved if a narrow-band filter is used at the output so that only frequencies equal or very nearly equal to a specific frequency, f'_0, can be passed. If the pump frequency f^p is varied, the input frequency which will be accepted by the amplifier will be given by

$$f = f^p - f'_0 \tag{II L-3}$$

for the case of lower-sideband up-converters, and by

$$f = f_0' - f^p \qquad \text{(II L-4)}$$

for the case of upper-sideband up-converters. In both cases the amplifiers will yield gain. The lower-sideband type introduces some negative-resistance amplification in addition to the up-converter amplification, however, and will therefore generally give more gain. For gain to be achieved, the variable-capacitance diode must see proper terminations at both frequencies, f and f_0'. Since f_0' is a fixed frequency, it is relatively easy to maintain proper termination at that frequency. The input frequency, f, varies, however, and the tuning range of the amplifier is determined largely by the range of f for which proper terminating conditions can be maintained. Because of the narrow-band output circuit used in devices of this type they are capable of tuning ranges of the order of an octave or more.[10]

A trial strip-line lower-sideband up-converter was constructed on this contract using the previously developed theory.[23] The measured 3-db bandwidth tuning range was 38.5 percent as compared to 40 percent for the design objective, and the peak gain was 12.6 db. The input band center was 946 Mc while the sideband output was at 4,037 Mc. The measured noise figure was in good agreement with the computed nominal noise figure of 2.1 db. The design and the measured performance of this device is discussed in Quarterly Progress Reports 2 and 3 for this contract.[2,16]

In Sec. II of Quarterly Progress Report 6 for this contract,[10] our previous theoretical work[23,16] on electronically tunable up-converters is further extended. The previous design theory neglected some of the parasitic parameters of the diode, which can become quite important if the up-converter is to operate with microwave input frequencies. Design procedures suitable for programming on a computer are developed for the cases of electronically tunable upper-sideband up-converters. The diode is assumed to be resonated by a single stub connected either in series with the diode, or in shunt, and all diode parasitic parameters are included. Procedures for computing the gain *vs.* frequency and the midband noise figure are also presented. The computed performance of a number of trial designs in the 1-to-2-Gc and 2-to-4-Gc tuning ranges are shown, and the results discussed.

Besides the discussions described above, additional discussions were presented in a paper presented at the *1961 PGMTT National Symposium in Washington, D.C.*,[24] in a paper published in the *IRE Transactions on Microwave Theory and Techniques*,[25] and in a letter to the editors of the *Proceedings of the IRE*.[26]

REFERENCES

1. G. L. Matthaei, Leo Young, and E. M. T. Jones, *Design of Microwave Filters, Impedance-Matching Networks and Coupling Structures*, a book prepared on SRI Project 3527, Contract DA 36-039 SC-87398, Stanford Research Institute, Menlo Park, California (January 1963).

2. W. J. Getsinger and G. L. Matthaei, "Microwave Filters and Coupling Structures," Quarterly Progress Report 2, SRI Project 3527, Contract DA 36-039 SC-87398, Stanford Research Institute, Menlo Park, California (July 1961).

3. W. J. Getsinger, "Coupled Rectangular Bars Between Parallel Plates," *IRE Trans. PGMTT*-10, pp. 65-72 (January 1962).

4. J. T. Bolljahn and G. L. Matthaei, "Microwave Filters and Coupling Structures," Quarterly Progress Report 1, SRI Project 3527, Contract DA 36-039 SC-87398, Stanford Research Institute, Menlo Park, California (April 1961).

5. J. T. Bolljahn and G. L. Matthaei, "A Study of the Phase and Filter Properties of Arrays of Parallel Conductors Between Ground Planes," *Proc. IRE* 50, pp. 299-311 (March 1962).

6. Leo Young and G. L. Matthaei, "Microwave Filters and Coupling Structures," Quarterly Progress Report 4, SRI Project 3527, Contract DA 36-039 SC-87398, Stanford Research Institute, Menlo Park, California (January 1962).

7. G. L. Matthaei, "Interdigital Band-Pass Filters," a paper presented on May 23, 1962, at the *1962 PGMTT National Symposium* at Boulder, Colorado.

8. G. L. Matthaei, "Interdigital Band-Pass Filters," *IRE Trans. PGMTT*-10, pp. 479-491 (November 1962).

9. G. L. Matthaei, Leo Young, and P. S. Carter, Jr., "Microwave Filters and Coupling Structures," Quarterly Progress Report 5, SRI Project 3527, Contract DA 36-039 SC-87398, Stanford Research Institute, Menlo Park, California (May 1962).

10. W. J. Getsinger, E. G. Cristal and G. L. Matthaei, "Microwave Filters and Coupling Structures," Quarterly Progress Report 6, SRI Project 3527, Contract DA 36-039 SC-87398, Stanford Research Institute, Menlo Park, California (August 1962).

11. Leo Young, "Stepped-Impedance Transformers and Filter Prototypes," *IRE Trans. PGMTT*-10, pp. 339-359 (September 1962).

12. Leo Young, "Prediction of Absorption Loss in Multilayer Interference Filters," *J. Opt. Soc. Am.*, 52, pp. 753-761 (July 1962).

13. Leo Young, "Inhomogeneous Quarter-Wave Transformers," *The Microwave Journal*, 5, pp. 84-89 (February 1962).

14. Leo Young, "The Practical Realization of Series-Capacitive Couplings for Microwave Filters," *The Microwave Journal*, 5, pp. 79-81 (December 1962).

15. Leo Young and B. M. Schiffman, "A Useful High-Pass Filter Design," to be published in *The Microwave Journal*.

16. P. S. Carter, Jr., Leo Young, G. L. Matthaei and E. M. T. Jones, "Microwave Filters and Coupling Structures," Quarterly Progress Report 3, SRI Project 3527, Contract DA 36-039 SC-87398, Stanford Research Institute, Menlo Park, California (October 1961).

17. B. M. Schiffman, P. S. Carter, Jr., and G. L. Matthaei, "Microwave Filters and Coupling Structures," Quarterly Progress Report 7, SRI Project 3527, Contract DA 36-039 SC-87398, Stanford Research Institute, Menlo Park, California (October 1962).

18. Leo Young, G. L. Matthaei and E. M. T. Jones, "Microwave Bandstop Filters with Narrow Stop Bands," a paper presented on May 23, 1962 at the *1962 PGMTT National Symposium* in Boulder, Colorado.

19. Leo Young, G. L. Matthaei and E. M. T. Jones, "Microwave Bandstop Filters with Narrow Stop Bands," *IRE Trans. PGMTT*-**10**, pp. 416-427 (November 1962).

20. G. L. Matthaei, *et al.*, "Design Criteria for Microwave Filters and Coupling Structures," Final Report, Chapter 28, SRI Project 2326, Contract DA 36-039 SC-74862, Stanford Research Institute, Menlo Park, California (January 1961).

21. P. S. Carter, Jr., "Magnetically-Tunable Microwave Filters Using Single-Crystal Yttrium-Iron-Garnet Resonators," *IRE Trans. PGMTT*-**9**, pp. 252-260 (May 1961).

22. Y. Sato and P. S. Carter, Jr., "A Device for Rapidly Aligning and Mounting Ferromagnetic Single Crystals Along Any Desired Axis," *IRE Trans. PGMTT*-**10**, pp. 611-612 (November 1962).

23. G. L. Matthaei, *et al.*, *op. cit.* Chapter 29.

24. G. L. Matthaei, "Design Theory of Up-Converters for Use as Electronically Tunable Filters," a paper presented on May 15, 1961, at the *1961 PGMTT National Symposium* in Washington, D.C.

25. G. L. Matthaei, "Design Theory of Up-Converters for Use as Electronicallly Tunable Filters," *IRE Trans. PGMTT*-**9**, pp. 425-435 (September 1961).

26. G. L. Matthaei, "An Electronically Tunable Up-Converter," *Proc. IRE* **49**, pp. 1703-1704 (November 1961).

III A NOVEL MAGNETICALLY TUNABLE WAVEGUIDE FILTER, AND A REFINED VERSION OF A PREVIOUS STRIP-LINE MAGNETICALLY TUNABLE FILTER DESIGN

A. GENERAL

During the past quarter, two additional magnetically tunable filters have been constructed which incorporate techniques discussed in previous reports,[1,2] along with some new techniques not previously treated. Most of the new techniques were tested in the waveguide filter discussed in the following pages. The strip-line filter demonstrates a simple form of consutruction which permits a magnet air gap which is quite small for the size of strip line used.

B. A MAGNETICALLY TUNABLE WAVEGUIDE FILTER USING TWO YIG RESONATORS

Figures III B-1(a), (b) show sectional views of a magnetically tunable waveguide filter which was constructed on this project during the past quarter, while Fig. III B-2 shows a photograph of the completed filter. This structure has several unusual features:

(1) It uses very small YIG resonators (0.025-inch-diameter) in order to reduce coupling between magnetostatic modes within the YIG material and the fields external to the YIG material.

(2) It uses a novel impedance transforming structure which greatly enhances the coupling between the YIG spheres and the waveguide structure, while at the same time the spheres are in regions which are sufficiently spacious so that the sphere's performance is not greatly disturbed by the surrounding metal walls.

(3) Because of the miniaturized structure around the YIG spheres, by machining away some unnecessary metal in the structure it is possible to use a biasing magnet with an air gap as small as 0.20 inch.

The waveguide structure shown is made of aluminum and was fabricated in three pieces which were afterwards fitted together with dowels and screws. The structure mates with standard *X*-band waveguide (which has

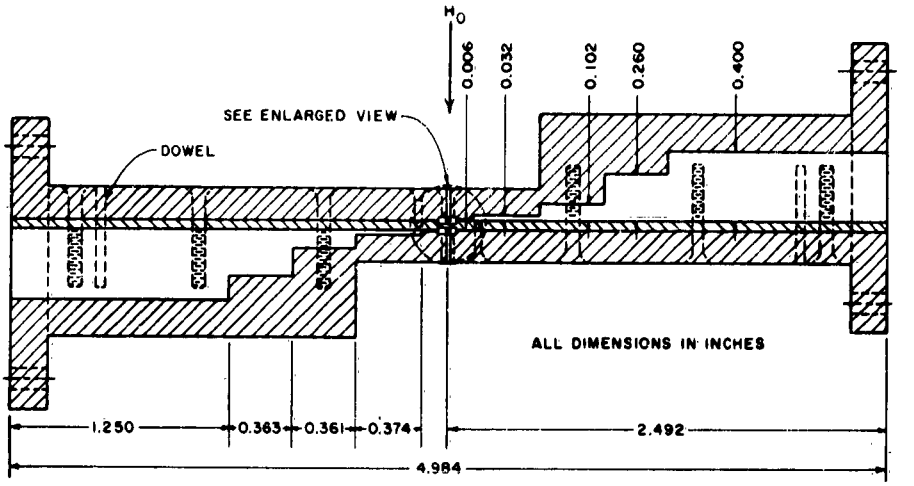

FIG. III B-1(a) SECTIONAL VIEW OF MAGNETICALLY TUNABLE WAVEGUIDE FILTER WITH TWO YIG RESONATORS

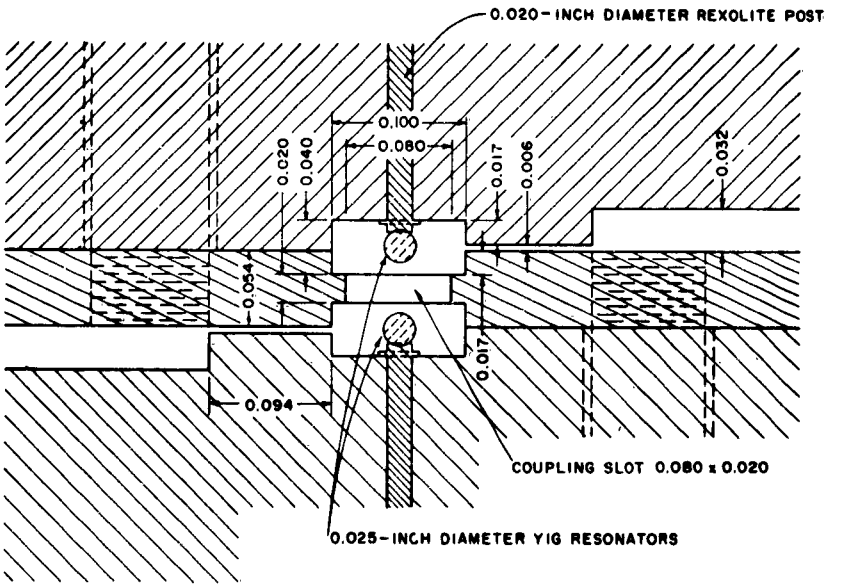

NOTES:

1. MATERIAL ALUMINUM
2. WIDTH INSIDE STRUCTURE 0.900 INCH THROUGHOUT
3. FILTER INPUT AND OUTPUT TO MATE WITH RG-52/U WAVEGUIDE
4. USES TWO 0.025-INCH DIA. YIG SPHERES AT CENTER OF FILTER STRUCTURE

RB-3527-657

FIG. III B-1(b) ENLARGED SECTIONAL VIEW OF CENTER PORTION OF MAGNETICALLY TUNABLE WAVEGUIDE FILTER WITH TWO YIG RESONATORS

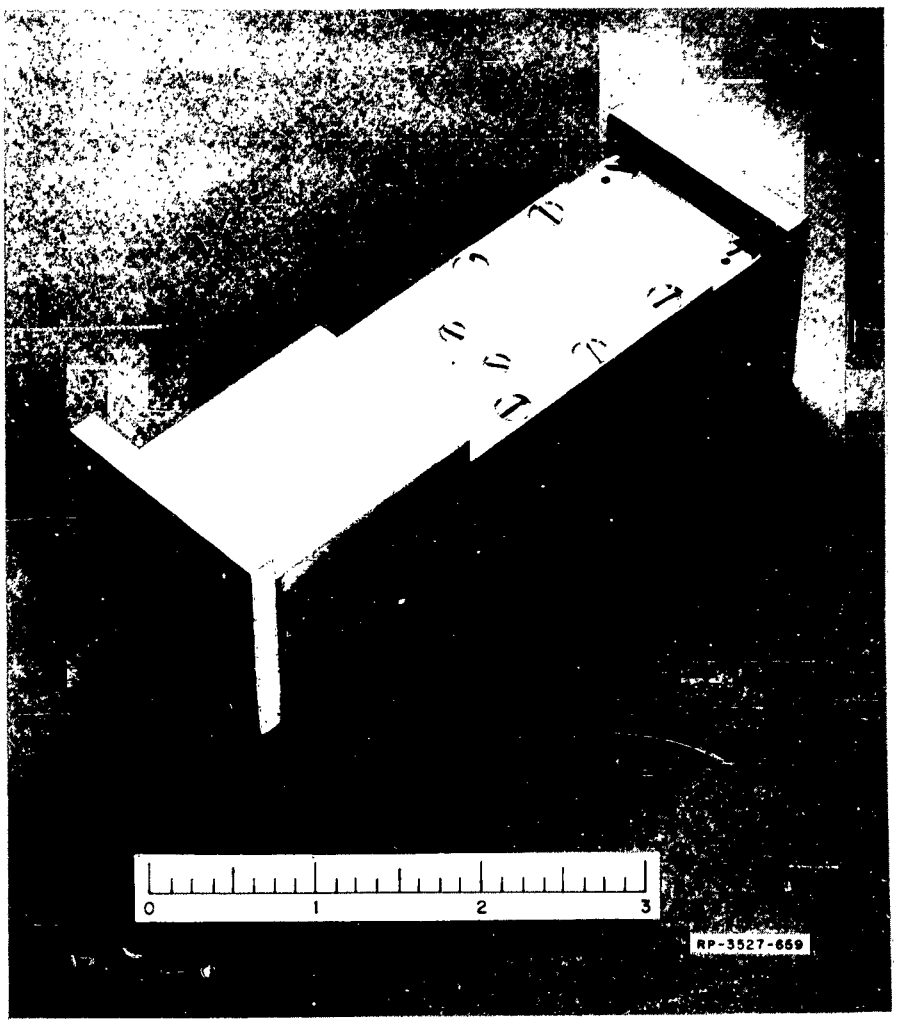

FIG. III B-2 PHOTOGRAPH OF THE FILTER IN FIGS. III B-1(a) AND (b)

inside dimensions of 0.400 inch by 0.900 inch), and the width of the structure shown is 0.900 inch throughout, except for the 0.080-inch-by-0.020-inch coupling slot between the resonator spheres. The coupling slot is oriented with its length parallel to the longitudinal axis of the guide. This causes the slot to disturb the current in the guide very little, and causes the circuit to have very high attenuation (in excess of 60 db) when the spheres are off ferrimagnetic resonance. However, when the signal frequency and applied biasing magnetic field are of the proper values to excite ferrimagnetic resonance, a component of RF magnetic dipole moment in the spheres is parallel to the length of the slot[1,2] and good coupling between the spheres is obtained, so as to give two-resonator filter performance.

C. DESIGN OF THE MAGNETICALLY TUNABLE WAVEGUIDE FILTER

As previously mentioned, it was decided to use 0.025-inch diameter spheres in this *X*-band filter in order to reduce coupling between possible magnetostatic modes within the YIG spheres and the fields external to the spheres. In some prior *X*-band waveguide experiments with larger spheres, we have experienced quite large spurious responses due to magnetostatic modes. Reducing the size of the spheres should reduce the excitation of such magnetostatic modes, at least as far as their excitation due to direct interaction with external fields is concerned. However, magnetostatic modes can also be excited by direct coupling between the desired uniform precession mode and magnetostatic modes. This type of coupling to magnetostatic modes can occur, for example, if the sphere is not perfectly round.[3] Assuming that the spheres are of good crystal structure with good surface polish and sphericity, making them as small as is feasible compared to a wavelength should help considerably in reducing difficulties with spurious responses due to magnetostatic modes.

By use of equations in Quarterly Progress Report 1, or in Sec. 17.09 of the book prepared on this contract,[2] we find that 0.025-inch-diameter YIG spheres next to a short-circuiting end wall in standard *X*-band waveguide should have an external Q of about $Q_e = 11,600$. Since the unloaded Q of *X*-band YIG resonators in a closed-in structure will probably not be over $Q_u = 2,000$ (and very likely less than that), an external Q of $Q_e = 11,600$ is much too large. Standard *X*-band waveguide has an inside

height of 0.400 inch, and by decreasing this height it is possible to reduce the external Q in direct proportion to the guide height.[1,2] However, the guide height must not be reduced too far or the metal top and bottom walls will be very close to the spheres and cause their operation to be disrupted as a result of currents induced in the adjacent metal surfaces.[1,2] From our past experience it appears that the guide height should be at least 1.3 times the diameter of the spheres, and larger if possible. In this case it was decided to make the guide 0.040-inch high in the region of the spheres, which is 1.6 times the diameter of the spheres. In this reduced-height guide the external Q will be about $Q_e = [(0.040)/(0.400)]\ (11,600) = 1,160$.

An external Q of 1,160, for a resonator whose unloaded Q might be of roughly the same value, is still too large to permit a reasonably low insertion loss in the filter. [See Eq. (III B-4) of Ref. 1, or Secs. 11.06 and 11.07 of Ref. 2 for equations for calculating the mid-band attenuation due to dissipation.] Now it can be shown that if a YIG resonator has an external Q of Q_e when it is connected to a terminating guide of impedance Z_0, if the impedance of the terminating guide is changed to Z_0', the external Q should become

$$Q_e' = Q_e \frac{Z_0'}{Z_0} \qquad \text{(III C-1)}$$

Thus, we could lower the external Q further (*i.e.*, increase the coupling between the resonator and the external load) if we could lower the effective impedance of the terminating guide. Since the guide impedance is directly proportional to the guide height, and since we do not wish to use a guide height less than 0.040 inch in the vicinity of the sphere, our problem resolves to this question: *With a YIG sphere in a 0.040-inch-high guide, can we obtain an effective terminating impedance like that of a guide whose height is considerably less than 0.040 inch*? As we shall see, at least as an approximation, the answer is yes.

In order to keep the dissipation loss in the filter down, it would be desirable to decrease the $Q_e = 1,160$ by at least a factor of five, which would give $Q_e' = 232$. Since the guide impedance is proportional to its height, by Eq. (III C-1) we conclude that the sphere must see a terminating impedance like that of a guide having a height of

$$b' = \frac{Q_e'}{Q_e} b \qquad \text{(III C-2)}$$

or

$$b' = \frac{232}{1,160} (0.040) = 0.008 \quad \text{inch} \quad .$$

Our approach will be to first obtain a step-transformer design which will match between standard-height *X*-band guide (which has $b = 0.400$ inch) and reduced-height guide having $b = 0.008$ inch. Then, one end of the transformer will be modified so as to present an impedance like that of 0.008-inch-high guide, at the center of a short section of 0.040-inch-high guide.

The required step transformer must have a transformation ratio of $0.400/0.008 = 50$. In order to cover the 8.2-to-12.4-Gc band with waveguide which is 0.900 inch wide, the transformer must have a fractional bandwidth $w_\lambda = 0.725$, on a reciprocal guide-wavelength basis [where $w_\lambda = 2(\lambda_{g1} - \lambda_{g2})/(\lambda_{g1} + \lambda_{g2})$, and λ_{g1} and λ_{g2} are the guide wavelength values at the operating band edges]. Tabulated impedance values for many quarter-wave-transformer designs are given in Refs. 4 and 5. A four-section, 50:1-impedance-ratio, Tchebyscheff transformer design with $w_\lambda = 0.80$ was selected, and from the tabulated normalized impedances the waveguide dimensions in Fig. III C-1 were obtained. This transformer has a theoretical maximum VSWR of 1.17 in its operating band.[4,5]

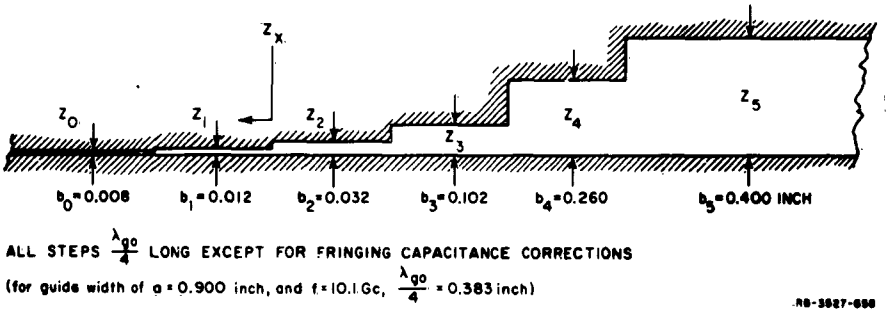

FIG. III C-1 A FOUR-SECTION, 50:1, TCHEBYSCHEFF, WAVEGUIDE IMPEDANCE TRANSFORMER

The next step in the design was to modify the first section (having $b_1 = 0.012$ inch) of the transformer so as to replace it with a short section of line having $b_A = 0.040$ inch, plus another section of line having a height and length such that the performance of the new line sections will be similar to that of the original uniform $b_1 = 0.012$-inch-high line section.

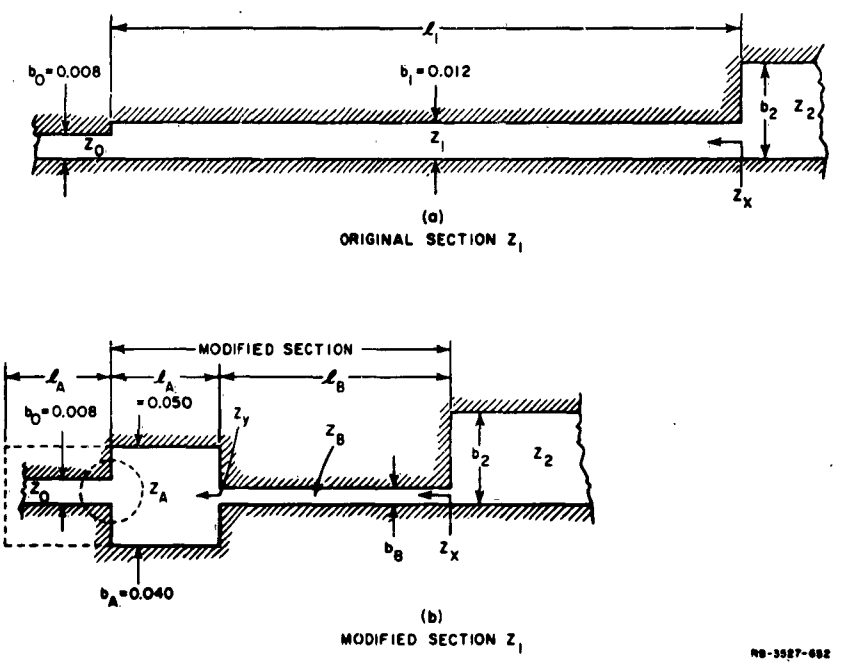

FIG. III C-2 ORIGINAL AND MODIFIED SECTION Z_1 OF TRANSFORMER, MODIFIED SO AS TO PROVIDE ADEQUATE SPACE FOR YIG SPHERE

Figure III C-2(a) shows the original first section of the transformer. At midband the length of this Z_1 section is $\lambda_{g0}/4$, and the impedance Z_x normalized with respect to Z_0 is

$$\frac{Z_x}{Z_0} = \left(\frac{Z_1}{Z_0}\right)^2 \quad . \qquad \text{(III C-3)}$$

We now wish to replace this line section of impedance Z_1 and length ℓ_1

by two line sections, one being of impedance Z_A (corresponding to a height of b_A = 0.040 inch) and of length ℓ_A, and the other being of impedance Z_B and of length ℓ_B, as is indicated by the solid line in Fig. III C-2(b). The length ℓ_A was chosen to be 0.050 inch, in order to provide sufficient room in the longitudinal direction so that the metal walls will not unduly disturb the resonance of the sphere. The height b_B and length ℓ_B were chosen so that the normalized impedance Z_x/Z_0 in Fig. III C-2(b) at the midband frequency will be the same as Z_x/Z_0 for the original structure in Fig. III C-2(a).

The values of b_B and ℓ_B were determined by trial and error procedures using a Smith chart, and making use of the fact the guide impedance Z_k is directly proportional to guide height b_k. By Eq. (III C-3), for Fig. III C-2(a)

$$\frac{Z_x}{Z_0} = \left(\frac{b_1}{b_0}\right)^2 = 2.25 \quad .$$

Next, Z_y in Fig. III C-2(b) was computed in normalized form. At midband, λ_{g0} = 1.530 inches, so that ℓ_A/λ_{g0} = 0.050/1.530 = 0.0326. Normalizing with respect to impedance Z_A, $Z_0/Z_A = b_0/b_A$ = 0.200. Using a Smith chart, moving ℓ_A/λ_{g0} towards the generator from Z_0/Z_A gives Z_y/Z_A = 0.21 + j0.205. Several values of b_B were tried until the value b_B = 0.006 inch was arrived at. For that value, $Z_y/Z_B = (Z_y/Z_A)(b_A/b_B)$ = 1.4 + j1.36. After moving towards the generator a distance ℓ_B/λ_{g0} = 0.605, a purely real value Z_x/Z_B = 3.05 was obtained. Renormalizing with respect to Z_0 gives $Z_x/Z_0 = (Z_x/Z_B)(b_B/b_0)$ = 2.29, which was deemed to be satisfactorily close to the desired value of Z_x/Z_0 = 2.25 computed above. In this manner the dimensions b_B = 0.006 inch and ℓ_B = 0.096 inch were arrived at.

Within the accuracy of the above calculations, the two lines Z_A and Z_B in Fig. III C-2(b) give exactly the same midband performance as does the single line of impedance Z_1 in Fig. III C-2(a). Note that the extra-high impedance of the Z_A line section is compensated for by an extra-low impedance in the Z_B line section. Though the circuit shown at (b) can be expected to deviate in performance from that at (a) as the frequency deviates from the midband value, the circuit at (b) should be reasonably broadband in its performance. This point is verified by

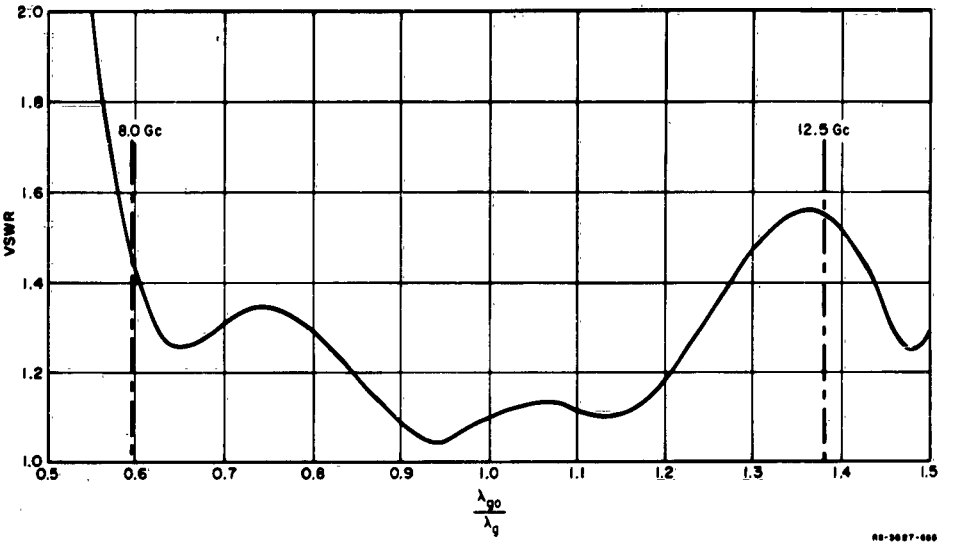

FIG. III C-3 COMPUTED VSWR OF THE 50:1 TRANSFORMER IN FIG. III C-1 WITH SECTION Z_1 REPLACED BY SECTIONS Z_A AND Z_B IN FIG. III C-2(b)

the computed response in Fig. III C-3, which shows the computed VSWR of the 50:1 impedance transformer in Fig. III C-1 with its Z_1 line section replaced by line sections Z_A and Z_B shown in Fig. III C-2(b). Note that the maximum VSWR in the band of interest is about 1.55 which, though larger than the 1.1 maximum VSWR value for the original transformer, is reasonably good. However, this design is obviously not optimum, and further study to provide techniques for optimum design of impedance transforming and coupling circuits of this type is contemplated.

In the actual filter circuit the Z_0 line of height $b_0 = 0.008$ inch in Fig. III C-2(b) was replaced by the YIG sphere, as indicated by dashed lines in the figure. Also, a short-circuit wall was placed a distance $\ell_A = 0.050$ inch to the left of the center of the sphere, as is also indicated by dashed lines in the figure. This distance was again governed by the need to keep the metal end wall a reasonable distance from the sphere in order to prevent induced currents in the wall from disturbing the sphere. The additional length of waveguide will introduce an additional, small self-reactance in the coupling to the sphere, but

this reactance should be small enough to be ignored without serious consequences. After corrections for fringing capacitances (as discussed in Refs. 4 and 5), the final dimensions of the input and output impedance transforming sections were as shown in Figs. III B-1(a), (b).

The dividing wall between the two spheres was made to be 0.020 inch thick, which resulted in a separation between the centers of the spheres of approximately 2.4 diameters. From past experience, this separation is believed to be adequate so that the spheres will not greatly distort each other's biasing *H*-field. Using the results of previous designs as a guide, trial values of 0.020 inch by 0.080 inch were estimated for the dimensions of the coupling slot between the spheres. It was expected that this slot would later be widened a little until the desired degree of coupling between spheres was obtained. However, initial tests indicated that the degree of coupling was about right with the dimensions as they were.

In working out the mechanical design of the filter, many of the contact surfaces of the joints in the device were partially recessed [not shown in Figs. III B-1(a), (b)] so as to leave a pressure lip along the edge of joints where good contact was important. In addition, at the joints in the short-circuit walls beside the YIG spheres a little silver paint was used in assembly to further insure a good contact.

D. MEASURED PERFORMANCE OF THE MAGNETICALLY TUNABLE WAVEGUIDE FILTER

The measured performance of the filter bore out quite well the validity of the design principles described above. Table III D-1 shows the measured values of midband attenuation, 3-db bandwidth, 30-db bandwidth, midband VSWR, and the required biasing magnetic field strength for different pass-band frequencies. Assuming that the response of this filter at 10 Gc corresponds to that of a two-resonator filter designed from an equal-element prototype,[6] for a midband attenuation of 2.4 db and a 30-db bandwidth of 276 Mc (as is indicated in Table III D-1 for f_0 = 10 Gc), then the computed unloaded Q of the resonators is Q_u = 1,040, while the external Q of the resonators is Q_e = 289. This value of Q_e is seen to agree reasonably well with the design value which was Q_e = 232, especially since it is known that the presence of the adjacent coupling slot will cause the Q_e value to be raised typically by about 20 percent

or somewhat more.[1,2] The estimated 1,040 value of unloaded Q for the spheres was lower than was hoped for. Because of a shortage of time, the linewidth of these spheres was not measured before inserting them in the filter, and it is probable that spheres with better unloaded Q's could be obtained.

Table III D-1

MEASURED PERFORMANCE OF THE MAGNETICALLY TUNABLE WAVEGUIDE FILTER

f_0 (Gc)	L_e (db)	Δf_{3db} (Mc)	Δf_{30db} (Mc)	VSWR at f_0	H_0 (k-oersted)
8.0	2.1	--	--	--	2.43
8.5	2.1	45.7	249	1.22	2.86
9.0	2.2	--	--	--	2.90
9.5	2.1	--	--	--	3.00
10.0	2.4	49.8	276	1.06	3.20
10.5	2.4	--	--	--	3.25
11.0	2.2	--	--	--	3.61
11.5	2.4	--	--	--	3.68
12.0	2.9	--	--	--	4.22
12.5	2.6	47.1	251	1.06	4.30

f_0 = Tuning frequency
L_e = Minimum attenuation at tuning frequency
Δf_{3db} = Bandwidth for 3 db attenuation with respect to L_e
Δf_{30db} = Bandwidth for 30 db attenuation with respect to L_e

Figure III D-1 shows the measured attenuation characteristics of the filter *vs.* biasing magnetic field. Here again the results are very much in line with what was hoped for. Note that there is only one stop-band spurious response, and its minimum attenuation is 38 db, a high value for a two-resonator magnetically tunable filter. Also note that the off-resonance attenuation is everywhere greater than the measuring range of the test equipment which in this case was from around 52 to 59 db. This very high off-resonance attenuation results from the very low impedance in the vicinity of the coupling slot between the two waveguides, and also from the small size of the coupling slot (which was made possible by the use of small YIG spheres).

One unexpected problem that became apparent after testing this filter was that though the spurious response activity in the stop-band of this filter was quite low, so that the stop-band performance was very good for a YIG filter with only two resonators, there were various small spurious responses which appeared in the pass-band of the filter.

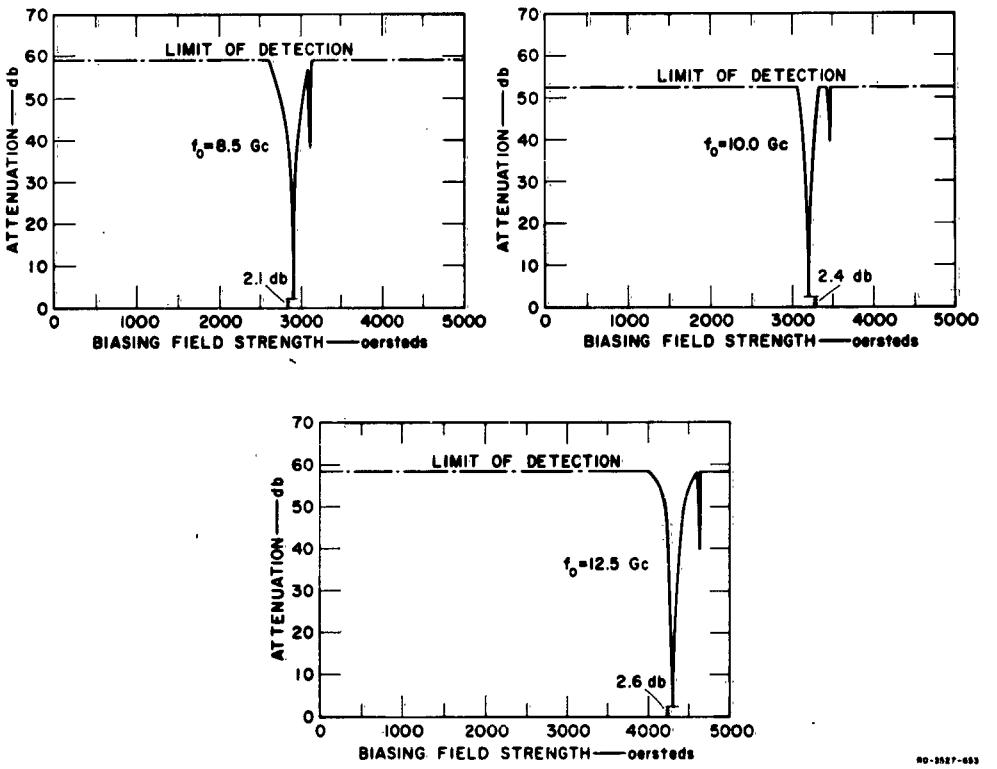

FIG. III D-1 ATTENUATION vs. BIASING FIELD STRENGTH FOR MAGNETICALLY TUNABLE WAVEGUIDE FILTER
These curves were obtained using a sweeping magnet power supply and a recorder

These can be seen from the responses shown in Fig. III D-2 which were taken using a sweeping magnet power supply, along with a recorder. These spurious responses are quite different in character from those that we have observed in our strip-line *S*-band filters.[1,2] In our *S*-band filters the stop-band spurious responses were generally more prominent than those in this present filter, and there were no spurious responses observable

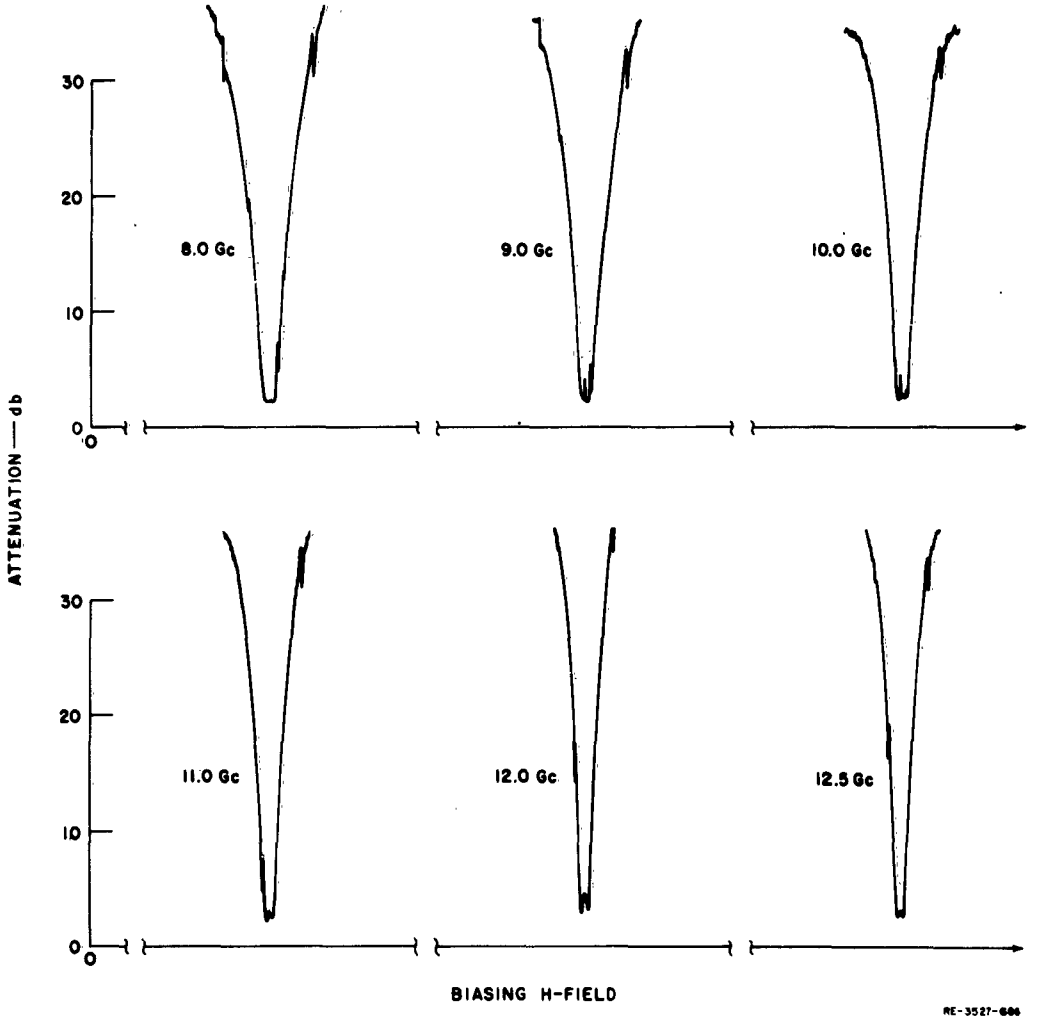

FIG. III D-2 PASS-BAND ATTENUATION vs. SWEPT BIASING FIELD STRENGTH FOR THE MAGNETICALLY TUNABLE WAVEGUIDE FILTER
These curves were obtained using a sweeping magnet power supply and a recorder

in the pass-band except for typically around 4.5 Gc where one of the stop-band spurious responses would tend to merge with the pass-band response. In the case of the data in Figs. III D-1 and III D-2 the stop-band spurious response never merges with the pass-band, and though there is movement of the pass-band spurious responses, as they move out of the pass-band they never grow into stop-band spurious responses, or at least not into stop-band spurious responses of any magnitude.

Though it will take further investigation to prove this point, it appears likely that these spurious responses which are occurring only in and around the pass-band of the spheres are responses due to direct coupling between the uniform precessional mode and the magnetostatic modes as a result of imperfections in the spheres (as contrasted with spurious responses excited by non-uniform external RF fields). The most likely imperfection to be giving this trouble is that the spheres may not be sufficiently spherical in shape.[3]

E. A MORE REFINED VERSION OF A PREVIOUS STRIP-LINE MAGNETICALLY TUNABLE FILTER DESIGN

One type of filter discussed previously[1,2] is a strip-line, two-resonator filter for the 2-to-4-Gc band, with the resonator spheres lying in a plane perpendicular to the biasing *H*-field. As a two-resonator filter this device had more stop-band spurious response activity than some other strip-line configurations we have investigated,[2,7] but it had the advantages that it was very easy to convert into a filter with three or more resonators, and it required an unusually small magnet air gap. When this filter was tested using three resonators, the spurious response activity which was apparent was greatly reduced.[1,2]

A more refined two-resonator version of the filter described above was constructed for use as one of the experimental models to be sent to the Signal Corps. This filter is shown in Fig. III E-1 with its upper half raised up. The significant electrical dimensions of this filter are the same as those given in Fig. III F-1 of Ref. 1 or in Fig. 17.08-3 of Ref. 2, but in this case the filter is fabricated in quite a different manner, and it is fabricated so as to minimize the magnet air gap required. In this case the filter is designed to split in half along a horizontal plane, the upper and lower housings being machined out of solid blocks of brass. After the housings were machined from brass, the

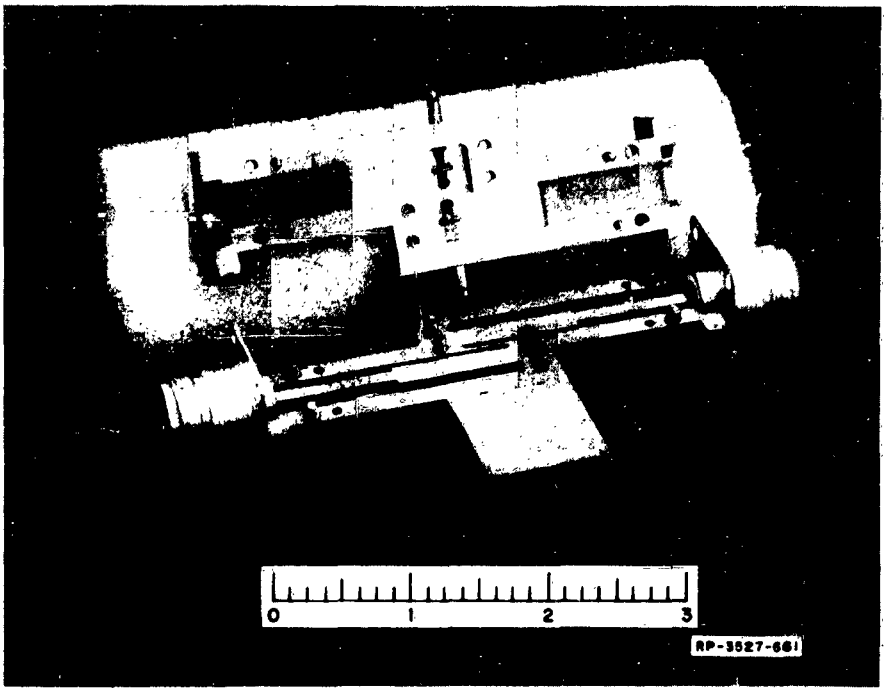

FIG. III E-1 A STRIP-LINE TWO-RESONATOR FILTER WITH YIG RESONATORS
The upper half is raised so that the YIG spheres and the strip lines may be seen

strip lines were soldered in place in one half of the structure, while the YIG spheres were mounted in the other half. Dielectric was used along the part of the strip lines in the regions next to the connectors in order to prevent possible flexing of the strip lines by forces in the connectors. Using this construction the magnet air gap required is only 0.260 inch. The housing structures for this filter could probably be made quite cheaply by die-casting methods. Figure III E-2 shows a close-up view of this filter mounted in an electromagnet purchased from a local manufacturer. Of course, by using a combination electromagnet and permanent magnet the size of the magnet could be reduced considerably.

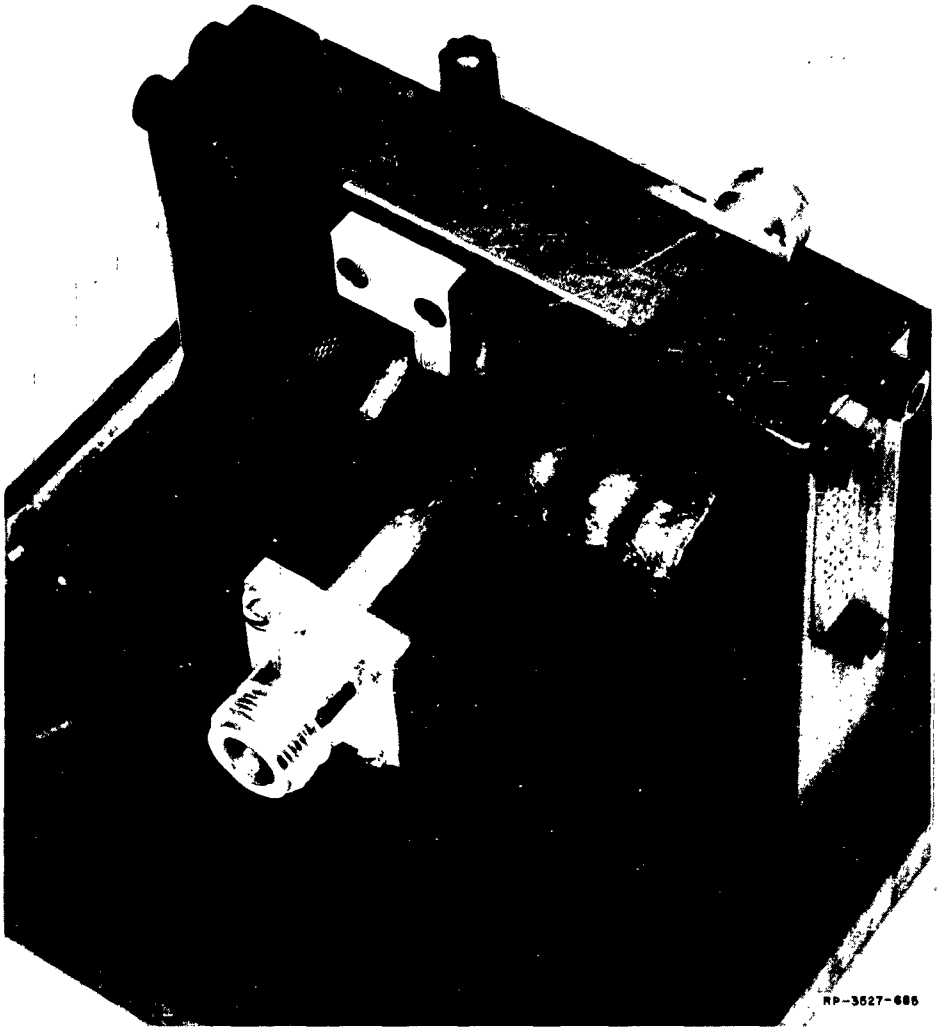

FIG. III E-2 CLOSE-UP VIEW OF FILTER IN FIG. III E-1 MOUNTED IN AN ELECTROMAGNET

The measured performance of this filter is much like that of the earlier experimental model[1,2] so the performance curves will not be repeated here. However, Table III E-1 shows the measured values of midband attenuation, 3-db bandwidth, 30-db bandwidth, midband VSWR, and biasing *H*-field required for resonance.

Table III E-1

MEASURED PERFORMANCE OF THE TWO-RESONATOR STRIP-LINE FILTER IN FIGS. III E-1 AND III E-2

f_0 (Gc)	L_c (db)	Δf_{3db} (Mc)	Δf_{30db} (Mc)	VSWR at f_0	H_0 (k-oersted)
2.0	2.3	18.71	93.0	1.02	0.66
2.5	1.4	--	--	--	0.84
3.0	1.1	18.88	99.0	1.3	1.00
3.5	1.2	--	--	--	1.20
4.0	1.2	18.24	100.9	1.6	1.44

REFERENCES

1. B. M. Schiffman, P. S. Carter, Jr., and G. L. Matthaei, "Microwave Filters and Coupling Structures," Quarterly Progress Report 7, SRI Project 3527, Contract DA 36-039 SC-87398, Stanford Research Institute, Menlo Park, California (October 1962).

2. G. L. Matthaei, Leo Young, and E. M. T. Jones, "Design of Microwave Filters Impedance Matching Networks and Coupling Structures," a book prepared on SRI Project 3527, Contract DA 36-039 SC-87398, Stanford Research Institute, Menlo Park, California, Chapter 17 (January 1963).

3. P. C. Fletcher and I. H. Solt, Jr., "Coupling of the Magnetostatic Modes," *J. Appl. Phys.*, Vol. 30S, pp. 181S-182S (April 1959).

4. Leo Young, and G. L. Matthaei, "Microwave Filters and Coupling Structures," Quarterly Progress Report 4, Sec. IV, SRI Project 3527, Contract DA 36-039 SC-87398, Stanford Research Institute, Menlo Park, California (January 1962).

5. G. L. Matthaei, Leo Young, and E. M. T. Jones, *Op. cit.*, Chapter 6.

6. G. L. Matthaei, Leo Young, and E. M. T. Jones, *Ibid.*, Sec. 11.07.

7. P. S. Carter, Jr., Leo Young, G. L. Matthaei, and E. M. T. Jones, "Microwave Filters and Coupling Structures," Quarterly Progress Report 3, SRI Project 3527, Contract DA 36-039 SC-87398, Stanford Research Institute, Menlo Park, California (October 1961).

IV BAND-STOP FILTERS

A. GENERAL

An exact method for the design of band-stop filters has been given in some detail in Quarterly Progress Report 7.[1] The main feature described there is a table of formulas (derived with the aid of a procedure given by Ozaki and Ishii[2]) for directly transforming a low-pass lumped-element prototype filter into a band-stop transmission-line filter that consists of alternating sections of quarter-wavelength connecting lines and stubs. The stubs are in shunt with the main line and are open-circuited at their outer ends, yielding a configuration that is here called the basic band-stop filter. Although this basic form is conceptually simple and easy to design it is not suitable for filters requiring very narrow stop-bands. The reason for this limitation is the difficulty of constructing stub lines with the high value of characteristic impedance required in such a filter. To overcome this difficulty, and also to allow greater freedom to the designer in general, other configurations of the band-stop filter are described here, together with design equations for converting the basic configuration to one of the newer types. Since the method of designing the basic filter (and other associated forms of band-stop filters) has been fully covered in Quarterly Progress Report 7,[2] it will not be reviewed here.

Two of these newer forms, both of which employ parallel-coupled lines, are completely consonant with the exact design procedure. A filter section of the first type, which is described in Sec. IV-B, has a stub resonator that is open-circuited on one end and short-circuited on the other,[2,3] and is separate from the main line. This type is particularly useful for filters with very narrow stop-bands because the stop-band width is essentially a function of the degree of coupling between the stub and main line.

The second type of filter employing coupled lines is suitable for wide bandwidths. This type of filter, described in Sec. IV-C, is similar to the first except that the stub is open-circuited on one end and directly connected to the main line at the other end. Because of its form it is here called a spur-line type of filter. In both types there is electromagnetic coupling between the stub and the main line along the full length

of the stub. Exact design equations and test results on filters designed by both the above methods are given herein.

In Sec. IV-D, test results are given on a filter configuration that uses short-circuited stubs capacitively coupled to the main line.[4,5] In the latter case the design formulas[1] (which were described in Quarterly Progress Report 7), although not exact, are a closer approximation to the exact design than earlier methods[4] from which they evolved. This form is particularly well suited to narrow stop-band filters.

In each of the three described cases it is required that a basic band-stop filter be designed as a first step. Then from this basic circuit (or its dual) one of the three alternative forms can be designed with the aid of the given equations.

B. PARALLEL-COUPLED-RESONATOR FILTER

A single section of the parallel-coupled-resonator type filter suitable for narrow stop-bands is shown in Fig. IV B-1. Also shown

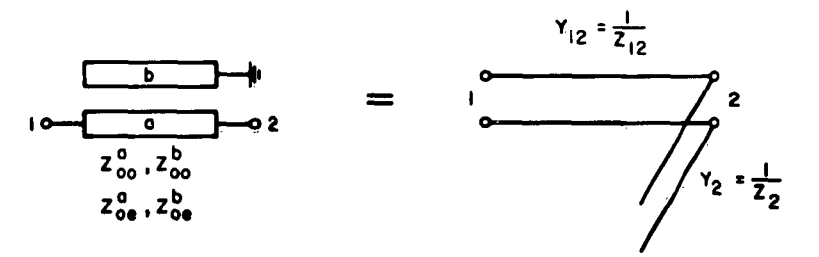

UNSYMMETRICAL CASE

$$\frac{C_a}{\epsilon} = \frac{\eta_0}{\sqrt{\epsilon_r}}(Y_{12} + Y_2) - \frac{C_{ab}}{\epsilon}$$

$$\frac{C_b}{\epsilon} = \frac{\sqrt{\epsilon_r}}{Y_2\eta_0}\left(\frac{C_{ab}}{\epsilon}\right)^2 - \frac{C_{ab}}{\epsilon}$$

with C_{ab} arbitrary (see text)

SYMMETRICAL CASE

$$\frac{C_a}{\epsilon} = \frac{C_b}{\epsilon} = \frac{\eta_0}{\sqrt{\epsilon_r}}\left[Y_{12} + Y_2 - \sqrt{Y_2(Y_{12} + Y_2)}\right]$$

$$\frac{C_{ab}}{\epsilon} = \frac{\eta_0}{\sqrt{\epsilon_r}}\sqrt{Y_2(Y_{12} + Y_2)}$$

RA-3527-690

FIG. IV B-1 PARALLEL-COUPLED TRANSMISSION-LINE SECTION AND EQUIVALENT SECTION OF BASIC FILTER

there, are the corresponding portion of the basic filter and design equations that enable the basic filter to be converted, section by section, into the parallel-coupled type. The coupled lines are completely specified by their even- and odd-mode impedances Z_{oe}^{a}, Z_{oe}^{b}, Z_{oo}^{a}, and Z_{oo}^{b} (or their odd- and even-mode admittances).[6,7] The superscripts a and b pertain to lines a and b in Fig. IV B-1.

Before the formulas can be applied it is necessary to partition the basic filter, shown in Fig. IV B-2, so that each section is complete according to Fig. IV B-1. Since there are more stubs (one more) than connecting lines, one quarter-wavelength section of connecting line must be inserted between the filter and one of the terminations. The characteristic impedance of the inserted section must of course equal the terminating impedance; although the filter amplitude response will be unaltered by this change, some time delay will be added to the signal.

The conversion formulas yield values for the distributed capacitances of the coupled lines as illustrated in Fig. IV B-3. These distributed capacitances C_a, C_b, and C_{ab}, pertaining to lines a and b shown in the form of a general π-network, are directly related to the even- and odd-mode admittances (or impedances) of the coupled lines.[6,7] The formulas give distributed capacitances directly because these quantities are most useful in designing coupled-rectangular-bar strip lines. The coupled lines may be symmetrical ($C_a = C_b$) or asymmetrical ($C_a \neq C_b$).

If it is desired that the coupled lines be symmetrical, the lower set of equations of Fig. IV B-1 is used. If the coupled lines are made unsymmetrical, the value of C_{ab} is arbitrarily chosen (subject to the condition that positive values are obtained for C_a and C_b) and the upper set of equations is used.

The relationship of the capacitances of the π-network of Fig. IV B-3 to the component capacitances (*i.e.*, parallel-plate and fringing capacitances) of parallel-coupled rectangular bars is easily seen in Fig. IV B-4. Since the capacitances C_a and C_b are not necessarily equal, the two coupled lines of each section need not be identical in cross section. However, as explained below, by restricting the heights of the two rectangular bars to be equal and further limiting the strip-line proportions, the coupled lines of both the symmetrical and asymmetrical type can be easily designed with the aid of Getsinger's graphs[8] of fringing capacitance.

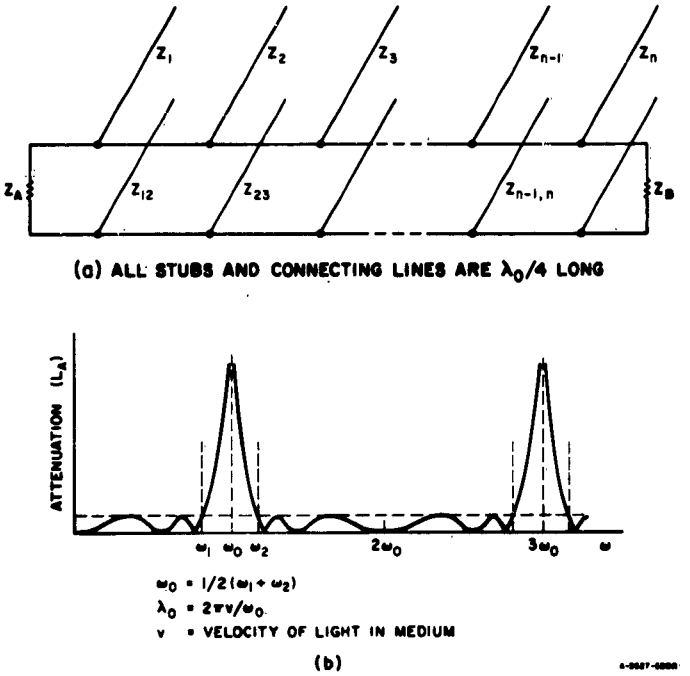

FIG. IV B-2 BASIC BAND-STOP FILTER

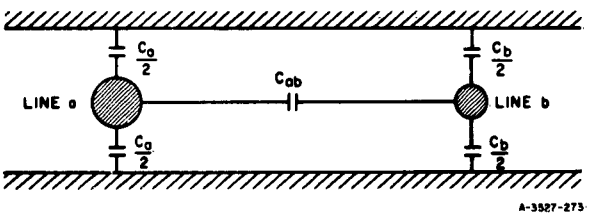

FIG. IV B-3 AN UNSYMMETRICAL PAIR OF PARALLEL-COUPLED LINES C_a, C_{ab}, AND C_b ARE LINE CAPACITANCES PER UNIT LENGTH

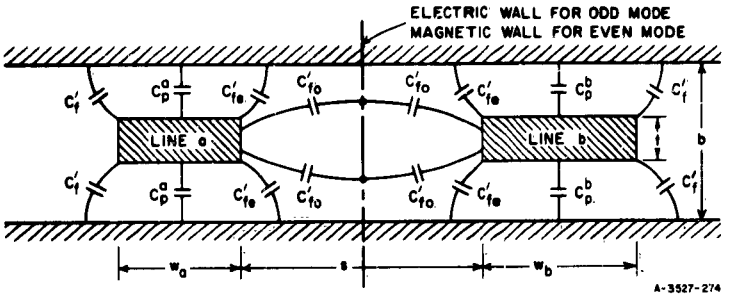

FIG. IV B-4 CROSS SECTION OF UNSYMMETRICAL, RECTANGULAR-BAR PARALLEL-COUPLED LINES

Getsinger[8] has derived equations for the fringing capacitances C'_{fe}, C'_{f0}, and C'_f, of rectangular bars shown in Fig. IV B-4, and has prepared convenient charts which relate C'_{fe}/ϵ, C'_{f0}/ϵ, and C'_f/ϵ to rectangular-bar strip-line dimensions. Here ϵ is the dielectric constant of the medium of propagation, so that the above ratios are dimensionless and of moderate size. Getsinger gives equations for the design of symmetrical, parallel-coupled, rectangular strip-lines, and here we adapt his equations to fit the unsymmetrical as well as the symmetrical case.[6]

Note that the shape of the strip lines in Fig. IV B-4 is specified in terms of the dimensions t, b, s, w_a, and w_b. To design a pair of lines such as those in Fig. IV B-4, to have odd- and even-mode admittances or impedances as determined implicitly by the calculated values of C_a/ϵ, C_{ab}/ϵ, and C_b/ϵ, first select a convenient value for t/b. Then, noting that

$$\frac{\Delta C}{\epsilon} = \frac{C_{ab}}{\epsilon} \quad , \qquad \text{(IV B-1)}$$

use Getsinger's chart[8] of $\Delta C/\epsilon$ and C'_{fe} *vs.* s/b to determine s/b, and also C'_{fe}/ϵ. Using t/b and Getsinger's chart of C'_f *vs.* t/b, determine C'_f/ϵ, and then compute

$$\frac{w_a}{b} = \frac{1}{2}\left(1 - \frac{t}{b}\right)\left[\frac{1}{2}\left(\frac{C_a}{\epsilon}\right) - \frac{C'_{fe}}{\epsilon} - \frac{C'_f}{\epsilon}\right] \qquad \text{(IV B-2)}$$

$$\frac{w_b}{b} = \frac{1}{2}\left(1 - \frac{t}{b}\right)\left[\frac{1}{2}\left(\frac{C_b}{\epsilon}\right) - \frac{C'_{f_a}}{\epsilon} - \frac{C'_f}{\epsilon}\right] \quad . \qquad \text{(IV B-3)}$$

When the ground plane spacing b is specified, the required bar widths, w_a and w_b, are determined. This procedure also works for the thin-strip case where $t/b = 0$. If either w_a/b or w_b/b is less than $0.35\ (1 - t/b)$, the width of the bar should be corrected using the approximate formula[8]

$$\frac{w'}{b} = \frac{0.07\left(1 - \frac{t}{b}\right) + \frac{w}{b}}{1.20} \quad , \qquad \text{(IV B-4)}$$

providing that $0.1 < (w'/b)/(1 - t/b) < 0.35$. In Eq. (IV B-4), w is the uncorrected bar width and w' is the corrected width. The need for this correction arises because of the interaction of the fringing fields at opposite sides of a bar, which will occur when a bar is relatively narrow.

The strip-line filter shown in Fig. IV B-5 was designed by the methods outlined here. The stop-band center frequency is 1.6 Gc. The prototype filter has two elements and a maximally flat response. The element values are $g_0 = g_3 = 1$, and $g_1 = g_2 = 1.414$. The characteristic impedance values of the basic two-stub filter designed with the aid of the formulas in Quarterly Progress Report 7 for a 5 percent width of the stop-band (between 3-db points) and 50-ohm terminations are $Z_1 = 949.9$ ohms and $Z_2 = 899.9$ ohms for the shunt-stub characteristic impedances, and $Z_{12} = 52.8$ for the connecting-line impedance. A quarter-wavelength section of 50-ohm impedance line was inserted between Stub 2 and the 50-ohm termination, thus yielding two complete L-sections ready to convert to two sections of parallel-coupled lines. The symmetrical type of coupled-line construction was chosen for the filter. The values of distributed capacitance (normalized to the permittivity of the medium) were then calculated with the aid of the formulas of Fig. IV B-1 and found to be: (1) for Section 1 consisting of Stub 1 and the connecting line, $C_a/\epsilon = C_b/\epsilon = 5.80$ and $C_{ab}/\epsilon = 1.73$, and (2) for Section 2 consisting of Stub 2 and the added 50-ohm section, $C_a/\epsilon = C_b/\epsilon = 6.12$ and $C_{ab}/\epsilon = 1.82$. With the aid of Getsinger's graphs the strip-line dimensions shown in the sketch Fig. IV B-6 were obtained.

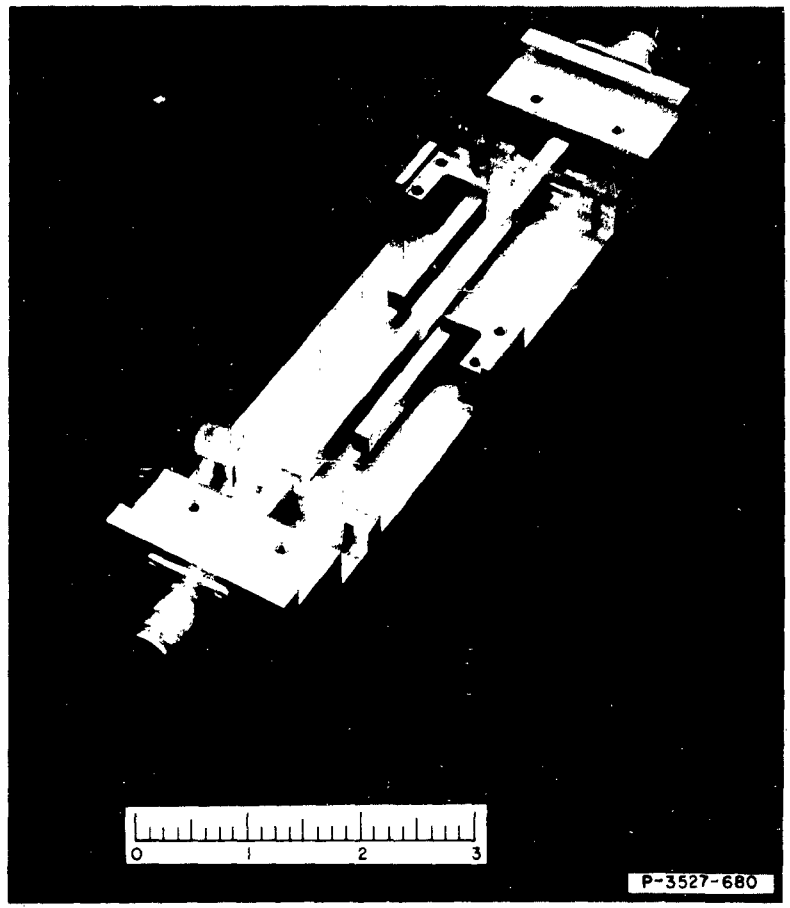

FIG. IV B-5 A PARALLEL-COUPLED-LINE, NARROW-BAND FILTER WITH COVER PLATE REMOVED

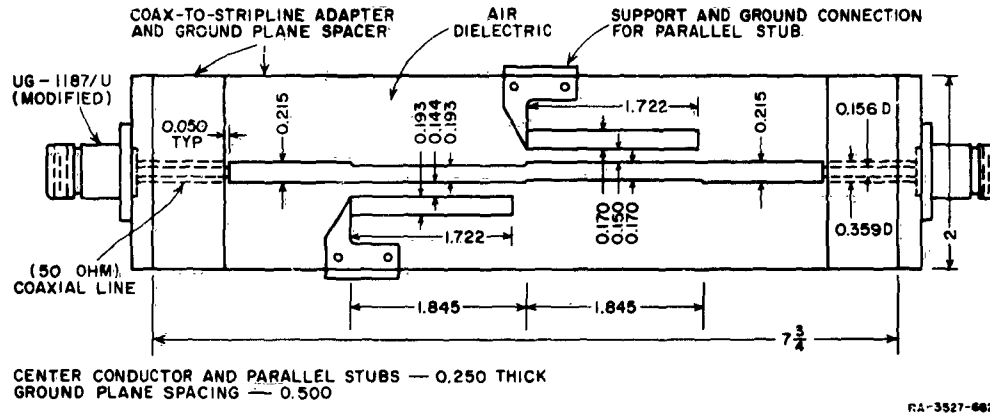

FIG. IV B-6 SKETCH OF A PARALLEL-COUPLED-LINE, NARROW-BAND FILTER WITH COVER PLATE REMOVED, SHOWING DIMENSIONS

The parallel-coupled resonator and its grounding wedge were milled from a solid piece of aluminum. Each resonator length is slightly less than $\lambda_0/4$, as determined experimentally, to allow for fringing capacity. The measured and computed responses of the filter are shown in Fig. IV B-7. The stop-band center frequency was found, after the final adjustments of the lengths of the resonators, to be f_0 = 1.608 Gc, and the curves of Fig. IV B-7 are so plotted. The measured attenuation loss and VSWR are seen to be in excellent agreement with the computed values over a very wide frequency range, even including the second stop-band at $3f_0$.

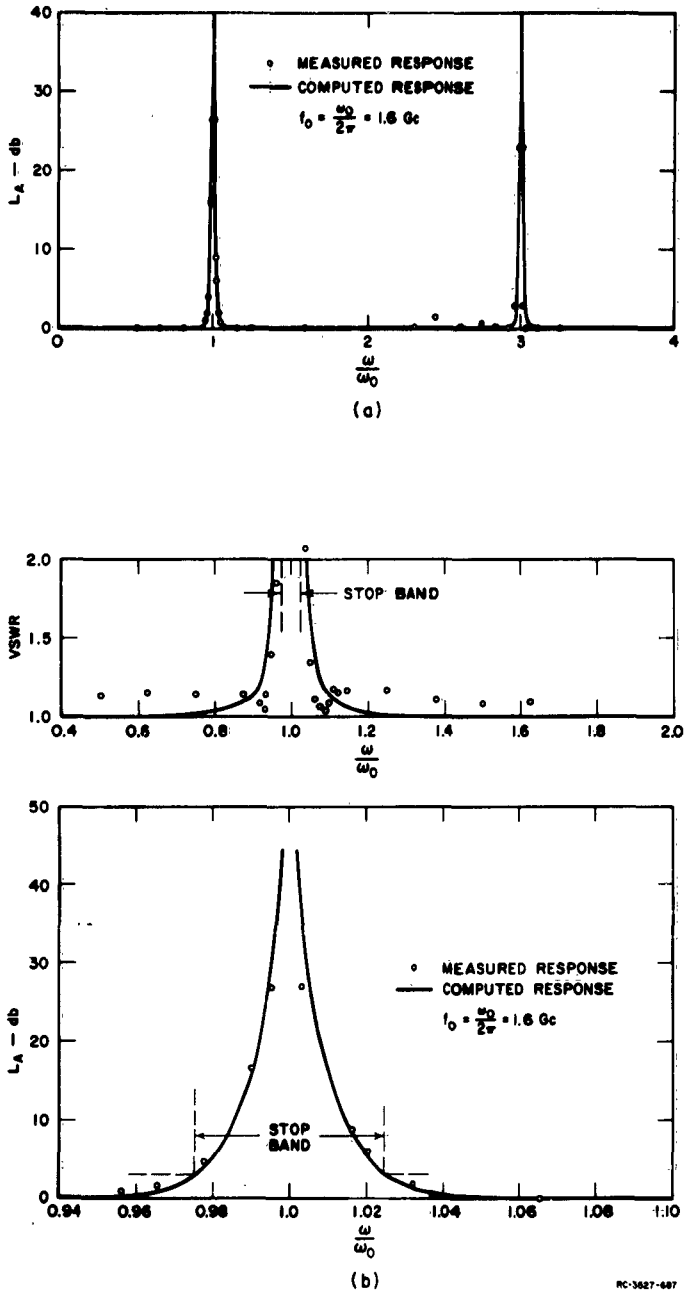

FIG. IV B-7 MEASURED AND COMPUTED RESPONSE OF FILTER IN FIG. IV B-5

C. SPUR-LINE TYPE OF FILTER

A second type of band-stop filter section employing coupled lines is shown, together with its design formulas, in Fig. IV C-1. Because of the direct connection (and the resulting strong coupling) of the stub to the line, this type of filter is similar to the basic type. In the limit, as the coupled lines are separated until there is very little

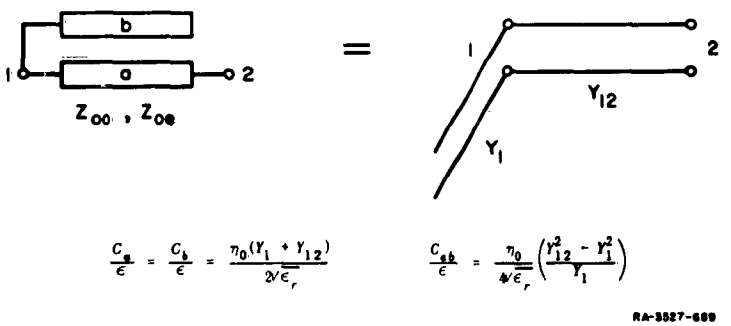

FIG. IV C-1 SPUR-LINE STUB RESONATOR AND EQUIVALENT SECTION OF BASIC FILTER

distributed coupling, the structure becomes almost identical to the basic shunt-stub filter section. The spur-line type of construction is thus suitable for filters with wide stop-bands. When the coupled lines are physically symmetrical, the energy stored in the resonant structure is determined mainly by the electromagnetic fields of the odd mode of propagation. This energy can be reduced and the bandwidth narrowed by reducing Z_{oo}—that is, by bringing the coupled lines close together—but this process has a practical limit. Furthermore, copper losses would tend to increase and thereby reduce the maximum attainable attenuation in the stop-band.

A two-resonator spur-line-type band-stop filter was designed with the aid of the formulas of Fig. IV C-1 for 60-percent stop-band bandwidth and 1.6-Gc stop-band center frequency. Here again, as for the narrow band filter described in Sec. IV-B, symmetrical coupled lines were used. The prototype circuit was chosen to have maximally flat response and its element values are, as before, $g_0 = g_3 = 1$, $g_1 = g_2 = 1.414$.

The basic filter element values were found to be $Z_1 = 119.3$ ohms and $Z_2 = 69.3$ ohms for the shunt stubs, and $Z_{12} = 86.05$ ohms for the connecting line. A quarter-wavelength section of 50-ohm line was then connected to one end of the filter so that it could be properly partitioned. The two possible circuits thus obtained and their methods of partitioning are shown in Fig. IV C-2(a) and (b). Trial paper designs based on those circuits yielded coupled rectangular bar lines of such proportions that it was feared that the discontinuities at the junctions of the two sections and main line would be large enough to badly degrade the performance. The circuit of Fig. IV C-2(c) was found superior in this respect. This circuit, which was used in the design of the filter, was derived from the basic circuit as follows: First the dual of the basic circuit was calculated by the equation

$$Z_D = \frac{Z_0^2}{Z} \qquad \text{(IV C-1)}$$

where $Z_0^2 = Z_A Z_B = (50)^2$, Z is the characteristic impedance of a stub or connecting line section and Z_D is the impedance of the dual of that section of line. (The dual of a shunt stub is a series short-circuited stub and the dual of a connecting line is again a connecting line.) Then a quarter-wavelength section of 50-ohm line was added to each end of the filter, and Kuroda's transformation[1] was used to move the two stubs outward, each to its end of the network, and at the same time transform the series stubs back to shunt stubs with the circuit of Fig. III C-2(c) as a result. This circuit was then partitioned so that it could be converted to a filter structure with two spur-line sections separated by a length of line of impedance $Z_{23} = 29.1$ ohms. The finished strip-line filter is shown in Fig. IV C-3. [Note that the two spurs point toward each other, and the spur-to-line junctions are separated by $3\lambda_0/4$. An alternative realization, in which the spurs point toward each other and their connecting points are separated $\lambda_0/4$, could be obtained from a series-stub

type filter in which the stubs are separated $3\lambda_0/4$. This latter circuit can be derived by applying Kuroda's transformation to the separate parts of the original shunt-stub basic circuit.] A sketch of the spur-line type filter with essential dimensions is given in Fig. IV C-4. The coupled lines were designed by the method described in Sec. IV-B.

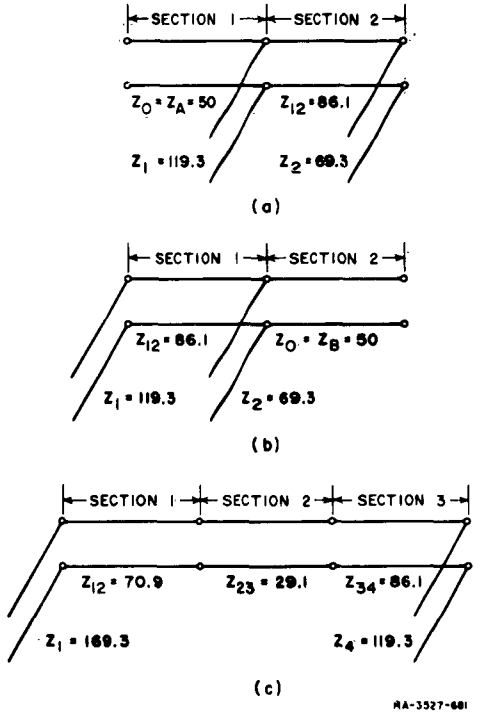

FIG. IV C-2 THREE POSSIBLE INTERMEDIATE STEPS IN CONVERTING A BASIC FILTER TO A SPUR-LINE FILTER

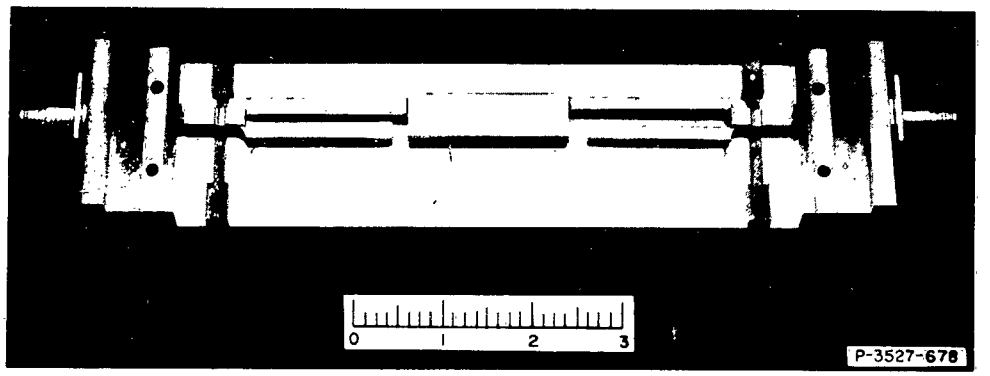

FIG. IV C-3 A SPUR-LINE BAND-STOP FILTER WITH COVER PLATE REMOVED

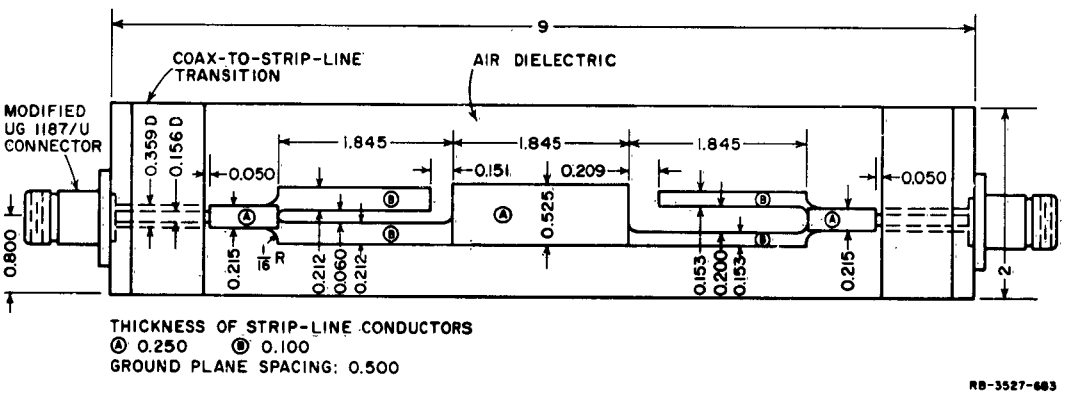

FIG. IV C-4 SKETCH OF A SPUR-LINE BAND-STOP FILTER WITH COVER PLATE REMOVED, SHOWING DIMENSIONS

The lengths of the spurs were individually adjusted to resonate at stop-band center as follows: The gap between the end of one spur and the center section of the main line was bridged with adhesive aluminum foil, thereby making that spur-line section non-resonant. The frequency of maximum attenuation of the remaining resonant spur line was then measured, and the unbridged spur was reduced in length about half the amount calculated to bring it to resonance at f_0 when considered to be a simple open-circuited shunt stub. (Half the calculated reduction in length was used as a safety precaution because the capacitance of the spur end to main line is reduced at the same time, and this latter value is not included in the calculation.) A few attempts brought the spur to resonance at the desired frequency and the same process was repeated for the other spur.

The measured values of attenuation loss and VSWR are shown to agree fairly well with the computed values, in Fig. IV C-5. The anomalous departure of measured values from computed values that does occur, mainly near the upper edge of the first stop-band and the lower edge of the

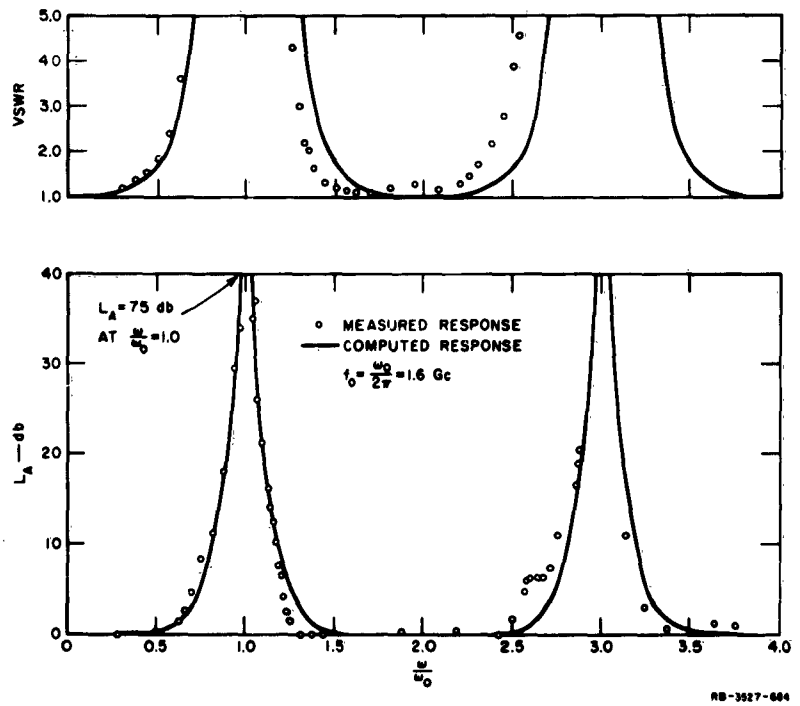

FIG. IV C-5 MEASURED AND COMPUTED VSWR AND ATTENUATION OF FILTER OF FIG. IV C-3

second stop-band, may be due to the remaining discontinuities between sections, which could not be eliminated entirely.

D. CAPACITIVELY-COUPLED-STUB FILTER

A method of designing an easily realizable narrow-band filter by modifying the exact design procedure was fully described in Quarterly Progress Report 7.[1] Although this design method is not exact, it yields a response curve that follows the desired response over a broad band. The modification consists of replacing each open-circuited high-impedance shunt stub with a short-circuited capacitively coupled stub of medium impedance—*i.e.*, the same order of magnitude as the connecting-line impedance, and of length slightly less than $\lambda_0/4$. The stubs are thus easily realized in coaxial or strip line, whereas by the exact method they would (in the case of very-narrow-band filters) be difficult or impossible to realize. In Quarterly Progress Report 7, a modified three-stub filter having ideally a 5-percent stop-band width and 0.1-db ripple in the pass-band was analyzed. The response in the frequency range 0 to $1.5f_0$ was shown to deviate no more than a negligible amount from the exact response, while the filter was usable over a still broader range.

This section describes a two-stub filter derived from an exact maximally flat design that is constructed in strip line. The stop-band width is 5 percent of the stop-band center frequency, and the basic filter, which is identical with the basic filter of Sec. IV-B, has a maximally flat response. The impedance of each stub of the capacitively coupled filter was arbitrarily set at 75 ohms for high unloaded Q. (This procedure allows an arbitrary choice of one design parameter for each resonator.) The other design parameters given in the schematic diagram in Fig. IV D-1(a)—the electrical length of each stub θ_{0i}, the gap susceptance $\omega_0 C_i$, and the impedance of the connecting line—were calculated by design formulas which have been previously given.[1,3]

A photograph of the filter is shown in Fig. IV D-2. Tuning screws are visible in the bottom plate under the main line end of each resonator. Similar screws were also put in the top plate. The short-circuit end supports of the resonators were so constructed that the stub lengths and capacitive gaps between the stubs and main line could be separately adjusted. The first step in adjusting the otherwise finished filter

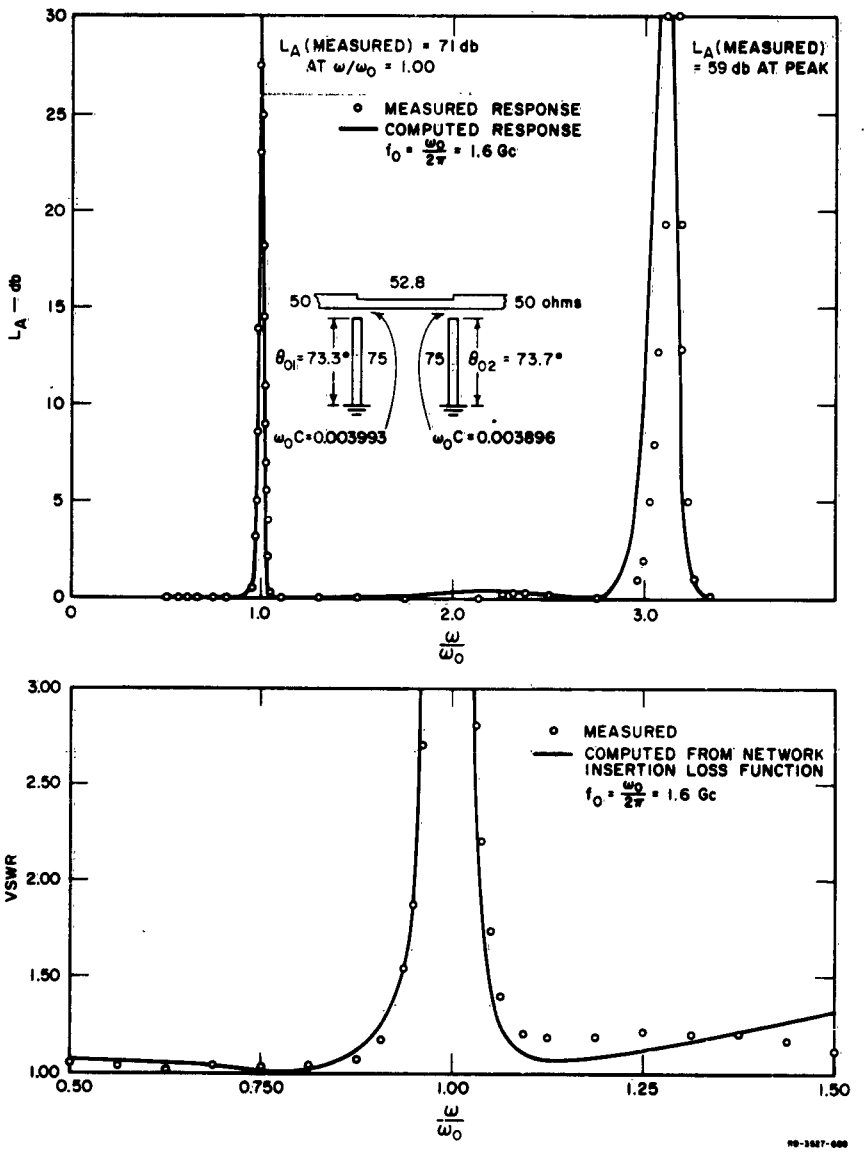

FIG. IV D-1 SCHEMATIC DIAGRAM OF CAPACITIVELY COUPLED FILTER, AND ITS MEASURED AND COMPUTED RESPONSE

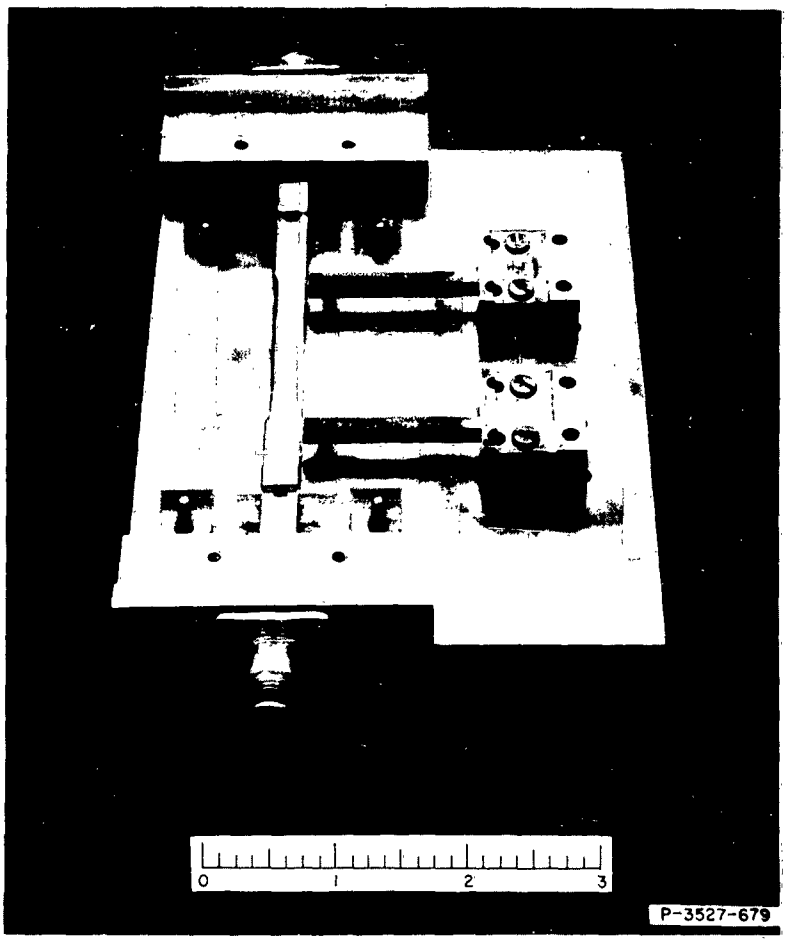

FIG. IV D-2 CAPACITIVELY COUPLED NARROW-BAND FILTER WITH COVER PLATE REMOVED

was the setting of the capacitive gaps of the two resonators for the proper loaded Q, and the second step was the tuning of each resonator to center frequency. This procedure, described more fully in Quarterly Progress Report 3,[5] p. 57, for a similar filter, was facilitated by the split-block construction of the resonator support that allowed separate adjustment of resonator length and capacitive gap. The measured response of the filter is seen to be very close to the computed response in Fig. IV D-1(a), (b), which shows attenuation and VSWR respectively. Figure IV D-3 gives the essential dimensions of this filter and reflects the final adjustments.

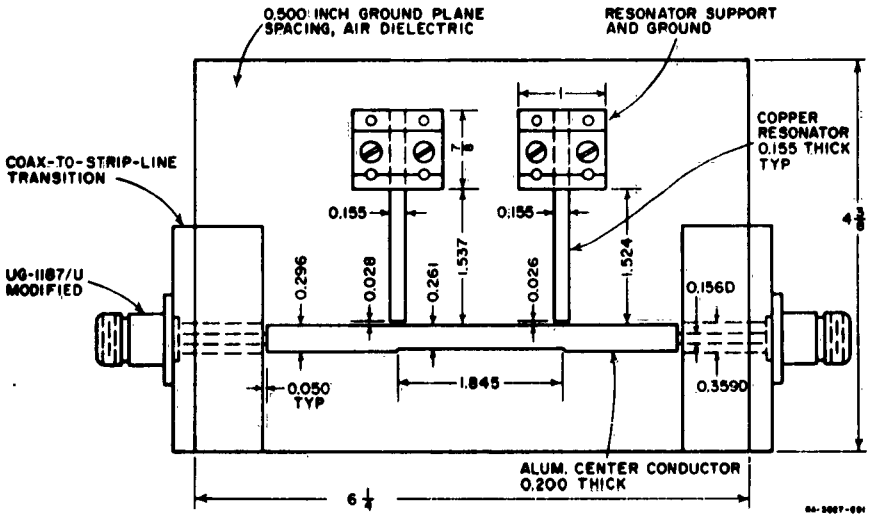

FIG. IV D-3 SKETCH OF CAPACITIVELY COUPLED NARROW-BAND FILTER WITH COVER PLATE REMOVED, SHOWING DIMENSIONS

E. DERIVATION OF THE DESIGN EQUATIONS FOR FILTER SECTIONS HAVING PARALLEL-COUPLED LINES

Design equations for symmetrical parallel-coupled band-stop filter sections of the type described in Sec. IV-B have been previously published (Ref. 7, p. 215); the equations for the unsymmetrical case are given herein. These latter equations were derived by applying the proper

terminal conditions to the general four-port consisting of two coupled transmission lines, and then solving the set of simultaneous equations obtained by expanding the matrix equation $V = IZ$ based on the 4×4 impedance matrix Z.[2] The general solution for the spur-line type filter was obtained in a similar way.

REFERENCES

1. B. M. Schiffman, P. S. Carter, Jr., and G. L. Matthaei, "Microwave Filters and Coupling Structures," Quarterly Progress Report 7, Section II, SRI Project 3527, Contract DA 36-039 SC-87398, Stanford Research Institute, Menlo Park, California (October 1962).

2. H. Ozaki and J. Ishii, "Synthesis of a Class of Strip-Line Filters," *IRE Trans. PGCT*-5, pp. 104-109 (June 1958).

3. E. M. T. Jones and J. T. Bolljahn, "Coupled-Strip-Transmission-Line Filters and Directional Couplers," *IRE Trans. PGMTT*-4, 2, pp. 75-81 (April 1956).

4. Leo Young, G. L. Matthaei, and E. M. T. Jones, "Microwave Band-Stop Filters with Narrow Stop Bands," *IRE Trans. PGMTT*-10, 6, pp. 416-427 (November 1962).

5. P. S. Carter, Jr., Leo Young, G. L. Matthaei, and E. M. T. Jones, "Microwave Filters and Coupling Structures," Quarterly Progress Report 3, SRI Project 3527, Contract DA 36-039 SC 87398, Stanford Research Institute, Menlo Park, California (October 1961).

6. Leo Young and G. L. Matthaei, "Microwave Filters and Coupling Structures," Quarterly Progress Report 4, SRI Project 3527, Contract DA 36-039 SC-87398, Stanford Research Institute, Menlo Park, California (January 1962).

7. G. L. Matthaei, Leo Young, and E. M. T. Jones, *Design of Microwave Filters, Impedance Matching Networks, and Coupling Structures*, Vol. 1, pp. 170-193, a book prepared on SRI Project 3527, Contract DA 36-039 SC 87398, Stanford Research Institute, Menlo Park, California (January 1963).

8. W. J. Getsinger, "Coupled Rectangular Bars Between Parallel Plates," *IRE Trans. PGMTT*-10, pp. 65-72 (January 1962).

V MULTIPLEXERS

A. GENERAL

Theory of the design of comb-line multiplexers having contiguous channels, a three-channel multiplexer trial design, and the calculated transducer loss per channel of the trial multiplexer design are discussed in Ref. 1, Secs. III-E and F. The design of Sec. III-F (Ref. 1), except for two minor changes,* was used as a prototype for a UHF three-channel comb-line multiplexer that is discussed in this report. The construction and illustrations of important components of the UHF three-channel comb-line multiplexer are described in Sec. V-C of this report. The tuning of the filters of the multiplexer and the staggering of the center frequencies of the filters is reported in Sec. V-D. Section V-E discusses the theory of designing multiplexers having guard-bands between channels.

B. THREE-CHANNEL COMB-LINE MULTIPLEXER RESPONSE

A photograph of the completed three-channel comb-line multiplexer is given in Fig. V B-1. The view is that seen when looking obliquely at the top of the multiplexer. The common input may be seen in the center of the photograph; the three remaining type-*N* connectors visible in the photograph are the output connectors of the three comb-line filters. Four resonator fine-tune screws are also visible on the top ground plane of each comb-line filter. The susceptance-annulling network cannot be seen in this particular view of the multiplexer.

The multiplexer attenuation, after final tuning and adjusting of the annulling network for an optimum response, is given in Fig. V B-2. Figure V B-3 gives the multiplexer attenuation in the pass-band using an expanded ordinate. The attenuation in the pass-band of the lower- and middle-frequency channels is typically 0.5 db. The attenuation in the pass-band of the highest-frequency channel is less by approximately 0.1 to 0.2 db. The VSWR of the multiplexer (measured at the common input) is shown in Fig. V B-4 and is less than 1.6 throughout the pass-band except at the multiplexer band edges.

* The normalized slope parameter, b_1/Y_A, was changed to 0.918 in order to optimize the resonator Q's. Y_B and Y_A were made equal to 0.02 mho.

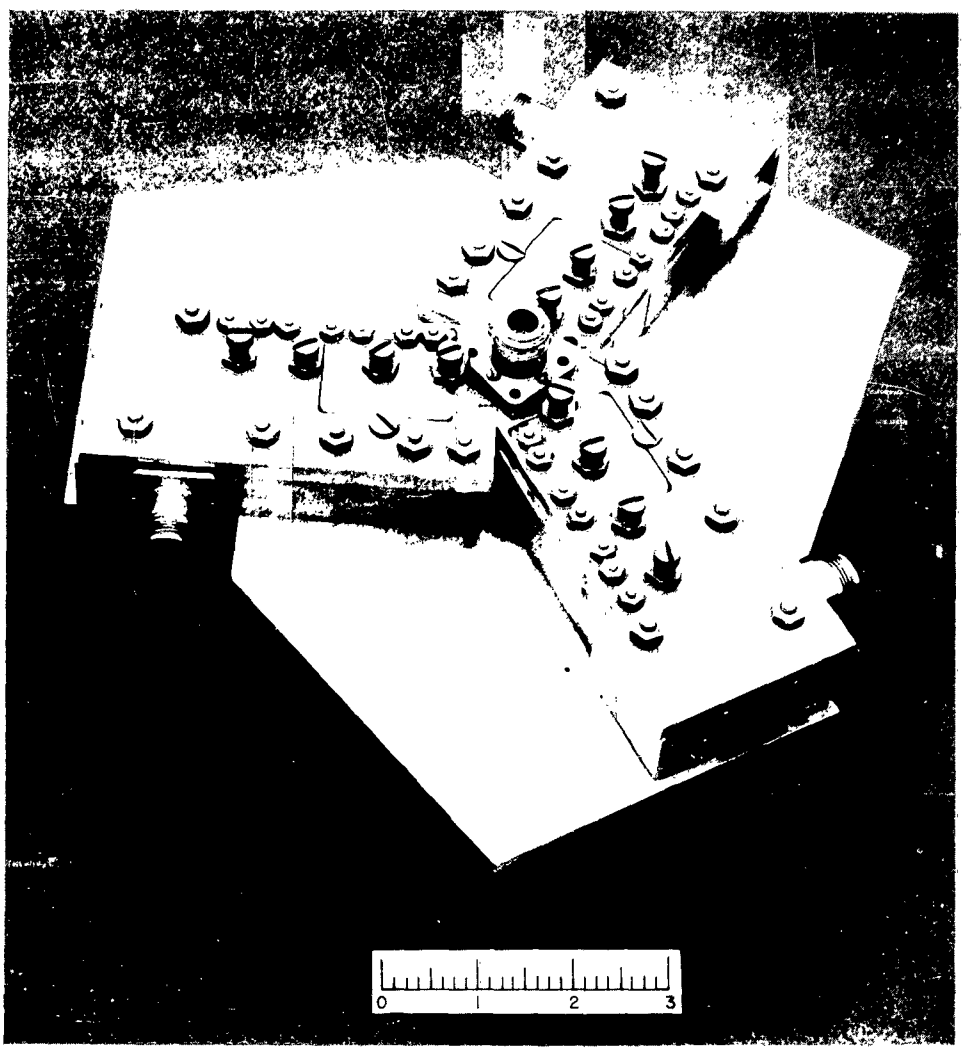

FIG. V B-1 PHOTOGRAPH OF THE THREE-CHANNEL COMB-LINE MULTIPLEXER

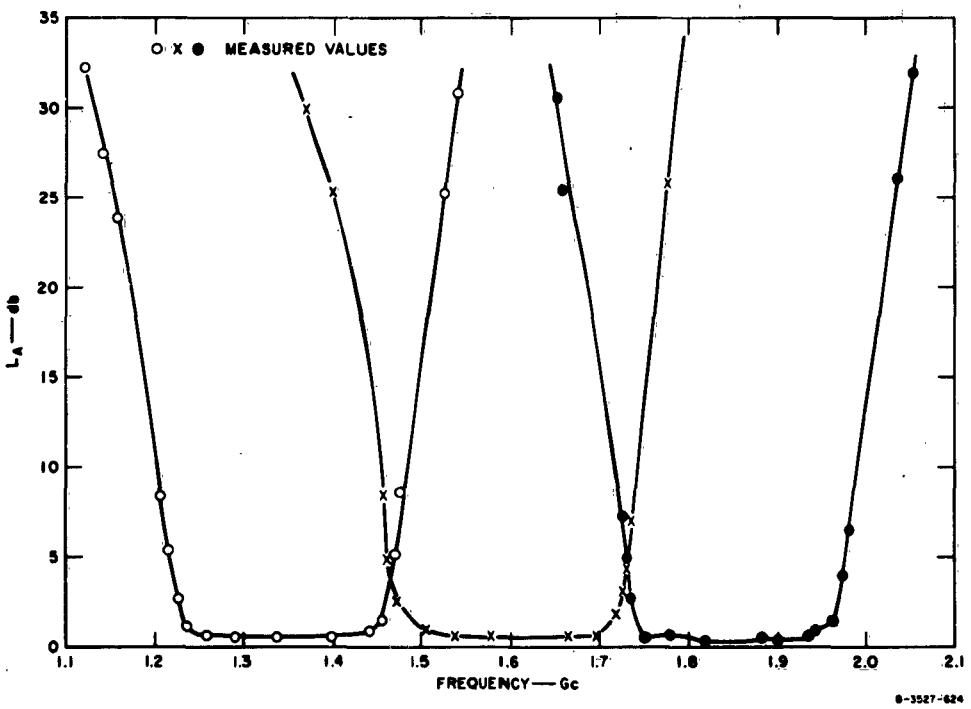

FIG. V B-2 ATTENUATION OF THE THREE-CHANNEL COMB-LINE MULTIPLEXER

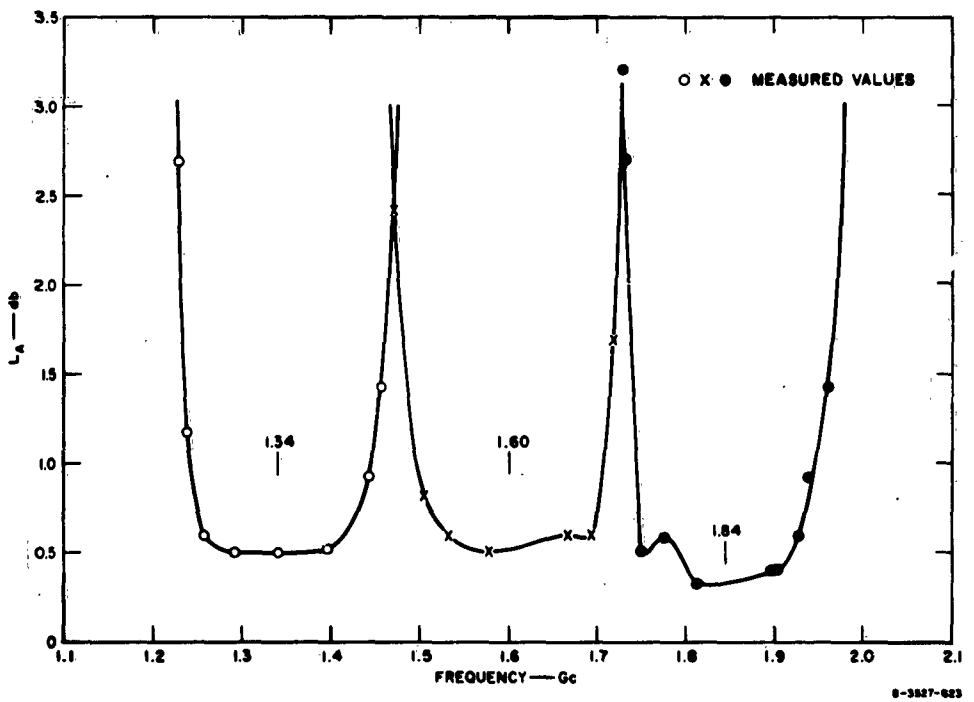

FIG. V B-3 ATTENUATION IN THE PASS BAND OF THE THREE-CHANNEL COMB-LINE MULTIPLEXER

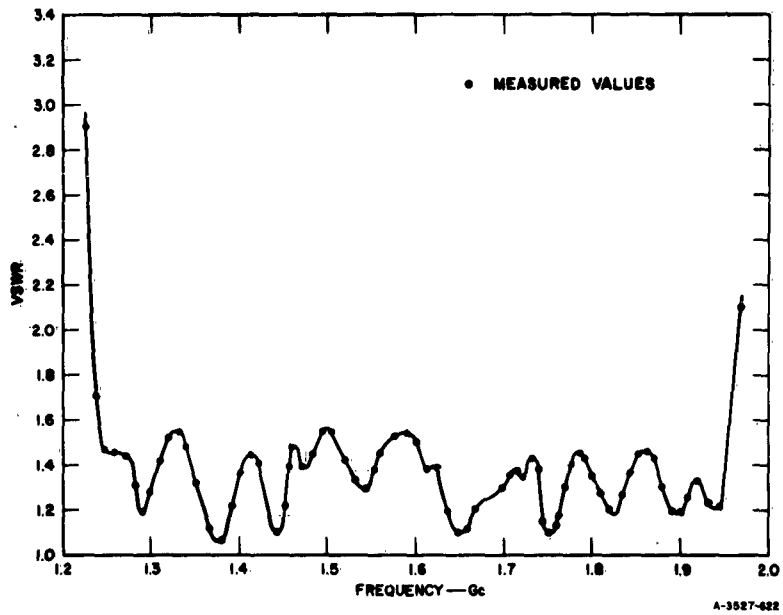

FIG. V B-4 VSWR IN THE PASS-BAND OF THE THREE-CHANNEL COMB-LINE MULTIPLEXER

The 3-db percentage bandwidths of each channel, defined as the difference of the frequencies at which the attenuation is 3 db, divided by the arithemetic mean of those frequencies, were determined and found to be 17, 16, and 13 percent for the lowest-, middle-, and highest-frequency channels, respectively. These percentages are larger than the corresponding values of the prototype multiplexer whose channel 3-db percentage bandwidths were found to be each 11 percent. Bandwidth spreading in actual filters relative to the design prototype has been noted before.[2] However, in the case of a comb-line filter having a design bandwidth of 10 percent, the bandwidth spreading was less than in the present cases. Bandwidth spreading is believed to be due to coupling effects beyond nearest neighboring line elements, which were neglected in the derivation of the design equations for comb-line filters.

C. CONSTRUCTION OF THE THREE-CHANNEL COMB-LINE MULTIPLEXER

The basic comb-line filter configuration is shown in Fig. V C-1. The mutual and self capacitances of the resonators, the lumped-capacitance resonator loadings, and the impedances of the large Z_0 coupling wires were calculated using the formulas of Table III E-1, Ref. 1. The relative spacings and dimensions of the resonators of the comb filters were determined using the design graphs of Getsinger.[3] The dimensions of the resonator widths and spacings in Fig. V C-1 are those independent of frequency, while the lengths of the resonators, coupling wires, and output coupling bars, denoted by L, s, and ℓ, respectively, depend on the center frequencies of the filters and are therefore tabulated in Table V C-1. Also in Table V C-1 are the AWG wire sizes of the large Z_0 coupling wires, the design center frequencies, and the experimentally measured center frequencies of the filters of the multiplexer. The deviation of the measured center frequencies from the design values results from the bandwidth spreading discussed in Sec. V-B.

A sketch of the top view of the multiplexer is given in Fig. V C-2, in which one of the filters is shown with its cover plate removed. The filters are arranged at approximately 120 degree intervals about a common coaxial line input and are electrically coupled to the common input by a direct connection of the large-Z_0 coupling wires to the inner conductor of the coaxial line. The common coaxial line is located at the center of the multiplexer by means of a permanently situated triangular section of

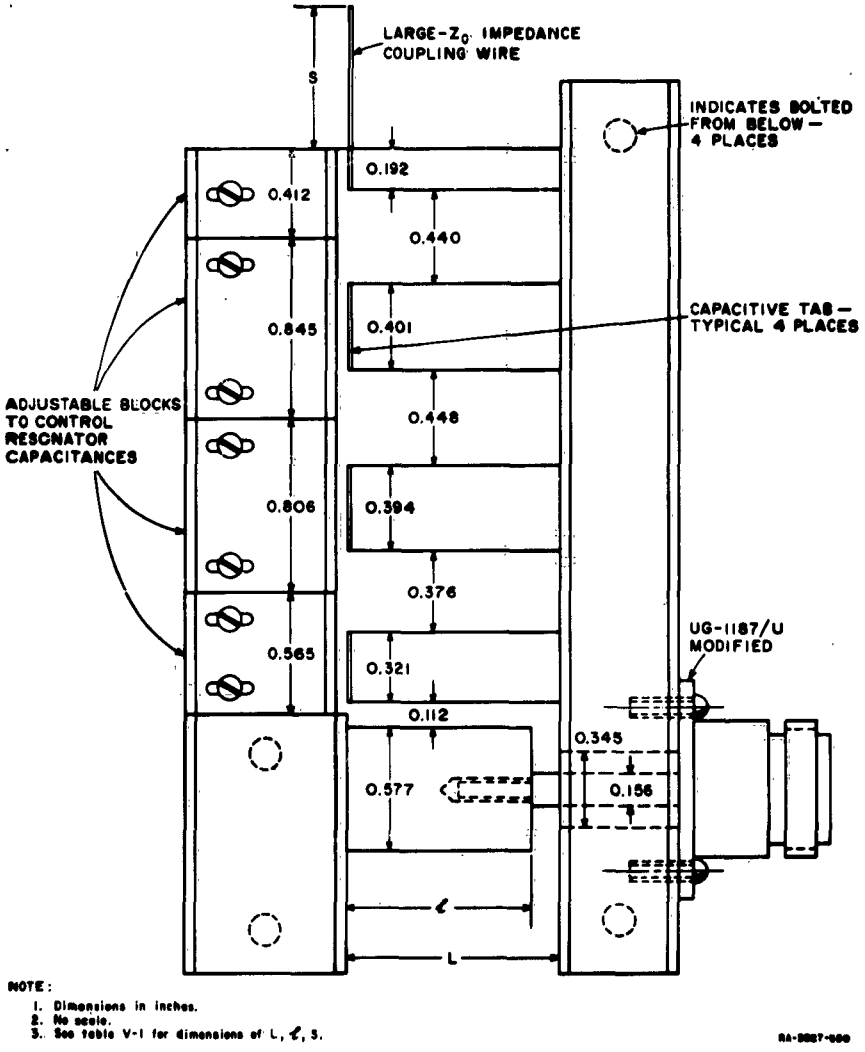

FIG. V C-1 BASIC COMB-LINE FILTER CONFIGURATION SHOWING IMPORTANT DIMENSIONS

Table V C-1

DATA FOR THREE-CHANNEL COMB-LINE MULTIPLEXER

FILTER	DESIGN CENTER FREQUENCY (Gc)	MEASURED CENTER* FREQUENCY (Gc)	L, RESONATOR LENGTH (in.)	ℓ_4 OUTPUT COUPLING BAR LENGTH (in.)	s, LARGE-Z_0 COUPLING WIRE LENGTH (in.)	LARGE-Z_0 COUPLING WIRE AWG WIRE SIZE
Low-Frequency Channel	1.50	1.34	0.983	0.863	0.655	No. 38 (3.96 mils)
Middle-Frequency Channel	1.67	1.60	0.882	0.738	0.580	No. 44 (2.00 mils)
High-Frequency Channel	1.86	1.85	0.791	0.674	0.527	No. 41 (2.75 mils)

* The measured center frequencies differ from the design center frequencies because of bandwidth spreading, which is discussed in Sec. V-B.

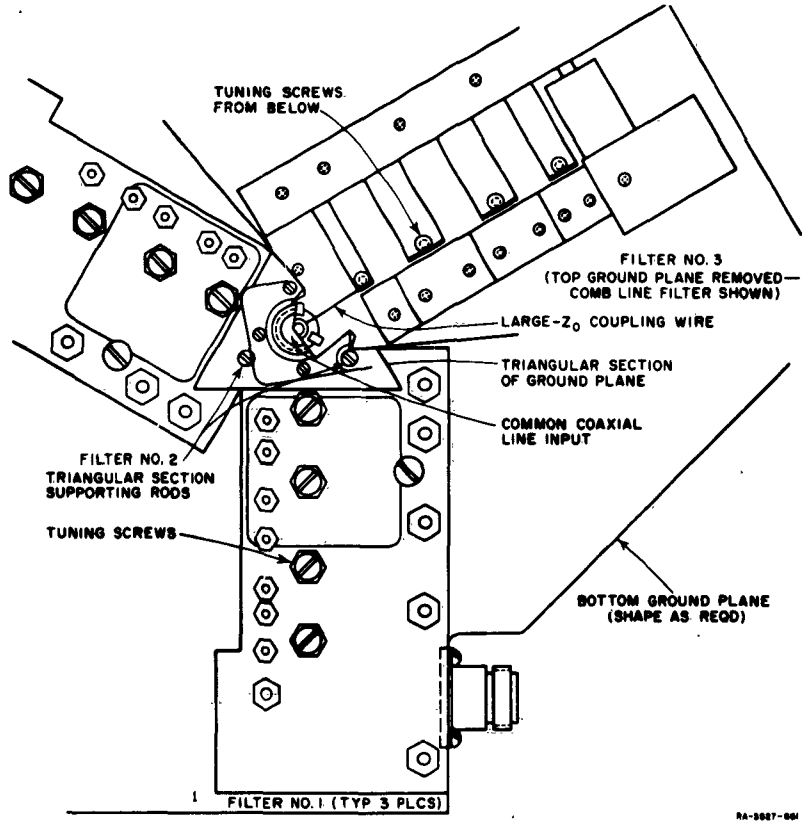

FIG. V C-2 SKETCH OF THE TOP VIEW OF THE THREE-CHANNEL COMB-LINE MULTIPLEXER SHOWING ONE OF THE COMB-LINE FILTERS WITH ITS COVER PLATE REMOVED

ground plane (visible in Figs. V B-1 and V C-2). Use of the triangular plate permits the removal of any filter cover plate without disturbing the common junction or the other filters. Three small, circular cylindrical rods connect the triangular section of ground plane to the bottom ground plane.

A detailed view of the common junction with the annulling network is given in Fig. V C-3. The center conductor of the common coaxial line is slightly longer than the outer conductor and is terminated in a small disc in which very small holes are drilled in order to facilitate soldering the coupling wire to the inner conductor. The inner conductor of the annulling stub screws into the inner conductor of the common input line. The annulling stub inner conductor is rounded at the junction end to provide clearance for the coupling wire and also to decrease the junction capacitance. The outer conductor of the annulling stub (see Fig. V C-4 for a drawing of the outer conductor of the annulling stub) fits into three longitudinal slots of the outer conductor of the common coaxial line input. Good electrical contact between the outer conductor of the annulling stub and both the bottom ground plane and the outer conductor of the common coaxial line is assured by the locking plug which screws into the bottom ground plane. This design of the common junction (Fig. V C-3) permits minimum distance, and almost symmetrical paths to both ground planes for the currents flowing in the inner wall of the outer conductor of the common coaxial line. The electrical length of the annulling stub is varied by moving the sliding short, while the admittance is varied by changing the diameter of the inner conductor.

D. TUNING THE MULTIPLEXER

The filters of the multiplexer were tuned using the alternating short-circuit and open-circuit procedure discussed by Dishal[4] and described in its application to the comb-line filter in Ref. 2. First, the large-Z_0 coupling wires of the lowest- and middle-frequency channels were disconnected from the common input while the highest-frequency channel of the multiplexer was tuned. During the tuning the inner conductor of the annulling stub was removed from the common junction. However, the outer conductor of the annulling stub was left intact in order to provide a minimum-distance path to the bottom ground plane for currents on the inner surface of the outer conductor of the common coaxial line input.

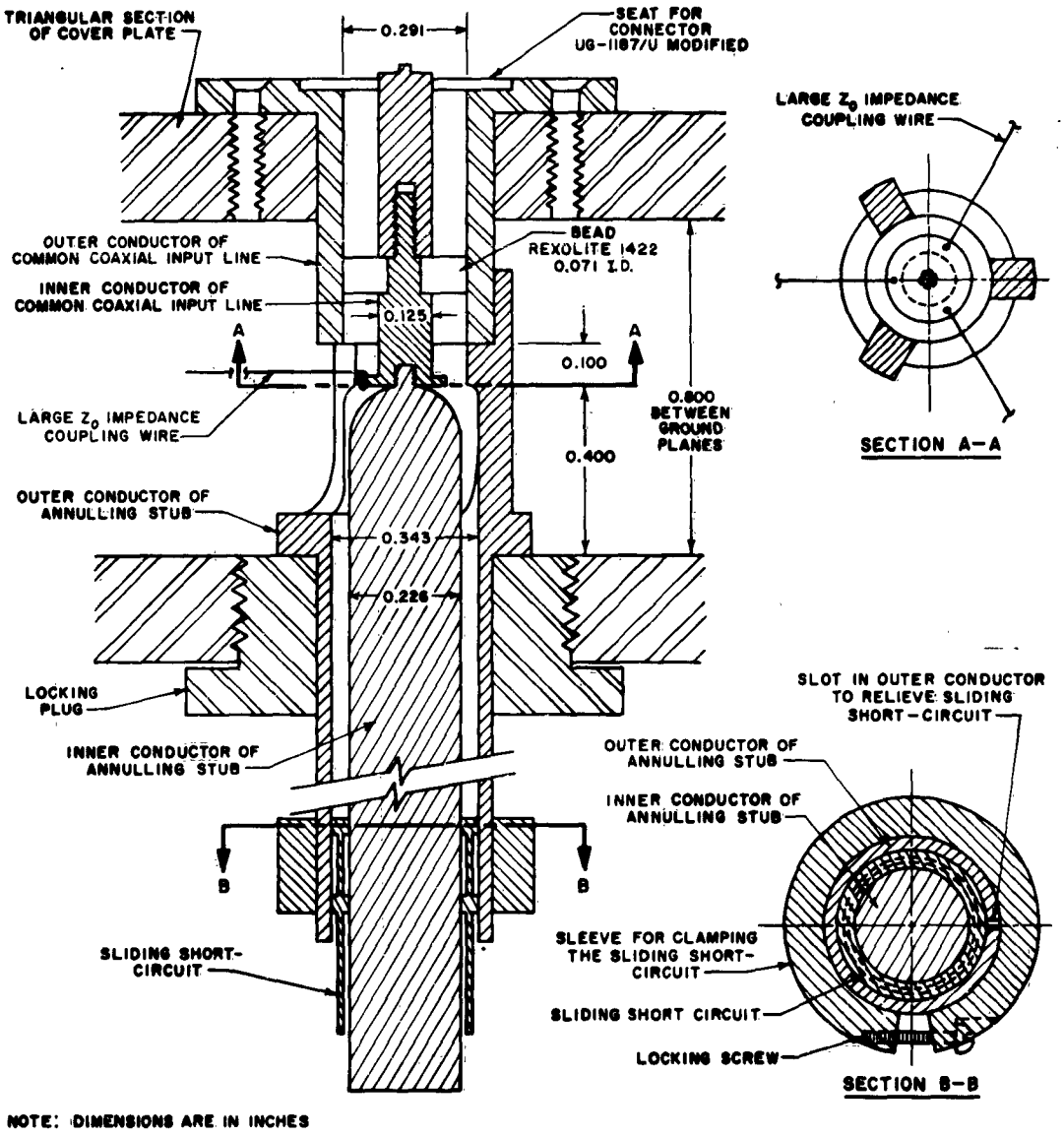

FIG. V C-3 DETAILED DRAWING OF THE COMMON JUNCTION

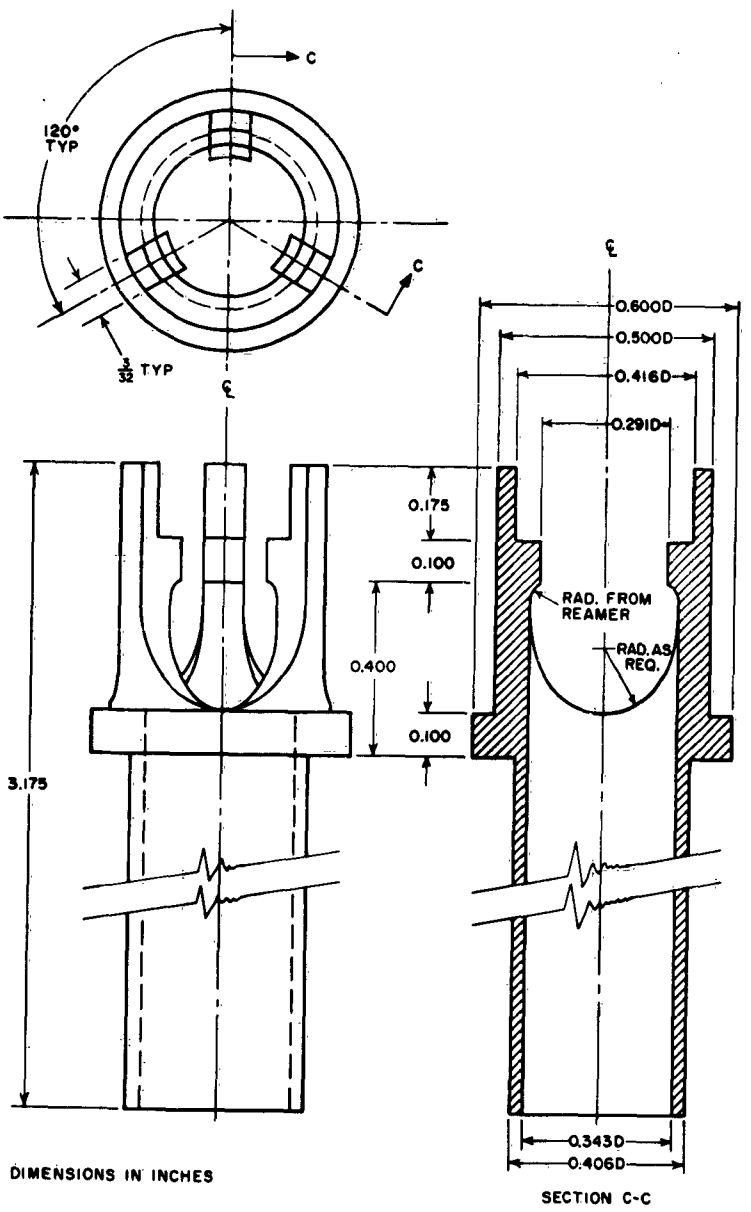

FIG. V C-4 DETAILED DRAWING OF THE ANNULLING STUB OUTER CONDUCTOR

After the highest-frequency channel was tuned, a load was placed on the output of that channel (the other channels remained decoupled during this time) and the reflection coefficient was observed on an oscilloscope using a reflectometer and an electronically swept signal generator. The reflection-coefficient trace on the oscilloscope was adjusted to the proper shape by varying only the tuning screws of the resonator to which the large-Z_0 coupling wire was attached. In this case the coupling of the end resonator was much different from the other resonators, and the bandwidth of the filter was sufficiently large so that the alternating short-circuit and open-circuit procedure did not give entirely satisfactory results in the pass-band response. However, it was known from the experience of tuning the comb-line filter described in Ref. 2 that this could be corrected by readjusting the tuning screws of the end resonator. Next, the attenuation of the highest-frequency channel was recorded using a pen recorder and a mechnically swept signal generator. Several frequencies at various points on the attenuation curve were then determined using a wave meter. From this data the band spreading and percentage bandwidth were calculated.

Using the data of the highest-frequency channel as a guide, the center frequency of the middle-frequency channel was computed such that the crossover of the attenuation curves of the middle- and highest-frequency channels would be at 4 db. A value of 4 rather than 3 db was used to allow for the effect of the susceptance-annulling network, which was to be added after all channels were tuned. It is this fact--*i.e.*, that the filters of the multiplexer must be tuned individually because of interaction, and the annulling network be added to the multiplexer only after all the filters are tuned--that makes tuning the multiplexer relatively complicated.

After the highest-frequency channel was tuned, its coupling wire was disconnected and then the middle-frequency channel was tuned using the same procedure. The center frequency of the middle-frequency channel had to be shifted and the filter retuned several times in order to obtain the proper crossover point in the attenuation curves. It was found that the middle-frequency channel had slightly more bandwidth spreading than the highest-frequency channel, so that the center frequency of the middle-frequency channel had to be decreased from the original calculated value.

Repeating the above procedure, the lowest-frequency channel was next tuned. The location of its center frequency was also found to be critical, and the filter was re-tuned several times in order to obtain the proper crossover.

During the testing of the three channels for VSWR and attenuation, several changes were made in the sizes of the various coupling wires in order to adjust the impedance levels of the three filters. The final values for the sizes of the large-Z_0 coupling wires are given in Table V C-1.

Next, the center conductor of the annulling stub was added, loads were placed on all channels, and all coupling wires were connected to the common coaxial-line input. A reflectometer was connected to the common input and the reflection coefficient was observed on an oscilloscope using an electronically swept signal generator whose sweep-width exceeded the multiplexer bandwidth. The sliding short-circuit of the annulling stub was positioned for an optimum response, and final adjustments of the tuning screws of the resonators to which the coupling wires were attached were made. Several times during the final adjustments the diameter of the inner conductor of the annulling stub was decreased slightly to further reduce the multiplexer susceptance. The fine tuning and susceptance annulling adjustments were stopped upon obtaining the response given in Figs. V B-2 and V B-3.

E. MULTIPLEXERS WITH GUARD-BANDS BETWEEN CHANNELS

The design of multiplexers having guard-bands between channels, rather than contiguous channels, differs primarily in the design of the susceptance-annulling network. It has been shown[1] that the susceptance in the pass-band of a multiplexer with contiguous channels may be partially cancelled by a properly designed annulling network. This is possible because (assuming the filters of the multiplexer to be designed from singly-terminated prototypes) the susceptance takes a somewhat monotonic form in the pass-band, going from capacitive to inductive near the center frequency of the multiplexer, and therefore is of a form that may be partially annulled by a properly designed resonant circuit. If the channels of the multiplexer are not contiguous, however, the susceptance assumes a much different form and, therefore, the susceptance-annulling network requires a different design.

For example, the admittance of a hypothetical multiplexer, using 1.0-db Tchebyscheff ripple, singly-terminated filters, is shown in Fig. V E-1. The frequency scale of Fig. V E-1 has been normalized with respect to ω_0, the center frequency in radians per second of the lowest-frequency channel. The admittance has been normalized so that the minimum

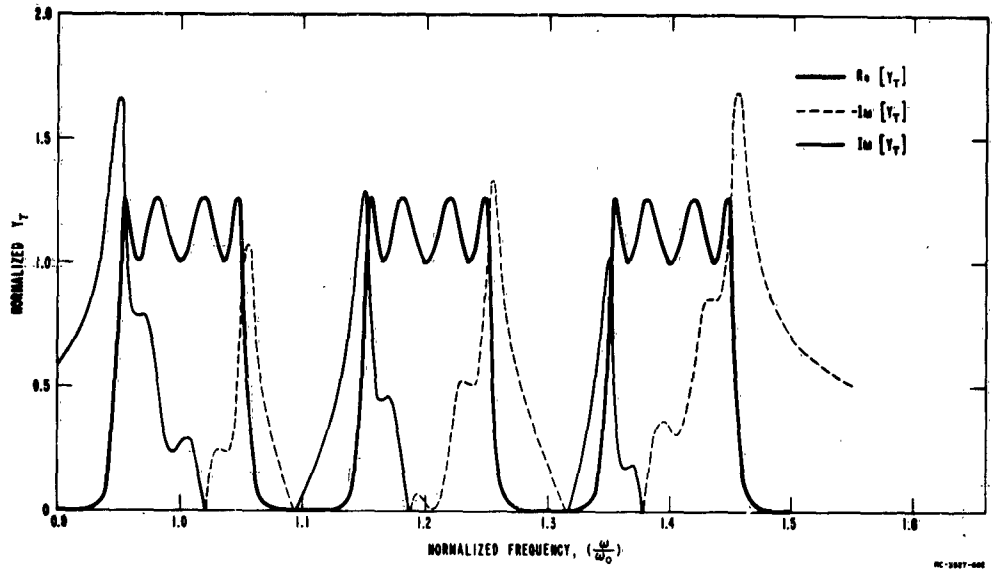

FIG. V E-1 ADMITTANCE OF A HYPOTHETICAL MULTIPLEXER USING 1.0-db CHEBYSHEV RIPPLE, SINGLY-TERMINATED FILTERS

value of its real part in the pass-band is 1.0. The multiplexer channels each have normalized bandwidths of $W = 0.1$, where W is the bandwidth in radians per second normalized with respect to the center frequency of the lowest-frequency channel. The normalized guard-bands are each 0.1. The susceptance of the multiplexer in the region of each of its channels resembles closely that of an individual filter in the absence of the others. This is because the guard-band is sufficiently large to limit significant contributions of susceptance from the other channels. If the guard-band were increased from its present value, the susceptance of the multiplexer (in the vicinity of each of its channels) would resemble still closer that of a given filter acting in the absence of the others. In that instance the design of the susceptance-annulling network is made easier. (The reasons are discussed in succeeding paragraphs.) On the other hand, if the guard-band were decreased, the susceptance of the other channels would contribute significantly to the total susceptance of the multiplexer (at a given frequency) and the form of the susceptance would depart appreciably from that of Fig. V E-1. In that instance, annulling the multiplexer susceptance in its pass-bands may be very difficult.

In the example of Fig. V E-1 the susceptance may be reduced by using an open-circuit transmission line as the annulling network. Because of the guard-bands, it is necessary to use a transmission line several wavelengths long at the multiplexer pass-band frequencies. Depending on the frequencies of operation and the guard-band width, this may be accomplished conveniently by using an open-circuited stub immersed in a dielectric which has a large relative dielectric constant. In the example of Fig. V E-1, the susceptance was reduced by adding to it the susceptance of an open-circuit transmission line having a normalized characteristic admittance of 1.427, and which was 2.5 wavelengths long at $\omega/\omega_0 = 1.0$. The resulting admittance is given in Fig. V E-2. Because we are using a hypothetical ideal lossless transmission line, there are poles of susceptance at the normalized frequencies 0.9, 1.1, 1.3, etc. Note that the susceptance is generally reduced but retains two large peaks in the pass-bands of the lowest- and highest-frequency channels.

One reason for this result is the fact that the contributions of susceptance from other channels have shifted the zeros of the susceptance of the three channels. Note that in Fig. V E-1 there are susceptance zeros

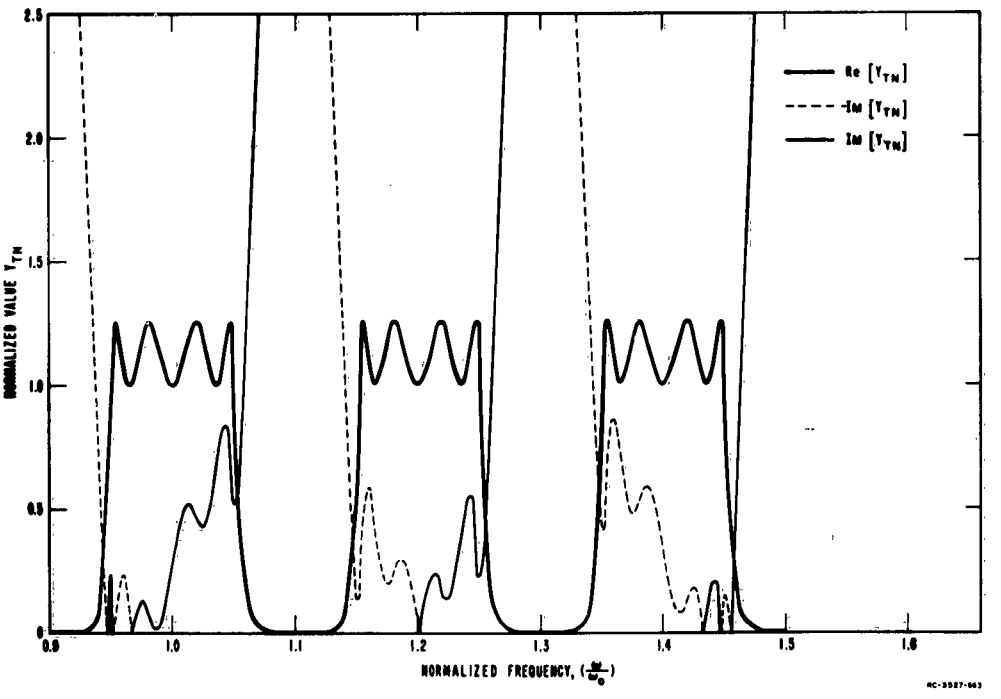

FIG. V E-2 ADMITTANCE OF HYPOTHETICAL MULTIPLEXER WITH ANNULLING STUB

at 1.02, 1.185, and 1.378 rather that at 1.0, 1.2, and 1.4, which would be their locations had there been no susceptance contributions from other channels. Important also, is that the frequency difference between susceptance zeros is 0.165 and 0.193 rather than 0.2. Thus, because the poles of the annulling stub repeat at a fixed frequency interval (0.2 in our example), it should be expected that the annulling of the multiplexer susceptance in its pass-bands will not be completely satisfactory.

The driving source was assumed to have an internal normalized admittance of 1.13 mho (the mean value of the real part of the multiplexer admittance in the pass-bands), and the values of input admittance were used as given in Fig. V E-2, to calculate the multiplexer attenuation. The result is given in Fig. V E-3. In the pass-bands of the three channels the attenuation is typically less than 0.3 db. However, in the low- and high-frequency channels the attenuation does rise to approximately 0.6 db because of insufficient reduction of susceptance in the pass-bands of these channels.

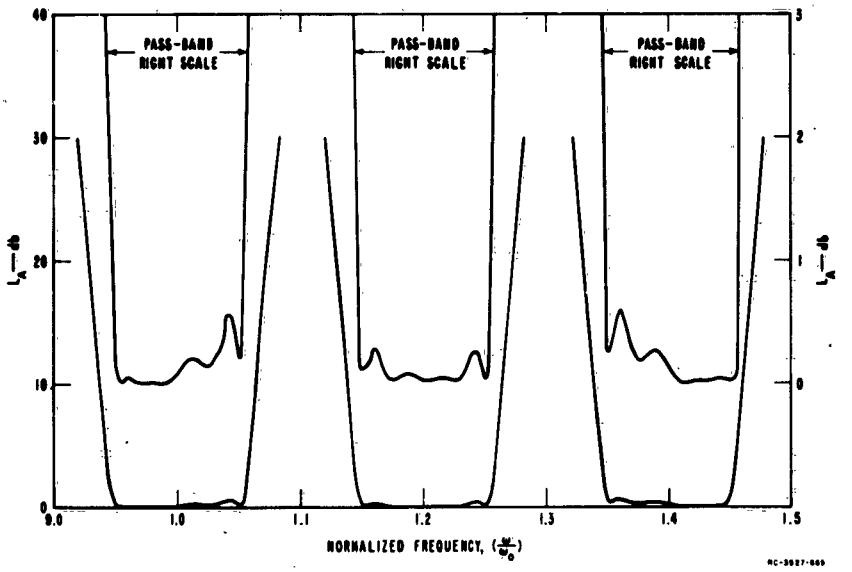

FIG. V E-3 ATTENUATION OF HYPOTHETICAL MULTIPLEXER WITH ANNULLING STUB

F. SUSCEPTANCE FORMULA FOR AN IDEAL MULTIPLEXER WITH GUARD-BANDS

In the investigation of designing multiplexers having contiguous channels,[1] Bode's integral formula[5] relating real and imaginary parts of passive admittances of minimum susceptance type was applied to the real part of the admittance of a hypothetical multiplexer. The normalized real part of the multiplexer admittance was supposed to be unity in the pass-band and zero outside. The analytical expression for the susceptance that resulted from Bode's formula was useful for sketching quickly the susceptance, and, particularly, for estimating the parameters of the anulling network.

We will generalize the expression of Ref. 1, which relates the real and imaginary parts of the hypothetical multiplexer having contiguous channels, to account for the case of an N-channel multiplexer with guard-bands between channels. The bandwidth of the N channels of the multiplexer may vary as well as the guard-band widths, so that the expression to be stated is general and includes the formula for contiguous channels as a special case.

A graph of the normalized real part of the input admittance of the hypothetical multiplexer with guard-bands between channels is given in Fig. V F-1. There are N channels with guard-bands between channels. The first channel begins at ω_1 and ends at ω_2. The second channel begins at ω_3 and ends at ω_4, and so on. For each channel the normalized real part of the admittance is unity in the pass-band and zero outside.

For all ω, the expression for the susceptance is

$$B(\omega) = \frac{1}{\pi} \ln \left| \frac{(\omega+\omega_1)(\omega-\omega_2)(\omega+\omega_3)(\omega-\omega_4) \ \ldots \ (\omega+\omega_{N-1})(\omega-\omega_N)}{(\omega-\omega_1)(\omega+\omega_2)(\omega-\omega_3)(\omega+\omega_4) \ \ldots \ (\omega-\omega_{N-1})(\omega+\omega_N)} \right| . \qquad \text{(V-F-1)}$$

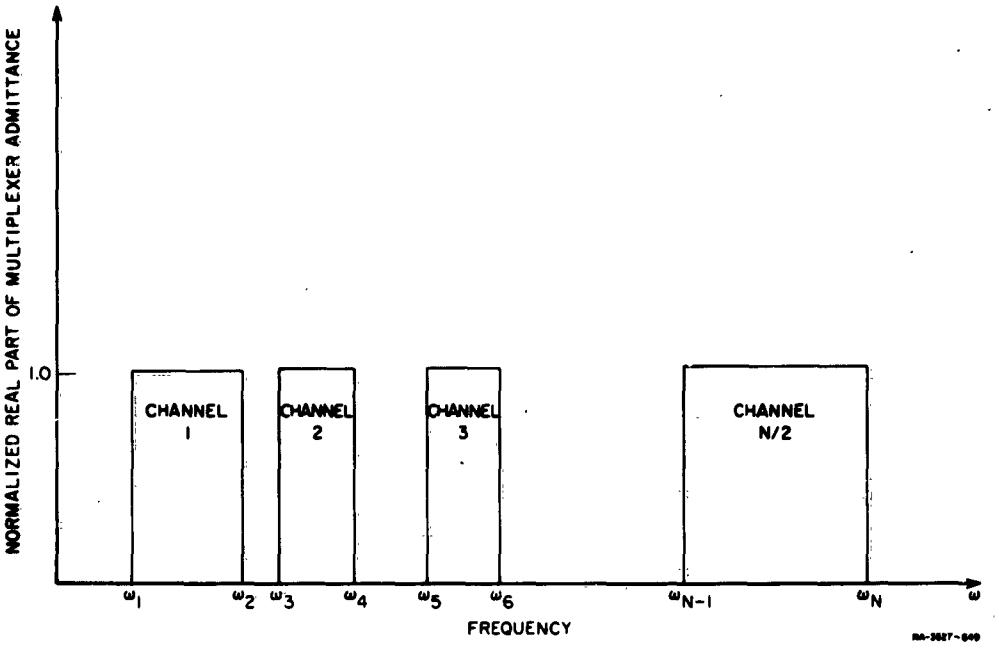

FIG. V F-1 NORMALIZED REAL PART OF THE ADMITTANCE OF A HYPOTHETICAL MULTIPLEXER WITH GUARD-BANDS BETWEEN CHANNELS

REFERENCES

1. W. J. Getsinger, E. G. Cristal and G. L. Matthaei, "Microwave Filters and Coupling Structures," Sixth Quarterly Progress Report SRI Project 3527, Contract DA-36039 SC-97398, Stanford Research Institute, Menlo Park, Calif. (August 1962).

2. G. L. Matthaei, L. Young, and P. S. Carter, Jr., "Microwave Filters and Coupling Structures," Fifth Quarterly Progress Report SRI Project 3527, Contract DA-36-039 SC-97398, Stanford Research Institute, Menlo Park, Calif. (May 1962).

3. W. G. Getsinger, G. L. Matthaei, "Microwave Filters and Coupling Structures," Second Quarterly Progress Report SRI Project 3527, Contract DA-36-039 SC-97398, Stanford Research Institute, Menlo Park, Calif. (July 1961).

4. M. Dishal, "Alignment and Adjustment of Synchronously Tuned Multiple-Resonator-Circuit Filters," *Proc. IRE* **39**, pp. 1448-1455 (November 1951).

5. H. Bode, *Network Analysis and Feedback Amplifier Design*, p. 335, (D. Van Nostrand Company, Inc., New York, N.Y., 1945).

VI. WIDEBAND INTERDIGITAL FILTERS WITH CAPACITIVELY LOADED RESONATORS

A. GENERAL

Some interdigital structures suitable for use as band-pass filters have been discussed in Sec. III of Quarterly Progress Report 4.[1] As described there, the coupled-line elements are short-circuited at one end and open-circuited at the other end, and were $\lambda/4$ long at the center frequency in the pass-band. In the filters to be considered in this section, the coupled-line elements are made less than $\lambda/4$ long at resonance, and capacitive loading to ground is added to the open-circuited end of each resonator. The specific arrangement of coupled-line elements, loading capacitances, and terminating admittances that will be considered here is illustrated in Fig. VI A-1. Note that the input and output lines are connected to loading capacitors. With this arrangement the structure will be most suitable for filters having moderate to wide bandwidths.

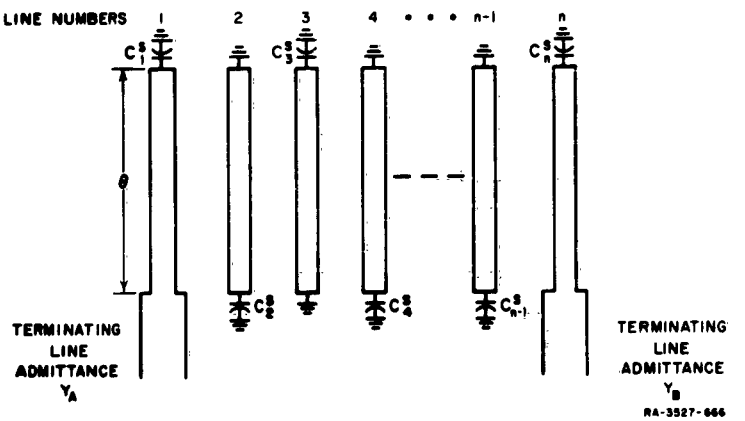

FIG. VI A-1 CAPACITIVELY LOADED INTERDIGITAL FILTER WITH UNGROUNDED END RESONATORS

These capacitively loaded interdigital filters have a number of very attractive features, including the following:

(1) They are very compact. They are even more compact in the dimension parallel to the coupled-line length than are the interdigital filters without capacitive loading. The calculated frequency response curves presented in Sec. VI-F demonstrate that capacitive loading can reduce the length of the coupled-lines by a factor of at least two.

(2) The second pass-band is centered at greater than three times the center frequency of the first pass-band. The more the resonators are shortened by capacitive loading, the higher in frequency will be the second pass-band. For example, if the resonators are $\lambda/8$ long at the center of the first pass-band, the second pass-band will be centered at between 4 and 4.5 times the center frequency of the first pass-band.

(3) The tolerances required in their manufacture are relatively relaxed as a result of the relatively large spacings between resonator elements.

(4) For a given bandwidth, number of resonators, and length of resonators, the spacing between resonators will be greater than for the comb-line filters described in Sec. II of Quarterly Progress Report 5.[2] This would be an advantage in maintaining tolerances during manufacture. This difference between capacitively loaded interdigital filters and comb-line filters becomes insignificant, however, as the resonators are made very short in terms of wavelength.

(5) The rates of cutoff and the strength of the stop-bands are enhanced by multiple-order poles of attenuation at zero frequency, and within the stop-bands above the first pass-band.

(6) These filters can be fabricated in structural forms which are self-supporting so that dielectric material need not be used. Thus, dissipation loss that would occur within the dielectric can be avoided.

If all possible couplings between the elements of an interdigital filter are taken into account, then even analysis of the filter behavior involves unwieldy mathematics. Synthesizing a structure to have a prescribed response would be even more difficult; thus it does not appear practical to attempt to devise an exact synthesis procedure. The synthesis procedure given here involves a number of simplifying approximations that permit straightforward, easy-to-use design calculations. Although the design formulas are approximate, the calculated frequency response presented in Sec. VI-E indicates that usable designs can be obtained for many practical applications.

For the benefit of readers who have filter design requirements but who are not particularly interested in filter theory as such, the design equations for capacitively loaded interdigital filters, and some calculated frequency responses, will be presented first. Readers who are also interested in the source of the design equations will find a discussion of their derivation in Sec. VI-F, and a discussion of the method of calculating frequency response in Sec. VI-G.

B. LOW-PASS PROTOTYPE FILTERS AND USE OF A LOW-PASS-TO-BAND-PASS TRANSFORMATION

The design procedures to be described are based on the use of low-pass prototype filter element values to give the band-pass filter its desired characteristics. Figures VI B-1(a), (b) show typical low-pass prototypes of the type under discussion, and they also define the manner in which the element values g_k are to be specified for the purpose of this discussion. The left side of Figs. VI B-2 and VI B-3 show typical maximally flat and Tchebyscheff responses such as can be achieved by filters of this type. Element values for prototype filters having such responses have been tabulated.[3,4] Notice that n is the number of reactive elements

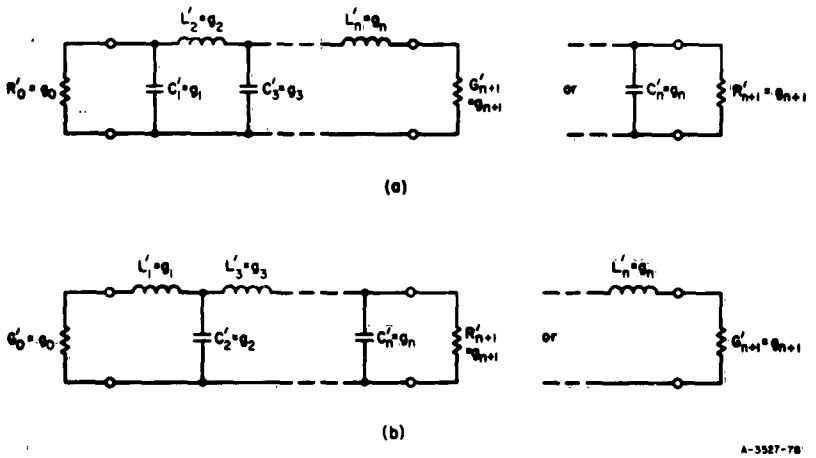

FIG. VI B-1 DEFINITION OF PROTOTYPE FILTER PARAMETERS $g_0, g_1, g_2, \cdots, g_n, g_{n+1}$. [A prototype circuit is shown at (a) and its dual is shown at (b). Either form will give the same response. An additional prototype parameter ω'_1 is defined in Figs. VI B-2 and VI B-3.]

PROTOTYPE RESPONSE

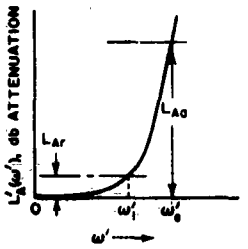

$$L'_A(\omega') = 10 \log_{10}\left[1 + \epsilon\left(\frac{\omega'}{\omega'_1}\right)^{2n}\right] \text{ db}$$

where

$$\epsilon = \text{antilog}_{10}\left(\frac{L_{Ar}}{10}\right) - 1$$

BAND-PASS FILTER RESPONSE

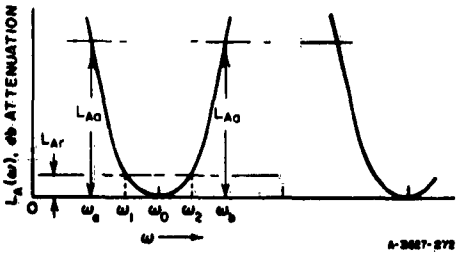

$$L_A(\omega) = L'_A(\omega') \text{ db}$$

where

$$\omega' = \frac{2\omega'_1}{w}\left|\frac{\omega - \omega_0}{\omega_0}\right|$$

$$\omega_0 = \frac{\omega_2 + \omega_1}{2}$$

and

$$w = \frac{\omega_2 - \omega_1}{\omega_0}$$

To determine n required for given values of ω_1/ω_0, L_{Ar}, ω_a/ω_0 and L_{Aa}, find smallest integer n value which satisfies

$$n \geq \frac{\log_{10}\left\{\frac{\left[\text{antilog}_{10}\left(\frac{L_{Aa}}{10}\right)\right] - 1}{\epsilon}\right\}}{2 \log_{10}\left(\frac{\omega'_a}{\omega'_1}\right)}$$

where

$$\omega'_a = \frac{2\omega'_1}{w}\left|\frac{\omega_a - \omega_0}{\omega_0}\right|$$

FIG. VI B-2 EQUATIONS AND PARAMETERS FOR MAXIMALLY FLAT RESPONSE

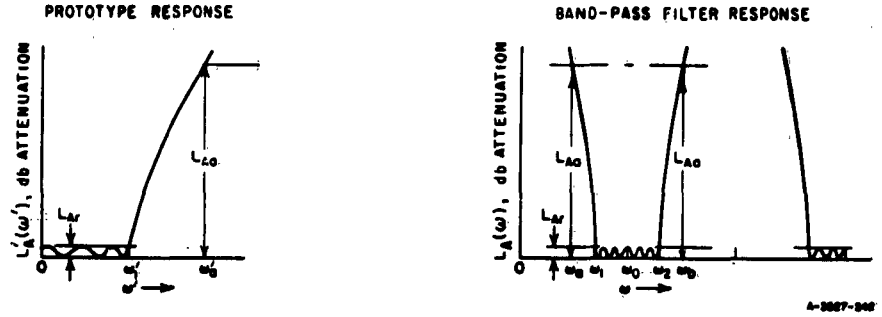

$$L'_A(\omega') = 10 \log_{10}\left\{1 + \epsilon \cos^2\left[n \cos^{-1}\left(\frac{\omega'}{\omega'_1}\right)\right]\right\} \text{ db}$$

for

$$\omega' \leq \omega'_1$$

$$L'_A(\omega') = 10 \log_{10}\left\{1 + \epsilon \cosh^2\left[n \cosh^{-1}\left(\frac{\omega'}{\omega'_1}\right)\right]\right\} \text{ db}$$

for

$$\omega' \geq \omega'_1$$

where

$$\epsilon = \left\{\left[\text{antilog}_{10}\left(\frac{L_{Ar}}{10}\right)\right] - 1\right\}$$

$$L_A(\omega) = L'_A(\omega') \text{ db}$$

where

$$\omega' = \frac{2\omega'_1}{w}\left|\frac{\omega - \omega_0}{\omega_0}\right|$$

$$\omega_0 = \frac{\omega_2 + \omega_1}{2}$$

and

$$w = \frac{\omega_2 - \omega_1}{\omega_0}$$

To determine n required for given values of ω_1/ω_0, L_{Ar}, ω_a/ω_0 and L_{Aa}, find smallest integer n value which satisfies

$$n \geq \frac{\cosh^{-1}\sqrt{\dfrac{\text{antilog}_{10}\left(\dfrac{L_{Aa}}{10}\right) - 1}{\epsilon}}}{\cosh^{-1}\left(\dfrac{\omega'_a}{\omega'_1}\right)}$$

where

$$\omega'_a = \frac{2\omega'_1}{w}\left|\frac{\omega_a - \omega_0}{\omega_0}\right|$$

FIG. VI B-3 EQUATIONS AND PARAMETERS FOR TCHEBYSCHEFF RESPONSE

and that, including the resistor terminations, the element values range from g_0 to g_{n+1}. A low-pass prototype with n reactive elements leads to a band-pass filter with n resonators.

The right sides of Figs. VI B-2 and VI B-3 show band-pass filter responses which correspond to the given low-pass prototype responses. The band-pass filter response will have the same type of pass-band characteristic as the prototype, but the width of the band-pass filter pass-band can be specified arbitrarily. Filters constructed with distributed-constant elements will also have other pass-bands centered at frequencies above ω_0. On the left sides of Figs. VI B-2 and VI B-3 will be found equations for determining the attenuation characteristic of the low-pass prototype as a function of the radian frequency variable ω', for specified ω' and n. On the right side of Figs. VI B-2 and VI B-3 will be found an approximate low-pass-to-band-pass transformation from which the attenuation characteristic of the low-pass prototype as a function of ω' can be mapped to the band-pass filter attenuation chatacteristic (centered at ω_0) as a function of the band-pass filter radian frequency variable ω. Since the attenuation is the same for both the low-pass and band-pass filters at frequencies ω' and ω, respectively, which are related as given by the mapping, the band-pass filter attenuation characteristic can be predicted by use of these data. At the bottom of Figs. VI B-2 and VI B-3 are equations for determining the value of n required in order to achieve a given amount of attenuation, L_{A_s} db, at a given frequency, ω_s.

The low-pass-to-band-pass transformation given in Figs. VI B-2 and VI B-3 is an approximate one, and is usually considered to be useful only for filters of narrow or moderate bandwidth. However, it appears to work fairly well for capacitively loaded interdigital filters even in cases of quite large bandwidth, as is verified by the nearly octave bandwidth design discussed in Sec. VI-E. One limitation of the low-pass-to-band-pass transformation is that it assumes the pass-band to have arithmetic symmetry about ω_0, whereas the capacitively loaded interdigital filters have a pass-band shape that is slightly narrower above ω_0 than below ω_0. The parameter w, which appears in the mapping equation, is the fractional bandwidth of the band-pass filter. This parameter will also be used in the filter design equations that are about to be presented. Our experience indicates that, because the design equations are based on various approximations, the actual fractional bandwidth of the filter will be about 6 to 10 percent smaller than the value of w used in the equations.

Thus, to allow for this shrinkage in bandwidth, it is suggested that a value of w which is about 6 to 10 percent larger than is actually desired be used in the design equations in Secs. VI-E. However, the actual desired value of w should be used in the mapping in Figs. VI B-2 and VI B-3.

C. PARALLEL-COUPLED LINES

As previously mentioned, interdigital filters consist of arrays of parallel lines between ground planes. The design equations for such filters to be given herein will yield the various line capacitances per unit length for the various lines in the filter array. From these values of capacitance per unit length, the actual dimensions of the lines can be determined. Definitions for these various line capacitances will now be given, and also equations for obtaining the line dimensions from the specified capacitances. In order to relate the design methods under discussion to existing design data that are extremely useful when adapted for the design of arrays of parallel lines, we will first consider the case of two unsymmetrical parallel-coupled lines. These methods will then be extended to the case of an array of parallel-coupled lines.

Case of Two Unsymmetrical Parallel-Coupled Lines--Some unsymmetrical parallel-coupled lines that are quite easy to design are shown in Fig. VI C-1. Note that the capacitance per unit length of each line has been separated into component parts. The capacitance C_p^a is the *parallel-plate* capacitance per unit length between one side of Line a and the adjacent ground plane, while C_p^b is the corresponding *parallel-plate* capacitance of Line b. The capacitance C_f' is the fringing capacitance per unit length for any of the outer corners of the strip lines. The fringing

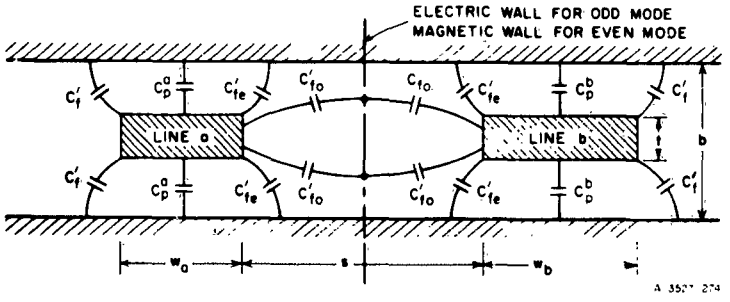

FIG. VI C-1 CROSS SECTION OF UNSYMMETRICAL, RECTANGULAR-BAR PARALLEL-COUPLED LINES

capacitances per unit length at the inner corners of each strip are designated C'_{fe} when the strips are excited in the even mode (*i.e.*, with equal voltages of the same phase); they are designated C'_{fo} when the strips are excited in the odd mode (*i.e.*, with voltages having equal amplitudes and opposite phases). Both bars have the same height, and both are assumed to be wide enough so that the interactions between the fringing fields at the right and left sides of each bar are negligible, or at least small enough to be easily corrected for. On this basis the fringing fields are the same for both bars, and their different total capacitances C_a and C_b to ground are due entirely to different parallel-plate capacitances C_p^a and C_p^b. For the structure shown in Fig. VI C-1,

$$\begin{aligned} C_a &= 2(C_p^a + C'_f + C'_{fe}) \\ C_{ab} &= (C'_{fo} - C'_{fe}) \\ C_b &= 2(C_p^b + C'_f + C'_{fe}) \quad . \end{aligned} \tag{VI C-1}$$

Getsinger[5] has derived equations for the fringing capacitances C'_{fe}, C'_{fo}, and C'_f, and has prepared convenient charts which relate C'_{fe}/ϵ, C'_{fo}/ϵ, and C'_f/ϵ to rectangular-bar strip-line dimensions. Here ϵ is the absolute dielectric constant of the medium of propagation, so that the above ratios are dimensionless and of moderate size. Getsinger gives equations for the design of *symmetrical*, parallel-coupled, rectangular strip-lines, and here we will adapt his equations to fit the unsymmetrical case.

Note that the shape of the lines in Fig. VI C-1 is fixed in terms of the dimensions t, b, s, w_a and w_b. To design a pair of lines such as those in Fig. VI C-1 so as to have specified odd- and even-mode admittances or impedances, first use equations such as those in Table VI D-1 to compute C_a/ϵ, C_{ab}/ϵ, and C_b/ϵ. Select a convenient value for line thickness t and plate spacing b, which fixes the ratio t/b. Then, noting that

$$\frac{\Delta C}{\epsilon} = \frac{C_{ab}}{\epsilon} \quad , \tag{VI C-2}$$

use Getsinger's chart[5] of $\Delta C/\epsilon$ and C'_{fe} *vs.* s/b to determine s/b, and also C'_{fe}/ϵ. Using t/b and Getsinger's chart of C'_f *vs.* t/b, determine C'_f/ϵ,

and then compute

$$\frac{w_a}{b} = \frac{1}{2}\left(1 - \frac{t}{b}\right)\left[\frac{1}{2}\left(\frac{C_a}{\epsilon}\right) - \frac{C'_{fa}}{\epsilon} - \frac{C'_f}{\epsilon}\right] \qquad \text{(VI C-3)}$$

$$\frac{w_b}{b} = \frac{1}{2}\left(1 - \frac{t}{b}\right)\left[\frac{1}{2}\left(\frac{C_b}{\epsilon}\right) - \frac{C'_{fa}}{\epsilon} - \frac{C'_f}{\epsilon}\right] \qquad \text{(VI C-4)}$$

When the ground plane spacing b is specified, the required bar widths, w_a and w_b, are determined. If either w_a/b or w_b/b is less than $0.35(1 - t/b)$, the width of the bar should be corrected using the approximate formula[5]

$$\frac{w'}{b} = \frac{0.07\left(1 - \frac{t}{b}\right) + \frac{w}{b}}{1.20} , \qquad \text{(VI C-5)}$$

provided that $0.1 < (w'/b)/(1 - t/b) < 0.35$. In Eq. (VI C-5) w is the uncorrected bar width and w' is the corrected width. The need for this correction arises because of the interaction of the fringing fields at opposite sides of a bar, which will occur when a bar is relatively narrow.

Case of an Array of Parallel-Coupled Lines--Figure VI C-2 shows an array of parallel-coupled lines such as is used in an interdigital filter. In the structure shown, all of the bars have the same t/b ratio and the other dimensions of the bars are easily obtained by generalizing the procedure just described for designing unsymmetrical parallel-coupled lines.

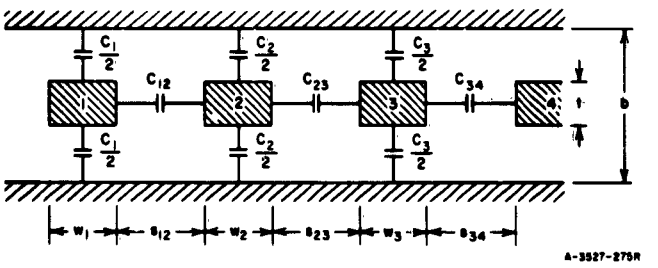

FIG. VI C-2 CROSS SECTION OF AN ARRAY OF PARALLEL-COUPLED LINES BETWEEN GROUND PLANES

In the structure in Fig. VI C-2 the electrical properties of the structure are characterized in terms of the self-capacitances, C_k, per unit length of each bar with respect to ground, and the mutual capacitances, $C_{k,k+1}$, per unit length between adjacent bars k and $k+1$. This representation is not necessarily always highly accurate; it is conceivable that a significant amount of fringing capacitance could exist between a given line element and, say, the line element beyond the nearest neighbor. However, at least for geometries such as that shown, experience has shown this representation to have satisfactory accuracy.

For design of the capacitively loaded interdigital-filter structures discussed herein, equations will be given for the normalized self and mutual capacitances, C_k/ϵ and $C_{k,k+1}/\epsilon$, per unit length for all the lines in the structure. Then the cross-sectional dimensions of the bars and spacings between them are determined as follows. First, choose values for t and b. Then, since

$$\frac{(\Delta C)_{k,k+1}}{\epsilon} = \frac{C_{k,k+1}}{\epsilon} , \qquad \text{(VI C-6)}$$

Getsinger's charts[5] can be used to determine $s_{k,k+1}/b$. In this manner, the spacings $s_{k,k+1}$ between all the bars are obtained. Also, using Getsinger's charts, the normalized fringing capacitance $(C'_{fe})_{k,k+1}/\epsilon$ associated with the gaps $s_{k,k+1}$ between bars are obtained. Then the normalized width of the kth bar is

$$\frac{w_k}{b} = \frac{1}{2}\left(1 - \frac{t}{b}\right)\left[\frac{1}{2}\left(\frac{C_k}{\epsilon}\right) - \frac{(C'_{fe})_{k-1,k}}{\epsilon} - \frac{(C'_{fe})_{k,k+1}}{\epsilon}\right] . \qquad \text{(VI C-7)}$$

In the case of the bar at the end of the array (the bar at the far left in Fig. VI C-2), C'_{fe}/ϵ for the edge of the bar that has no neighbor must be replaced by C'_f/ϵ, which is also obtained from Getsinger's charts. Thus, for example, for Bar 1 in Fig. VI C-2,

$$\frac{w_1}{b} = \frac{1}{2}\left(1 - \frac{t}{b}\right)\left[\frac{1}{2}\left(\frac{C_1}{\epsilon}\right) - \frac{C'_f}{\epsilon} - \frac{(C'_{fe})_{1,2}}{\epsilon}\right] . \qquad \text{(VI C-8)}$$

If $w_k/b < 0.35\ (1 - t/b)$ for any of the bars, the width correction given in Eq. (VI C-5) should be applied to the affected bars.

D. DESIGN EQUATIONS

The approximate design equations for the capacitively loaded interdigital filter illustrated in Fig. VI A-1 are summarized in Table VI D-1. Based on previous experience[1] with interdigital filters without loading capacitances, these design equations are thought to be most practical for filters having moderate to wide bandwidth. The calculated frequency responses presented in Sec. VI-E demonstrate that the design equations are usable for bandwidths up to an octave wide, and perhaps these design equations would be usable down to bandwidths on the order of 30 percent. These design equations are generalized to the case of unequal terminating admittances at the ends of the filter, and the lumped-element prototype on which designs are based need not be either symmetrical or antimetrical.*

To use Table VI D-1 for the design of capacitively loaded interdigital filters, first use Fig. VI B-2 or VI B-3 to estimate the number, n, of reactive elements required in the low-pass prototype in order to give the desired rate of cutoff with the desired pass-band characteristics. When the prototype cutoff frequency ω_1' and the element values g_0, g_1, ..., g_{n+1} have been obtained from tables[3,4] or by computations,[6] these values can be inserted into the equations of Table VI D-1. It is suggested that the value of filter fractional bandwidth, w, used with Eq. (1) of Table VI D-1 be 6 to 10 percent larger than is actually desired, since experience has shown that there will be some bandwidth shrinkage due to the approximate nature of the design equations. In the equations in Figs. VI B-2 and VI B-3, however, the desired value of w should be used. It is also suggested that the resonance frequency ω_0 be chosen 5 to 9 percent above the desired arithmetic average of the band-edge frequencies, since the capacitively loaded interdigital filters do not give a frequency response that has arithmetic symmetry about ω_0.

The parameters, d, h_A, and h_B are essentially admittance scale factors. For the interdigital filters without capacitive loading discussed in Quarterly Progress Report 4,[1] the frequency response of the filter did not depend on the parameters d, h_A, or h_B when dissipation loss is neglected.

* A network is antimetrical if the impedance-vs.-frequency function looking into one end of the network is the reciprocal of that looking into the other end of the network. Prototypes with resistor terminations at both ends, having either maximally flat or Tchebyscheff responses with one or more frequencies ω where zero transducer loss occurs, are either symmetrical or antimetrical.

Table VI D-1

DESIGN EQUATIONS FOR INTERDIGITAL FILTERS OF THE FORM IN FIG. VI A-1

Use the equations in Fig. VI B-2 or VI B-3 to select a low-pass prototype with the required value of $n \geq 4$. The input and output elements in this filter count as resonators, so that there are n elements for an n-reactive-element prototype. Choose $\theta_0 = 2\pi\ell/\lambda_0$ = the electrical length of the elements at the resonance wavelength λ_0 in the medium surrounding the line elements. Compute:

$$\theta_1 = \theta_0 \frac{\omega_1}{\omega_0} = \theta_0 \left(1 - \frac{w}{2}\right) \tag{1}$$

$$\frac{J_{2,3}}{Y_A} = \frac{1}{g_0}\sqrt{\frac{2g_2 d}{g_3}}, \quad \left.\frac{J_{k,k+1}}{Y_A}\right|_{k=3 \text{ to } n-3} = \frac{2g_2 d}{g_0\sqrt{g_k g_{k+1}}} \tag{2}$$

$$\frac{J_{n-2,n-1}}{Y_A} = \frac{\sqrt{h_B}}{g_0\sqrt{h_A}}\sqrt{\frac{Y_B g_0}{Y_A g_{n+1}} \cdot \frac{2g_2 d}{g_{n-2}}} \tag{3}$$

$$S = \left(1 - \frac{\omega_1}{\omega_0}\cot\theta_0 \tan\theta_1\right)^{-1}, \quad T = S\left(\frac{\omega_1}{\omega_0}\cot\theta_0 + \tan\theta_1\right) \tag{4}$$

$$\left.N_{k,k+1}\right|_{k=2 \text{ to } n-2} = \sqrt{\left(\frac{J_{k,k+1}}{Y_A}\right)^2\left[1 - \left(\frac{\cos\theta_0}{\cos\theta_1}\right)^2\right] + \left(\frac{\omega_1' g_2 d \tan\theta_1}{g_0}\right)^2} \tag{5}$$

$$\frac{Z_1}{Z_A} = \omega_1' g_0 g_1 T \tag{6}$$

$$\frac{Y_2}{Y_A} = h_A\left[\frac{\omega_1' g_2 (1-d) S \tan\theta_1}{g_0} + SN_{2,3} - \frac{J_{2,3}}{Y_A}\sin\theta_0\right] \tag{7}$$

$$\left.\frac{Y_k}{Y_A}\right|_{k=3 \text{ to } n-2} = h_A\left[(N_{k-1,k} + N_{k,k+1})S - \left(\frac{J_{k-1,k}}{Y_A} + \frac{J_{k,k+1}}{Y_A}\right)\sin\theta_0\right] \tag{8}$$

$$\frac{Y_{n-1}}{Y_A} = h_A\left[\frac{\omega_1' g_2 S \tan\theta_1}{g_0}\left(\frac{g_0 g_{n-1}}{g_2 g_{n+1}} - d\right) + SN_{n-2,n-1} - \frac{J_{n-2,n-1}}{Y_A}\sin\theta_0\right] \tag{9}$$

Table VI D-1 (*continued*)

$$\frac{Z_B}{Z_A} = \omega_1' g_n g_{n+1} T\left(\frac{Y_A}{Y_B}\right) \tag{10}$$

$$\left.\frac{Y_{k,k+1}}{Y_A}\right|_{k=2 \text{ to } n=2} = \frac{J_{k,k+1}}{Y_A} h_A \sin\theta_0 \quad . \tag{11}$$

The normalized self-capacitances per unit length for the coupled-line elements are:

$$\frac{C_1}{\epsilon} = \frac{376.7}{\sqrt{\epsilon_r}} Y_A \frac{1 - \sqrt{h_A}}{(Z_1/Z_A)} \tag{12}$$

$$\frac{C_2}{\epsilon} = \frac{376.7}{\sqrt{\epsilon_r}} Y_A\left(\frac{Y_2}{Y_A}\right) - \sqrt{h_A}\,\frac{C_1}{\epsilon} \tag{13}$$

$$\left.\frac{C_k}{\epsilon}\right|_{k=3 \text{ to } n-2} = \frac{376.7}{\sqrt{\epsilon_r}} Y_A\left(\frac{Y_k}{Y_A}\right) \tag{14}$$

$$\frac{C_{n-1}}{\epsilon} = \frac{376.7}{\sqrt{\epsilon_r}} Y_A\left(\frac{Y_{n-1}}{Y_A}\right) - \sqrt{h_B}\,\frac{C_n}{\epsilon} \tag{15}$$

$$\frac{C_n}{\epsilon} = \frac{376.7}{\sqrt{\epsilon_r}} Y_A \frac{1 - \sqrt{h_B}}{(Z_n/Z_A)} \tag{16}$$

where ϵ and ϵ_r are the absolute and relative dielectric constants, respectively, of the medium surrounding the resonator line elements. The d, h_A, and h_B are dimensionless admittance scale factors whose values should be chosen to give a convenient admittance level in the filter (see text).

The normalized mutual capacitances per unit length between adjacent coupled-line elements are:

$$\frac{C_{1,2}}{\epsilon} = \frac{376.7}{\sqrt{\epsilon_r}} Y_A \frac{\sqrt{h_A}}{(Z_1/Z_A)} \tag{17}$$

$$\left.\frac{C_{k,k+1}}{\epsilon}\right|_{k=2 \text{ to } n-2} = \frac{376.7}{\sqrt{\epsilon_r}} Y_A\left(\frac{Y_{k,k+1}}{Y_A}\right) \tag{18}$$

$$\frac{C_{n-1,n}}{\epsilon} = \frac{376.7}{\sqrt{\epsilon_r}} Y_A \frac{\sqrt{h_B}}{(Z_n/Z_A)} \quad . \tag{19}$$

Table VI D-1 (*concluded*)

The lumped loading capacitances are:

$$C_1^s = \frac{Y_A \cot \theta_0}{\omega_0 (Z_1/Z_A)} \tag{20}$$

$$C_2^s = \frac{Y_A \cot \theta_0}{\omega_0} \left(\frac{Y_2}{Y_A} + \frac{Y_{2,3}}{Y_A} \right) \tag{21}$$

$$C_k^s \Big|_{k=3 \text{ to } n-2} = \frac{Y_A \cot \theta_0}{\omega_0} \left(\frac{Y_k}{Y_A} + \frac{Y_{k-1,k}}{Y_A} + \frac{Y_{k,k+1}}{Y_A} \right) \tag{22}$$

$$C_{n-1}^s = \frac{Y_A \cot \theta_0}{\omega_0} \left(\frac{Y_{n-1}}{Y_A} + \frac{Y_{n-2,n-1}}{Y_A} \right) \tag{23}$$

$$C_n^s = \frac{Y_A \cot \theta_0}{\omega_0 (Z_n/Z_A)} \tag{24}$$

where the resonance frequency, ω_0, is in radians per second, admittances are in mhos, and impedances are in ohms to give capacitances in farads.

For the capacitively loaded interdigital filters, however, the value of d influences the amplitude of the ripples in the pass-band.* The calculated frequency responses presented in Sec. VI-E indicate that d should be between 0.5 and 1.0 for octave-bandwidth filters, with a value of $d = 0.65$ giving best results. The choice of d is not extremely critical, however, and the optimum value can readily be determined by a few trial designs. That is, values are assumed for d, h_A, and h_B, and if the resulting frequency response is not satisfactory, another value of d is tried.

* For the design equations presented in Table III E-1 of Quarterly Progress Report 4,[1] d has been set equal to 0.5. A single parameter $h = h_A = h_B$ appears in Quarterly Progress Report 4, since equal terminating admittances were assumed in that report. The h-parameter was also introduced in Quarterly Progress Report 4 at a different stage in the derivation of the equations. Except for these differences, the design equations presented here in Table VI D-1 reduce to those in Table III E-1 of Quarterly Progress Report 4 for the case of no capacitive loading.

The prime consideration in the choice of the admittance scale factors h_A and h_B is that the dimensions of the coupled lines be such that the resonators have high unloaded Q in order that dissipation loss be low. The dimensions that optimize the unloaded Q of interdigital filters are not known. For air-filled coaxial-line resonators, however, it is known that a characteristic impedance of 76 ohms gives the highest unloaded Q. Various approximate studies suggest that the optimum impedance for stripline resonators of nearly square cross section, such as are shown in Fig. VI C-2, is not greatly different than 76 ohms. Thus, it is suggested that h_A and h_B be chosen such that Eq. (VI D-1) is satisfied (at least when air dielectric is used):

$$\left.\frac{2C_{k-1,k}}{\epsilon} + \frac{C_k}{\epsilon} + \frac{2C_{k,k+1}}{\epsilon}\right|_{\substack{k=n/2 \text{ for } n \text{ even} \\ =(n+1)/2 \text{ for } n \text{ odd}}} \approx 5.4. \qquad \text{(VI D-1)}$$

Equation (VI D-1) corresponds to making the coupled-line impedance 70 ohms for the resonators in the center of the filter, under the conditions that the adjacent lines are excited with voltages of equal amplitude but of opposite phase (this is a generalized odd-mode admittance condition). The trial designs mentioned above for determining the best value of d will also provide values of odd-mode admittance at the filter center for a given combination of d, h_A, and h_B. The parameters h_A and h_B can then be adjusted to satisfy Eq. (VI D-1).

Once values for d, h_A, and h_B have been determined, the remaining calculations to determine the capacitances per unit length of the line elements, C_k/ϵ and $C_{k,k+1}/\epsilon$ are straightforward. From these capacitances, the line dimensions are determined as discussed in Sec. VI-C. The lumped loading capacitances at the ends of the resonators can be constructed in many configurations, such as those in Fig. VI D-1. Each configuration would require estimates of the fringing fields in order to determine the dimensions for the loading capacitances. Data for estimating the fringing fields associated with the loading capacitances are available in other works.[5,7-11] Since the estimates of fringing capacitances will be approximate, tuning screws should be incorporated into the first model of a given filter to trim the loading capacitances. It is anticipated that the fringing capacitances associated with Fig. VI D-1(c) will be discussed in a future report on Contract DA 36-039-AMC-00084(E), after a capacitively loaded filter is constructed and tested.

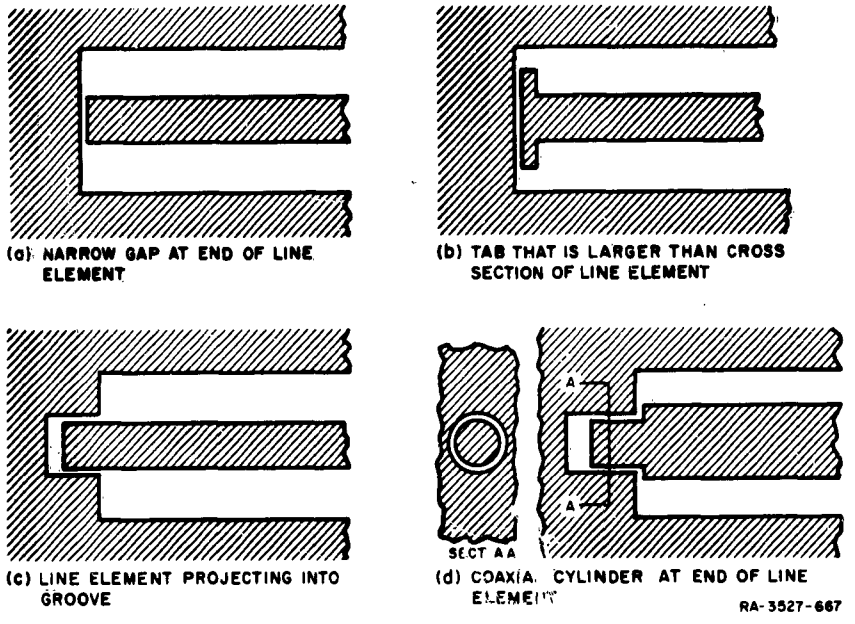

FIG. VI D-1 VARIOUS CONFIGURATIONS FOR LOADING CAPACITANCES AT ENDS OF LINE ELEMENTS

E. CALCULATED FREQUENCY RESPONSES

Some trial designs for capacitively loaded interdigital filters have been worked out using an $n = 8$ reactive-element, Tchebyscheff prototype with ripple amplitude $L_{Ar} = 0.10$ db. The element values for this prototype are $g_0 = 1$, $g_1 = 1.1897$, $g_2 = 1.4346$, $g_3 = 2.1199$, $g_4 = 1.6010$, $g_5 = 2.1699$, $g_6 = 1.5640$, $g_7 = 1.9444$, $g_8 = 0.8778$, $g_9 = 1.3554$, and $\omega_1' = 1$. The line elements were chosen $\lambda/8$ long at the resonance frequency ω_0, so $\theta_0 = \pi/4$. The ratio ω_1/ω_0 was chosen equal to 0.65, which would give 2.08-to-1.0 bandwidth if the frequency response had arithmetic symmetry about ω_0. Equal terminating admittances $Y_A = Y_B = 0.02$ mho were used, and the admittance scale factors $h_A = h_B = 0.18$ were chosen to be the same as an interdigital filter without capacitive loading whose measured performance was presented in Sec. III-E of Quarterly Progress Report 4.[1] The relative dielectric constant, ϵ_r, was set equal to unity. The parameter d was given the values 0.25, 0.5, 0.65, and 1.0, and the resulting filter parameters calculated by Table VI D-1 are summarized in Tables VI E-1 through VI E-4, respectively.

Table VI E-1

LINE-ELEMENT PARAMETERS FOR AN OCTAVE-BANDWIDTH, CAPACITIVELY LOADED INTERDIGITAL FILTER WITH ADMITTANCE-SCALING PARAMETER $d = 0.25$

k	$\frac{C_{k,k+1}}{\epsilon}$	$\frac{Y_{k,k+1}}{Y_A}$	k	$\frac{C_k}{\epsilon}$	$\omega_0 C_k^s$ mho	$\frac{Y_k}{Y_A}$
1 and 7	1.412	---	1 and 8	1.916	0.00884	---
2 and 6	0.558	0.0740	2 and 7	0.758	0.00565	0.2085
3 and 5	0.373	0.0496	3 and 6	0.560	0.00396	0.0744
4	0.369	0.0490	4 and 5	0.550	0.00343	0.0729

$$\frac{Z_1}{Z_A} = \frac{Z_8}{Z_A} = 2.264 \quad , \qquad \frac{376.7/\sqrt{\epsilon_r}}{2\frac{C_{3,4}}{\epsilon} + \frac{C_4}{\epsilon} + 2\frac{C_{4,5}}{\epsilon}} = 186 \text{ ohms}$$

Table VI E-2

LINE-ELEMENT PARAMETERS FOR AN OCTAVE-BANDWIDTH, CAPACITIVELY LOADED INTERDIGITAL FILTER WITH ADMITTANCE-SCALING PARAMETER $d = 0.50$

k	$\frac{C_{k,k+1}}{\epsilon}$	$\frac{Y_{k,k+1}}{Y_A}$	k	$\frac{C_k}{\epsilon}$	$\omega_0 C_k^s$ mho	$\frac{Y_k}{Y_A}$
1 and 7	1.412	---	1 and 8	1.916	0.00884	---
2 and 6	0.789	0.1047	2 and 7	0.593	0.00583	0.1866
3 and 5	0.747	0.0991	3 and 6	1.098	0.00699	0.1458
4	0.738	0.0980	4 and 5	1.099	0.00686	0.1459

$$\frac{Z_1}{Z_A} = \frac{Z_8}{Z_A} = 2.264 \quad , \qquad \frac{376.7/\sqrt{\epsilon_r}}{2\frac{C_{3,4}}{\epsilon} + \frac{C_4}{\epsilon} + 2\frac{C_{4,5}}{\epsilon}} = 93 \text{ ohms}$$

Table VI E-3

LINE-ELEMENT PARAMETERS FOR AN OCTAVE-BANDWIDTH, CAPACITIVELY LOADED INTERDIGITAL FILTER WITH ADMITTANCE-SCALING PARAMETER $d = 0.65$

k	$\frac{C_{k,k+1}}{\epsilon}$	$\frac{Y_{k,k+1}}{Y_A}$	k	$\frac{C_k}{\epsilon}$	$\omega_0 C_k^s$ mho	$\frac{Y_k}{Y_A}$
1 and 7	1.412	---	1 and 8	1.916	0.00884	---
2 and 6	0.899	0.1194	2 and 7	0.504	0.00588	0.1748
3 and 5	0.971	0.1289	3 and 6	1.431	0.00876	0.1900
4	0.960	0.1274	4 and 5	1.429	0.00892	0.1896

$$\frac{Z_1}{Z_A} = \frac{Z_8}{Z_A} = 2.264 \quad , \qquad \frac{376.7/\sqrt{\epsilon_r}}{2\frac{C_{3,4}}{\epsilon} + \frac{C_4}{\epsilon} + 2\frac{C_{4,5}}{\epsilon}} = 71 \text{ ohms}$$

Table VI E-4

LINE-ELEMENT PARAMETERS FOR AN OCTAVE-BANDWIDTH, CAPACITIVELY LOADED INTERDIGITAL FILTER WITH ADMITTANCE-SCALING PARAMETER $d = 1.00$

k	$\frac{C_{k,k+1}}{\epsilon}$	$\frac{Y_{k,k+1}}{Y_A}$	k	$\frac{C_k}{\epsilon}$	$\omega_0 C_k^e$, mho	$\frac{Y_k}{Y_A}$
1 and 7	1.412	--	1 and 8	1.916	0.00884	--
2 and 6	1.116	0.1481	2 and 7	0.318	0.00596	0.1501
3 and 5	1.493	0.1982	3 and 6	2.230	0.01285	0.2960
4	1.476	0.1959	4 and 5	2.198	0.01372	0.2918

$$\frac{Z_1}{Z_A} = \frac{Z_8}{Z_A} = 2.264 \quad , \quad \frac{376.7/\sqrt{\epsilon_r}}{2\frac{C_{3,4}}{\epsilon} + \frac{C_4}{\epsilon} + 2\frac{C_{4,5}}{\epsilon}} = 46 \text{ ohms}$$

The capacitances in Table VI E-1 through VI E-4 could be used to determine physical dimensions for use in constructing the filters, as was explained in Secs. VI-C and VI-D. The admittances listed in Tables VI E-1 through VI E-4 are useful for calculating the frequency response of each filter, as is explained in Sec VI-G.

For each of the filter designs presented in the paragraph above, the transducer loss has been calculated as a function of frequency. These calculations are based on open-wire-line equivalent circuits of the filters, as is discussed in Sec. VI-G. Dissipation loss was neglected. Figures VI E-1 through VI E-4 show the frequency response for $d = 0.25$, 0.50, 0.65, and 1.0, respectively. Taking $d = 0.65$ seems about the best choice, since this value keeps all the ripples below 0.35 db. However, the value of d is not critical; the highest ripples for $d = 0.50$ and 1.0 are 0.4 db and 0.5 db, respectively.

If an exact synthesis procedure had been followed, these eight-resonator filters would be capable of producing an equal-ripple response with eight frequencies of zero transducer loss, neglecting the effects of dissipation loss. The fact that these filters do not duplicate the 0.1-db, equal-ripple characteristics of the low-pass prototype from which these were designed, is a result of the approximations made in derivation of the design equations. The approximate synthesis procedure gives best control of the frequency response at the resonance frequency, ω_0, and at the lower-band-edge frequency, ω_1. Note that Figs. VI E-1 through VI E-4 have exactly 0.10 db tranaducer loss at ω_0, and the lower edge of each pass-band is near the specified value of 0.65 ω_0. If the frequency response had arithmetic

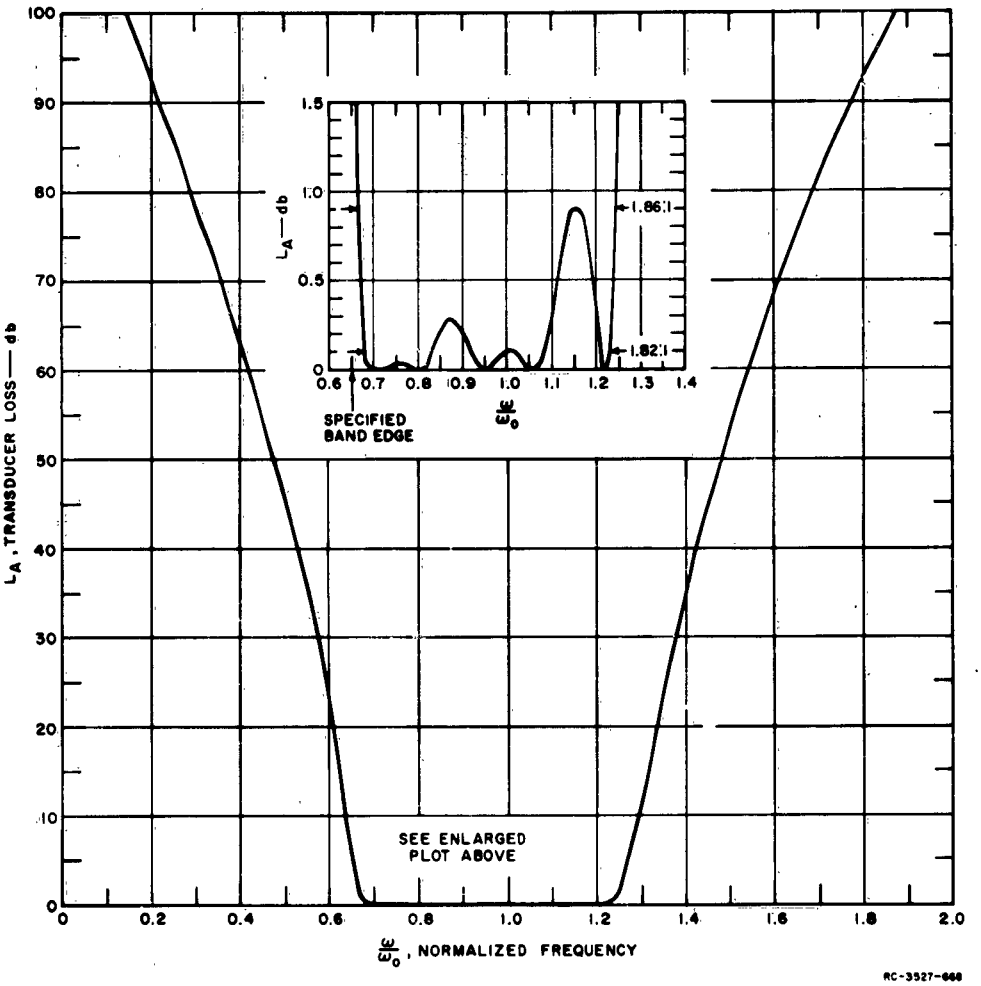

FIG. VI E-1 FREQUENCY RESPONSE OF A CAPACITIVELY LOADED INTERDIGITAL FILTER DESIGNED WITH ADMITTANCE-SCALING PARAMETER d = 0.25

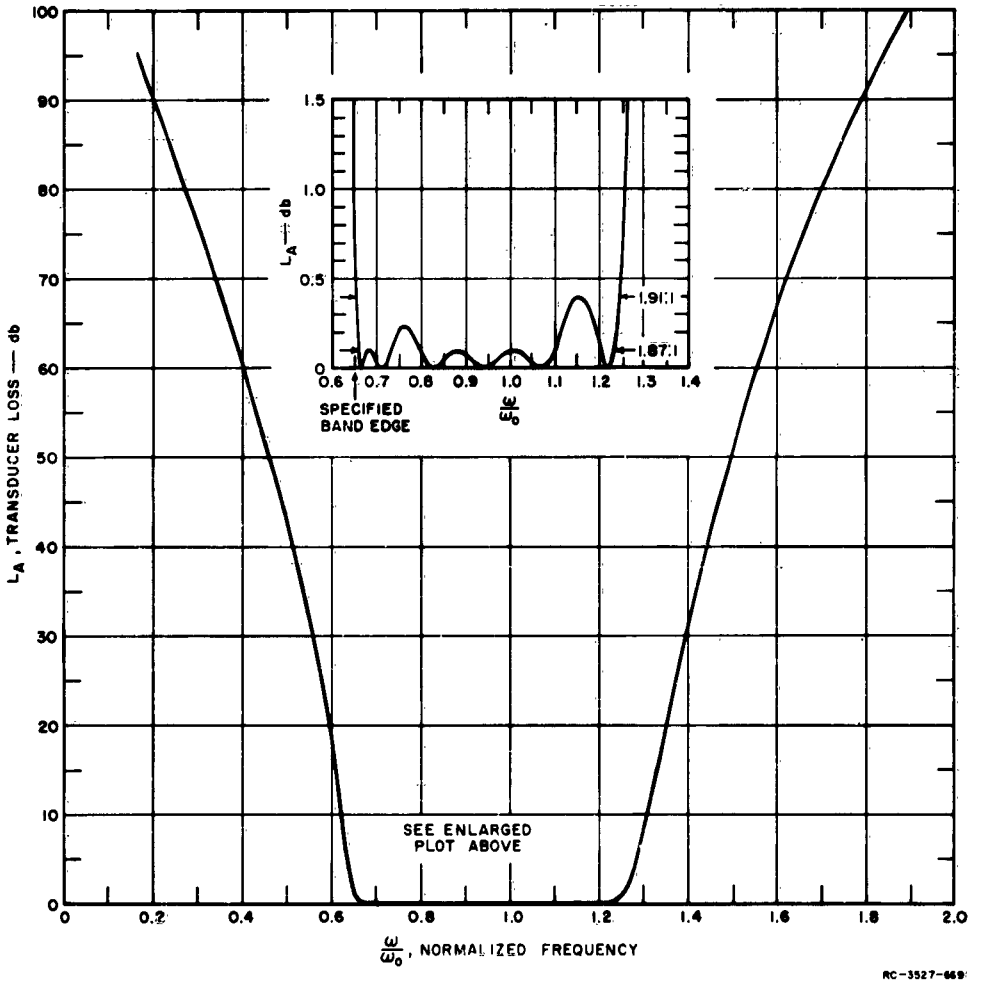

FIG. VI E-2 FREQUENCY RESPONSE OF A CAPACITIVELY LOADED INTERDIGITAL FILTER DESIGNED WITH ADMITTANCE-SCALING PARAMETER d = 0.50

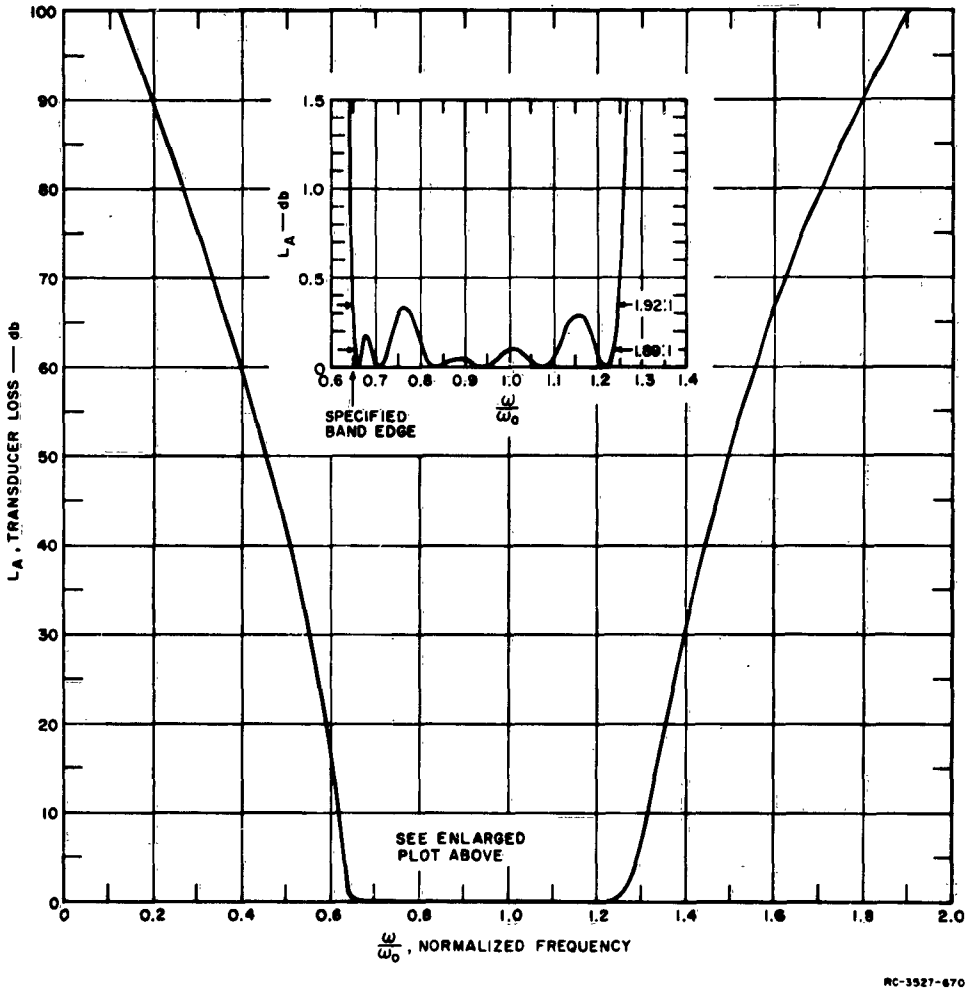

FIG. VI E-3 FREQUENCY RESPONSE OF A CAPACITIVELY LOADED INTERDIGITAL FILTER DESIGNED WITH ADMITTANCE-SCALING PARAMETER d = 0.65

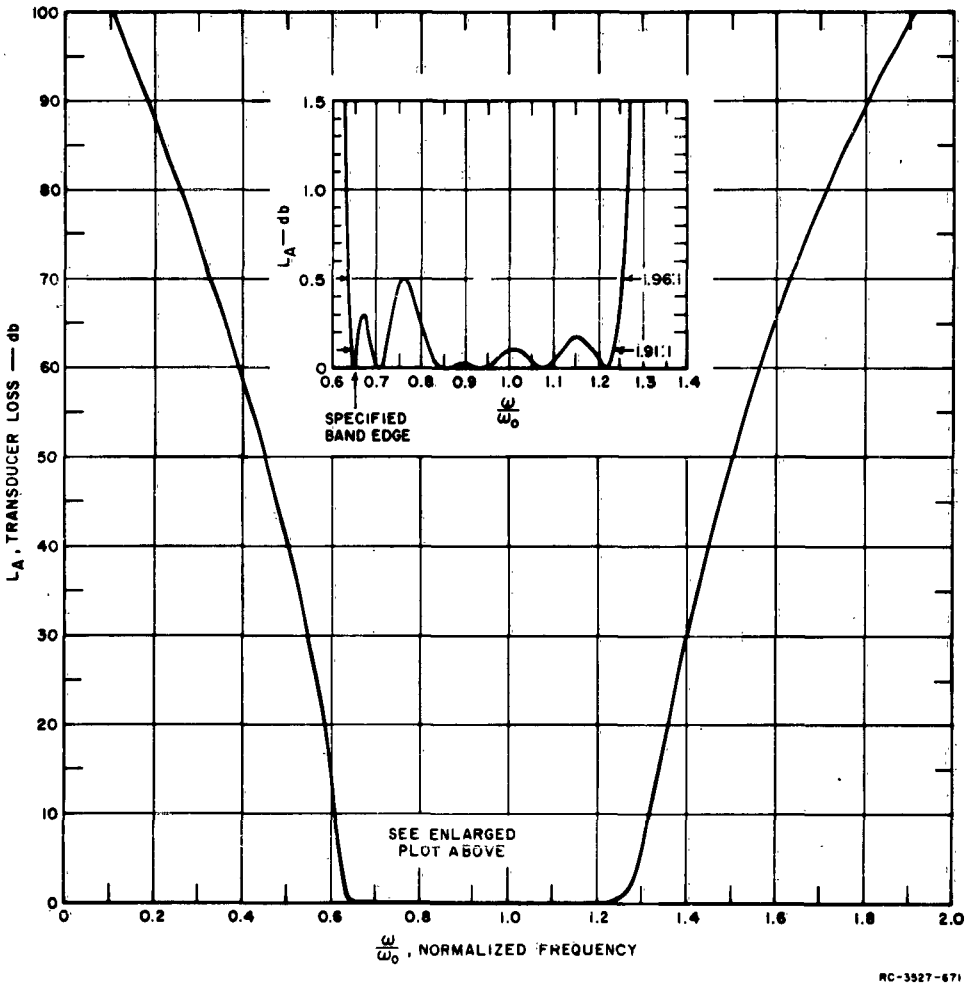

FIG. VI E-4 FREQUENCY RESPONSE OF A CAPACITIVELY LOADED INTERDIGITAL FILTER DESIGNED WITH ADMITTANCE-SCALING PARAMETER d = 1.00

symmetry about ω_0, the upper edge of the pass-band would be at 1.35 ω_0. The upper band-edge is actually as much as 9 percent below 1.35 ω_0. An additional departure from the ideal response is that there are only two frequencies of zero transducer loss above ω_0, rather than the four possible frequencies.

The departures noted above of the frequency response of capacitively-loaded interdigital filters from the desired response are probably due to two factors. One factor is that the susceptance of each loading capacitance is a linear function of frequency, while the susceptance of each short-circuited, coupled-line element is proportional to a cotangent function of frequency, cot $(\theta_0\omega/\omega_0)$. The other factor is that this cotangent function is not symmetrical about the resonance frequency, ω_0, when $\theta_0 < \pi/2$ due to capacitance loading. It is found, for example, that the image admittance and image phases of the individual sections in the filters are not symmetrical about ω_0. In addition, the image admittance as a function of frequency does not have zero slope at ω_0, but has a negative slope of cot $(\theta_0\omega/\omega_0)$ evaluated at ω_0. Interdigital filters without capacitive loading, on the other hand, have image parameters and frequency responses with arithmetic symmetry about ω_0. The frequency response of the interdigital filter without capacitive loading described in Sec. III-E of Quarterly Progress Report 4[1] was calculated, and exact arithmetic symmetry was confirmed. The ripples all fell within 0.063 to 0.105 db, as compared to the 0.1-db ripple of the low-frequency prototype from which the filter was designed.*

To demonstrate the wide-stop-band potentialities of the capacitively-loaded interdigital filter, the transducer loss is shown in Fig. VI E-5 over an extended frequency range for the filter having $d = 0.65$. The first spurious pass-band does not occur until nearly 4.5 times the resonance frequency ω_0 within the main pass-band. If the coupled-line elements were made even shorter than $\lambda/8$ at ω_0, the stop-band would extend over an even larger frequency range. For example, if the coupled-line elements were $\lambda/16$ at ω_0, the first spurious pass-band would occur at slightly less than 8.5 ω_0.

* The close correspondence between this calculated frequency response and the measured data presented in Quarterly Progress Report 4 also demonstrates the validity of the method described in Sec. VI-G of this report for calculating frequency response. The calculated bandwidth was 2.06:1 as compared with the measured 1.95:1, and as compared to the design goal of 2.08:1. The calculated frequency response had eight frequencies of perfect input match, which is the maximum possible number for an eight-resonator filter. The measured frequency response, however, had only six frequencies of best input match.

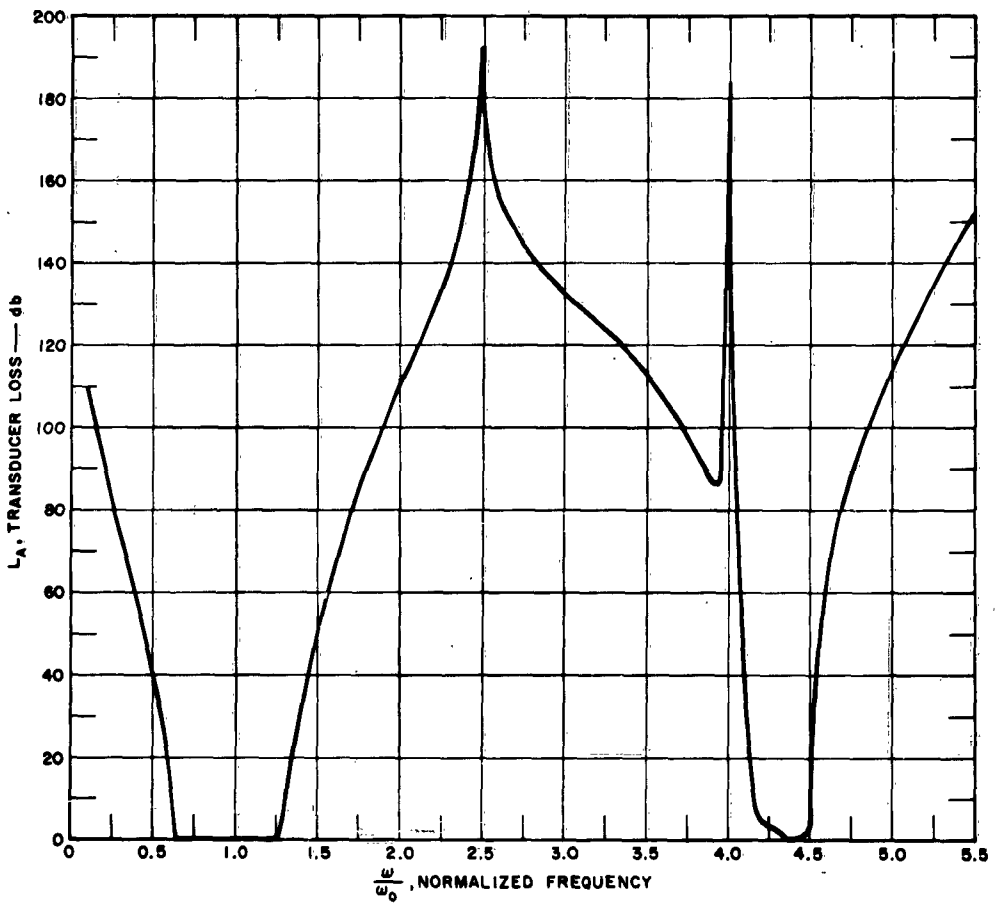

FIG. VI E-5 FREQUENCY RESPONSE OVER AN EXTENDED FREQUENCY RANGE FOR THE CAPACITIVELY LOADED INTERDIGITAL FILTER WITH ADMITTANCE-SCALING PARAMETER d = 0.65

That these predicted wide stop-bands can actually be obtained in practice is indicated by the following arguments. Consider the case where the capacitive loading is chosen to make the coupled-line elements $\lambda/8$ long at the resonance frequency ω_0, as is the case for the filters whose frequency responses are shown in this report. For these same coupled-line lengths, in order for a pass-band to exist at $2\omega_0$, there would have to be no reactive loading on the ends of the line elements. The capacitive loading that exists completely detunes any pass-band that might otherwise exist at $2\omega_0$. For a pass-band to exist at $3\omega_0$, the reactive loading at the ends of the line elements should be inductive rather than capacitive. At $4\omega_0$, the line elements are $\lambda/2$ long, and the sum of the magnetic coupling and electric coupling between adjacent line elements is zero.* Thus, a pass-band cannot exist at $4\omega_0$. The first spurious pass-band would occur when the length of each line element is $\lambda/2$ longer than the original $\lambda/4$--that is, at $4.5\ \omega_0$—if the susceptance of each loading capacitance were the same at $4.5\ \omega_0$, as it is at ω_0. Since the susceptance of each loading capacitance is actually greater at the higher frequency, the first spurious pass-band will be tuned lower than $4.5\ \omega_0$, but not as low as $4\ \omega_0$. This behavior of the frequency response is what is observed in Fig. VI E-5.

Although the capacitively loaded interdigital filters discussed in this report do not yield as good pass-band characteristics as do interdigital filters without capacitive loading, Figs. VI E-2, VI E-3 and VI E-4 demonstrate that filter characteristics can be obtained that are very satisfactory for many practical applications. It is to be expected that if the same number of resonators were used in a capacitively loaded filter having less than octave bandwidth, the ripples within the pass-band would more closely approach the ripple amplitude of the low-pass prototype used in the design.

F. DERIVATION OF DESIGN EQUATIONS

The design equations for capacitively loaded interdigital filters presented in Table VI D-1 are based on the use of low-pass, lumped-element prototypes whose element values are known to give prescribed low-pass frequency responses. The parameters of the capacitively loaded interdigital filters are related to the prototype element values by a method due to Matthaei[13] wherein the image admittance and image phase of sections of the

* This can be seen, for example, by the fact that the image impedance for filter 2 in Fig. 2(a) of Ref. 12 goes to infinity when the line elements are $\lambda/2$ long ($\theta = \pi$).

filter are made equal to the image admittance and image phase of corresponding sections of the prototype at certain important frequencies. Splitting the low-pass prototype into sections involves modifying the prototype from a ladder network of alternating series reactances and shunt susceptances, to a network of shunt capacitances separated by ideal admittance inverters. This modification of the prototype is similar to a concept introduced by Cohn,[6] and enlarged upon by Matthaei.[13] The image admittance and image phase of the filter sections are found by means of open-wire-line equivalent circuits for the coupled-line elements forming interdigital filter.

The open-wire-line equivalent circuit for the capacitively loaded interdigital filter can be drawn by considering the two types of coupled sections in Fig. VI A-1. Each pair of coupled lines from Lines 2 and 3 through Lines $(n-2)$ and $(n-1)$ is of the same configuration as the two lines on the left in Fig. VI F-1, and has the open-wire-line equivalent circuit on the right in Fig. VI F-1. Figure VI F-1 is simply obtained from Fig. III F-4 of Quarterly Progress Report 4[1] by adding the lumped loading capacitances at the ends of the coupled lines. The Y^a_{oo} and Y^a_{oe} in Fig. VI F-1 are the odd-mode and even-mode characteristic admittances, respectively, for Line a. The Y^b_{oo} and Y^b_{oe} are the odd-mode and even-mode characteristic admittances, respectively for Line b. The capacitances are as given by Eq. VI C-1, and v is the velocity of propagation in the medium surrounding the coupled lines.

The end pair of coupled lines in Fig. VI A-1 are of the same configuration as the two lines, and have the open-wire-line equivalent circuit, shown in Fig. VI F-2. Figure VI F-2 is an extension of Fig. III F-7 of Quarterly Progress Report 4.[1] In this equivalent circuit, the location of the tuning capacitance was not considered as obvious as for the circuit in Fig. VI F-1. Therefore, the open-wire-line equivalent circuit of Fig. VI F-2 was derived directly from the open-circuit impedance and short-circuit admittance matrices that apply in general to any two parallel-coupled transmission lines. The elements of these matrices are given by Jones and Bolljahn[12] for the case of equal-size coupled lines, and their results can readily be generalized to the case of unequal coupled lines.*

Combining the two types of open-wire-line circuits on Figs. VI F-1 and VI F-2, the open-wire-line equivalent circuit for the entire filter

* N.B. The admittance-matrix elements given by Eq. (9) of Jones and Bolljahn[12] have incorrect algebraic signs on Y_{12}, Y_{21}, Y_{34}, Y_{43}, Y_{14}, Y_{41}, Y_{23} and Y_{32}.

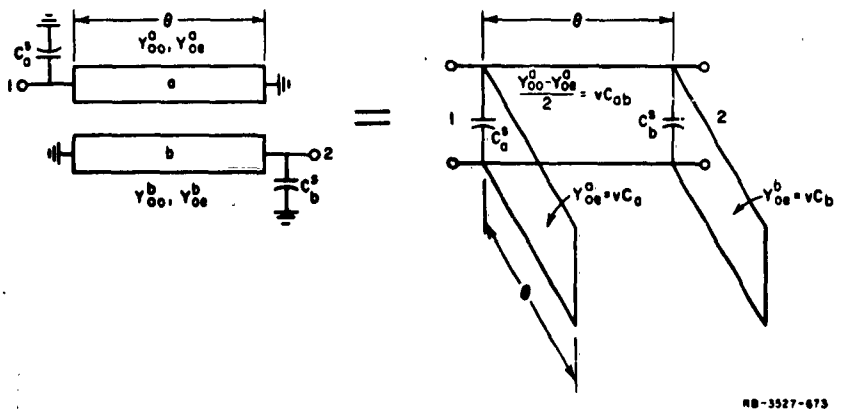

FIG. VI F-1 CAPACITIVELY LOADED, PARALLEL-COUPLED LINES USED AS INTERIOR RESONATORS IN FIG. VI A-1

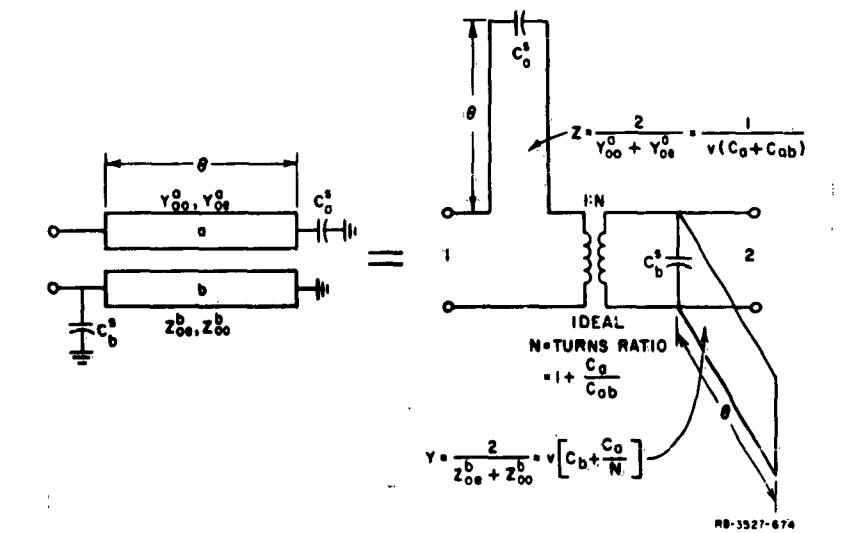

FIG. VI F-2 CAPACITIVELY LOADED, PARALLEL-COUPLED LINES USED AT THE ENDS OF THE FILTER STRUCTURE SHOWN IN FIG. VI A-1

is as shown in Fig. VI F-3. To relate this equivalent circuit to the prototype, Fig. VI F-3 is broken into sections as in Fig. VI F-4, the interior sections $S_{2,3}$ through $S_{n-2,n-1}$ being made symmetrical. The transformers have also been removed to increase the resemblance between Fig. VI F-4 and the modified prototype to be presented later in this section.

The first condition applied to the interior sections of Fig. VI F-4 is the resonance condition. This condition is that when a purely real admittance terminates any of the interior sections, the input admittance is also purely real at the frequency ω_0. The tuning capacitances that satisfy this condition are:

$$C'_{k,k+1}\Big|_{k=2 \text{ to } n-2} = \frac{\cot \theta_0}{\omega_0 h_A} (Y'_{k,k+1} + Y_{k,k+1}) \qquad \text{(VI F-1)}$$

where $\theta_0 = 2\pi\ell/\lambda_0$ is the electrical length of the coupled-line elements at ω_0, ℓ being the physical length of the coupled lines, and λ_0 being the wavelength within the medium surrounding the coupled lines at ω_0. The admittance scale factor h_A is defined in Fig. VI F-4. Other conditions to be applied to the interior sections of Fig. VI F-4 involve the image admittance of these sections, which is:

$$(Y_I)_{k,k+1}\Big|_{k=2 \text{ to } n-2} = \frac{Y_{k,k+1} \csc \theta}{h_A} \sqrt{1 - \left(\frac{Y_{k,k+1} + Y'_{k,k+1}}{Y_{k,k+1}}\right)^2 \left(1 - \frac{\omega \tan \theta}{\omega_0 \tan \theta_0}\right)^2 \cos^2 \theta}$$

(VI F-2)

where $\theta = \theta_0 \omega/\omega_0$ is the electrical length of the coupled-line elements at any frequency ω. Equation (VI F-2) was obtained by the usual procedure of taking the geometric mean of the short-circuit admittance parameter of one end of the section divided by the open-circuit impedance parameter of the same end.* It is assumed in Eq. (VI F-2) that the tuning capacitances satisfy Eq. (VI F-1).

* A worthwhile reduction in the complexity of the algebraic manipulations results from taking advantage of the symmetry of the sections. Each section can be divided in half, and the open-circuit and the short-circuit placed at the midplane.

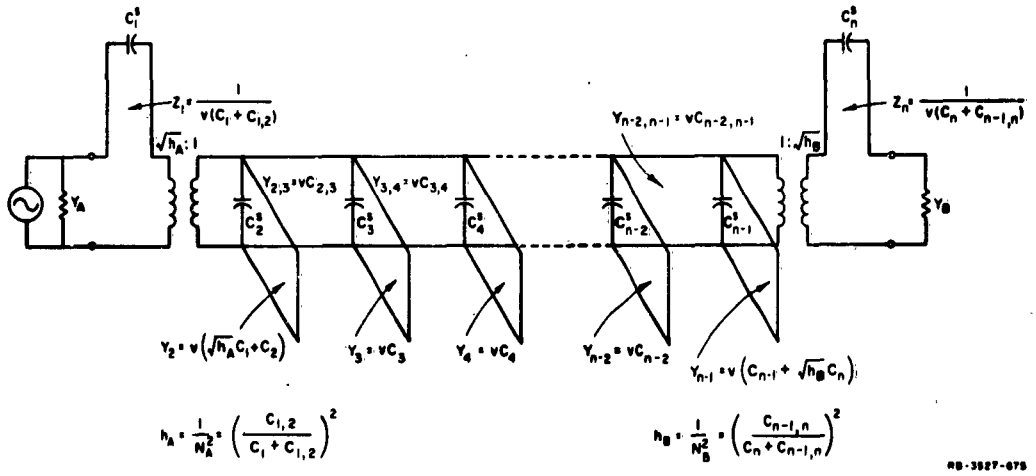

FIG. VI F-3 AN OPEN-WIRE-LINE EQUIVALENT CIRCUIT FOR THE CAPACITIVELY LOADED INTERDIGITAL FILTER SHOWN IN FIG. VI A-1
All lines are of electrical length θ.

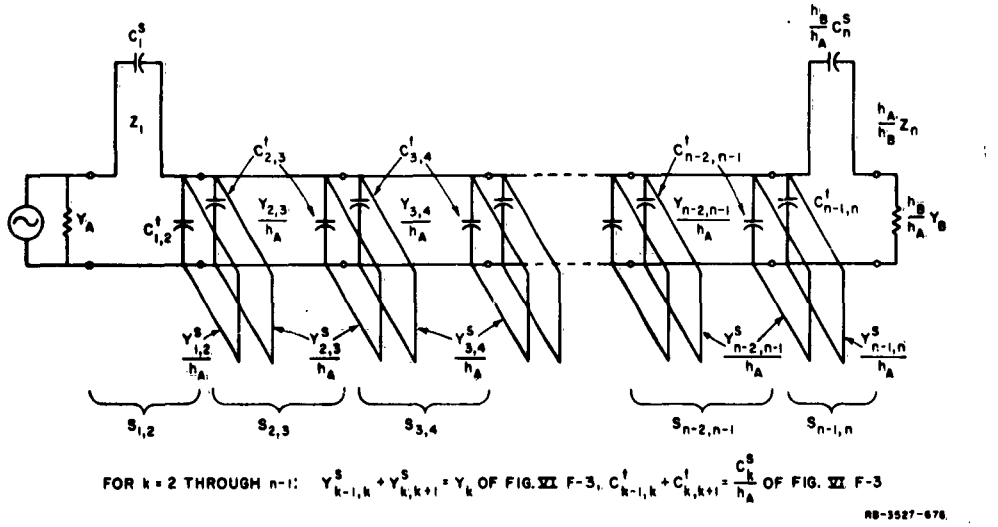

FIG. VI F-4 THE CIRCUIT OF FIG. VI F-3 SPLIT INTO SYMMETRICAL INTERIOR SECTIONS, AND THE TRANSFORMERS REMOVED

Consideration will now be given to the modified prototype shown in Fig. VI F-5. Modification of the prototype in the forms shown in Fig. VI B-1 to obtain Fig. VI F-5 in which admittance inverters* appear has been described by Matthaei.[13] Figure VI F-5 is slightly more general than Fig. 19 of Matthaei[13] in that unequal terminating admittances are permitted, but slightly less general in that all the element values have been renormalized so that the terminating admittances are the same as in

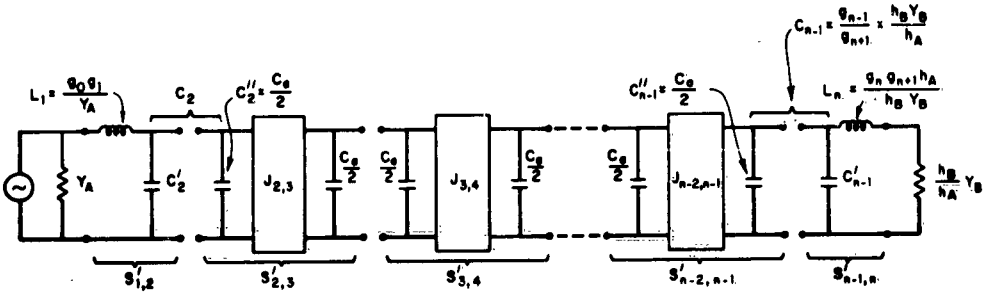

$$C_2' = (1-d)\frac{g_2 Y_A}{g_0}, \quad C_2'' = C_{n-1}'' = \frac{C_a}{2} = d g_2 \frac{Y_A}{g_0}, \quad C_{n-1}' = \left(\frac{g_0 g_{n-1}}{g_2 g_{n+1}} - d\right)\frac{g_2 Y_A}{g_0}$$

$$J_{2,3} = \frac{Y_A}{g_0}\sqrt{\frac{2dg_2}{g_3}}, \quad J_{n-2,n-1} = \frac{Y_A}{g_0}\sqrt{\frac{g_0 h_B Y_B}{g_{n+1} h_A Y_A} \cdot \frac{2dg_2}{g_{n-2}}}$$

$$J_{k,k+1}\Big|_{k=3 \text{ TO } n=3} = \frac{Y_A}{g_0}\frac{2dg_2}{\sqrt{g_k g_{k+1}}}$$

RA-3527-677

FIG. VI F-5 MODIFIED PROTOTYPE FOR DERIVING DESIGN EQUATIONS FOR CAPACITIVELY LOADED INTERDIGITAL FILTERS

Fig. VI F-4. In order for unequal terminating admittances to be possible, there must be at least one admittance inverter in Fig. VI F-5, which requires $n \geq 4$. Except for the above-mentioned re-normalization, the elements L_1, C_2, C_{n-1}, and L_n have the same values that they had in Fig. VI B-1. The other shunt capacitances have been chosen such that each interior section, $S_{2,3}'$ through $S_{n-2,n-1}'$, is symmetrical. The parameter d specifies what fraction of C_2 is split into C_2'' to be part of $S_{2,3}'$, and similarly for C_{n-1}. These choices completely specify[13] the values for the admittance-inverter parameters, $J_{k,k+1}$, as is shown at the bottom of Fig. VI F-5.

* Admittance inverters are defined as having a constant image admittance J and a constant image phase of ±90 degrees at all frequencies. (Thus they operate like a quarter-wavelength line of characteristic admittance J at all frequencies.) These inverters are introduced here only for mathematical convenience, and no attempt will be made to realize actual circuits that behave as admittance inverters.

The image admittance of each of the interior sections of the modified prototype is readily found to be:

$$(Y_I')_{k,k+1}\Big|_{k=2 \text{ to } n-2} = J_{k,k+1}\sqrt{1-\left(\frac{\omega' d g_2 h_A Y_A}{J_{k,k+1} g_0}\right)^2} \quad . \qquad \text{(VI F-3)}$$

Both the modified prototype and the open-wire-line equivalent circuit of the filter are now in forms where the end sections consist of a series reactance and a shunt susceptance, and the interior sections are symmetrical. Attention will now be turned to relating the equivalent-circuit parameters in Fig. VI F-4 to the prototype parameters in Fig. VI F-5, with the interior sections being considered first. The first condition applied requires that the image admittance of each interior filter section, Eq. (VI F-2), evaluated at the resonance frequency ω_0 be equal to the image admittance of the corresponding prototype section, Eq. (VI F-3), evaluated at $\omega' = 0$. This condition gives the characteristic admittance of the connecting open-wire-lines in Fig. VI F-4 in terms of the admittance-inverter parameters:

$$Y_{k,k+1}\Big|_{k=2 \text{ to } n-2} = J_{k,k+1} h_A \sin\theta_0 \quad , \qquad \text{(VI F-4)}$$

which is Eq. (11) in Table VI D-1. Equations (VI F-1) and (VI F-4) are sufficient to also ensure that the image phase shift of each interior section in Fig. VI F-4 is the same at $\omega = \omega_0$ as the image phase shift of the corresponding prototype section at $\omega' = 0$.

The second condition applied requires that the image admittance of each interior filter section, Eq. (VI F-2), evaluated at the lower band-edge frequency ω_1 be equal to the image admittance of the corresponding prototype section, Eq. (VI F-3), evaluated at the band-edge frequency $\omega' = -\omega_1'$. These frequencies are as defined in Figs. VI B-2 and VI B-3. After some algebraic manipulation, this condition produces Eq. (VI F-5):

$$Y^2_{k,k+1}\Big|_{k=2 \text{ to } n-2} = S\, h_A Y_A N_{k,k+1} - J_{k,k+1} h_A \sin\theta_0 \qquad \text{(VI F-5)}$$

where we define

$$S = \left(1 - \frac{\omega_1}{\omega_0} \cot \theta_0 \tan \theta_1\right)^{-1}$$

$$N_{k,k+1}\Big|_{k=2 \text{ to } n-2} = \sqrt{\left(\frac{J_{k,k+1}}{Y_A}\right)^2 \left[1 - \left(\frac{\cos \theta_0}{\cos \theta_1}\right)^2\right] + \left(\frac{\omega_1' g_2 d \tan \theta_1}{g_0}\right)^2} \quad .$$

The parameters S and $N_{k,k-1}$ are introduced only to shorten the form of some of the design equations, and have no particular physical significance. Combining Eq. (VI F-5) with the relationship at the lower left-hand corner of Fig. VI F-4, the characteristic admittances of some of the shunt stubs in Fig. VI F-3 are found to be:

$$Y_k\Big|_{k=3 \text{ to } n-2} = S\, h_A Y_A N_{k-1,k} + S\, h_A Y_A N_{k,k+1} - (J_{k-1,k} + J_{k,k+1}) h_A \sin \theta_0 \quad . \qquad \text{(VI F-6)}$$

This is Eq. (8) in Table VI D-1. Equations (VI F-1) and (VI F-5) are also sufficient to ensure that the image phase shift of each interior section in Fig. VI F-4 is the same at $\omega = \omega_1$ as the image phase shift of the corresponding prototype section at $\omega' = -\omega_1'$.

The end sections $S_{1,2}$ and $S_{n-1,n}$ in Fig. VI F-4, and $S'_{1,2}$ and $S'_{n-1,n}$ in Fig. VI F-5 are sufficiently simple that only reactances and susceptances need be considered, instead of considering image admittances. For the series stub at the left-hand end of Fig. VI F-4, its input reactance at $\omega = \omega_0$ is required to be the same as the reactance of the inductance L_1 in Fig. VI F-5 at $\omega' = 0$—that is, zero reactance. This specifies the end-loading capacitance in terms of the characteristic impedance and length of the end stub:

$$C_1' = \frac{\cot \theta_0}{\omega_0 Z_1} \quad . \qquad \text{(VI F-7)}$$

The characteristic impedance Z_1 is determined by making the input impedance of the series stub at the left-hand end of Fig. VI F-4, evaluated at $\omega = \omega_1$,

be the same as the reactance of the inductance L_1, evaluated at $\omega' = -\omega_1'$, which gives:

$$Z_1 = \frac{\omega_1' g_0 g_1}{Y_A} T \qquad \text{(VI F-8)}$$

where T is defined as

$$T = S\left(\frac{\omega_1}{\omega_0} \cot \theta_0 + \tan \theta_1\right) \quad .$$

Equations (VI F-7) and (VI F-8) appear in Table VI D-1 as Eqs. (20) and (6), respectively.

For the shunt stub at the left-hand end of Fig. VI F-4, its susceptance in parallel with the tuning capacitance $C_{1,2}'$, evaluated at $\omega = \omega_0$, is required to be the same as the susceptance of the capacitance C_2' in Fig. VI F-5 at $\omega' = 0$--that is, zero shunt susceptance. Therefore:

$$C_{1,2}' = \frac{Y_{1,2}' \cot \theta_0}{h_A \omega_0} \quad . \qquad \text{(VI F-9)}$$

Substituting Eq. (VI F-9) along with Eq. (VI F-1) evaluated for $k = 2$ into the relationships at the bottom of Fig. VI F-4, we have:

$$C_2' = \frac{Y_A \cot \theta_0}{\omega_0}\left(\frac{Y_2}{Y_A} + \frac{Y_{2,3}}{Y_A}\right) \qquad \text{(VI F-10)}$$

which is the same as Eq. (21) of Table VI D-1. The shunt susceptance of stub $Y_{1,2}'$ in Fig. VI F-4 in parallel with $C_{1,2}'$ evaluated at $\omega = \omega_1$ is now made equal to the susceptance of C_2' of Fig. VI F-5 evaluated at $\omega' = -\omega_1'$. This condition, along with Eq. (VI F-9), gives the stub characteristic admittance:

$$Y_{1,2}' = \frac{h_A Y_A \omega_1' (1 - d) g_2 S \tan \theta_1}{g_0} \quad . \qquad \text{(VI F-11)}$$

Equation (7) of Table VI D-1 results from taking the sum of Eq. (VI F-11) and Eq. (VI F-5) evaluated for $k = 2$.

The end section $S_{n-1,n}$ in Fig. VI F-4 is related to end section $S'_{n-1,n}$ in Fig. VI F-5 following the same procedure given above for sections $S_{1,2}$ and $S'_{1,2}$. The resulting equations are given in Table VI D-1 as Eqs. (9), (10), (23), and (24).

Equations (12) through (19) of Table VI D-1 follow directly from the definitions of the characteristic admittances and characteristic impedances of the open-wire transmission lines in Fig. VI F-3. Use is made of the fact that the velocity of propagation in the medium surrounding the coupled-line elements can be written:

$$v = \frac{1}{\sqrt{\mu_0 \epsilon}} = \frac{1}{\sqrt{\mu_0 \epsilon}} \times \sqrt{\frac{\mu_0}{\epsilon_0}} \times \frac{\sqrt{\epsilon_r}}{\sqrt{\epsilon_r}} = \frac{\sqrt{\epsilon_r}}{376.7\ \epsilon} \qquad \text{(VI F-12)}$$

where

μ_0 = the permeability of free space = $4\pi \times 10^{-7}$ henry/meter

ϵ_0 = the absolute permittivity of free space = 8.85×10^{-12} farad/meter = 0.225 picofarad/inch

ϵ = the absolute permittivity of the medium surrounding the coupled-line elements

ϵ_r = the relative permittivity (dielectric constant) of the medium surrounding the coupled-line elements

$\sqrt{\mu_0/\epsilon_0}$ = 376.7 ohms = characteristic impedance of free space.

Equation (VI F-12) applies for the usual case where, in order to minimize dissipation loss, only nonmagnetic materials would be used in constructing the filter.

G. METHOD OF FREQUENCY-RESPONSE CALCULATION

The frequency responses presented in Sec. VI-E were calculated using the open-wire-line equivalent circuit of Fig. VI F-3. The validity of such open-wire equivalent circuits is based on the fact that the pairs of coupled lines on the left-hand side of Figs. VI F-1 and VI F-2 have exactly the same short-circuit admittances as functions of frequency as do the open-wire-line equivalent circuits on the right-hand side of the same figures. In order

to obtain a valid equivalent circuit for an entire filter by cascading several of the equivalent circuits as in Figs. VI F-1 and VI F-2, the coupling beyond adjacent coupled-line elements of the filter must be negligible. That coupling beyond nearest neighbor is insignificant for coupled-line proportions similar to Fig. VI C-2 is demonstrated by the experimental results obtained with the interdigital filter of Sec. III in Quarterly Progress Report 4,[1] with the comb-line filter of Sec. II in Quarterly Progress Report 5,[2] and with comb-line filters used in the multiplexer of Sec. III in this report.

As a specific check on the digital-computer program outlined in this section, the frequency response was calculated for the interdigital filter without capacitive loading whose measured performance was presented in Sec. III of Quarterly Progress Report 4.[1] The calculated frequency response was in close agreement with both the design objectives for the filter, and with the measured performance. The calculated bandwidth was 2.06:1 compared with the design objective of 2.08:1, and compared with the measured bandwidth of 1.95:1. The amplitude of the calculated VSWR peaks within the pass-band fell between 1.27:1 and 1.36:1, compared with the design objective of 1.35:1, and compared with the measured values of 1.35:1 to 1.5:1. The number of frequencies of minimum input-VSWR was eight for the calculated data, and six for the measured data.

The frequency response of the open-wire-line equivalent circuit of Fig. VI F-3 was calculated using the general-circuit parameters, A, B, C, D, of the circuit exclusive of the terminating admittances. The general-circuit parameters of the entire equivalent circuit was found by taking the matrix product of the various filter parts that are cascaded to form the entire circuit:

$$\begin{bmatrix} A & B \\ C & D \end{bmatrix} = \begin{bmatrix} 1 & jX_1 \\ 0 & 1 \end{bmatrix} \begin{bmatrix} \sqrt{h_A} & 0 \\ 0 & \dfrac{1}{\sqrt{h_A}} \end{bmatrix}$$

(VI G-1 continued)

$$\times \left\{ \prod_{k=2}^{n-2} \begin{bmatrix} 1 & 0 \\ j\left[\frac{\omega}{\omega_0}\left(\omega_0 C_k^s\right) - Y_k^s \cot\theta\right] & 1 \end{bmatrix} \begin{bmatrix} \cos\theta & j\frac{\sin\theta}{Y_{k,k+1}} \\ jY_{k,k+1}\sin\theta & \cos\theta \end{bmatrix} \right\}$$

$$\times \begin{bmatrix} 1 & 0 \\ j\left[\frac{\omega}{\omega_0}\left(\omega_0 C_{n-1}^s\right) - Y_{n-1}^s \cot\theta\right] & 1 \end{bmatrix} \begin{bmatrix} \frac{1}{\sqrt{h_B}} & 0 \\ 0 & \sqrt{h_B} \end{bmatrix} \begin{bmatrix} 1 & jX_n \\ 0 & 1 \end{bmatrix}$$

(VI G-1 concluded)

where

$$\theta = \theta_0 \frac{\omega}{\omega_0} \qquad \text{(VI G-2)}$$

$$X_1 = \frac{1}{Y_A}\left(\frac{Z_1}{Z_A}\right) \frac{\frac{Z_1}{Z_A} - \frac{Y_A \cot\theta}{(\omega/\omega_0)(\omega_0 C_1^s)}}{\frac{Z_1}{Z_A}\cot\theta + \frac{Y_A}{(\omega/\omega_0)(\omega_0 C_1^s)}} \text{ ohms} \qquad \text{(VI G-3)}$$

$$X_n = \frac{1}{Y_A}\left(\frac{h_A}{h_B}\right)\left(\frac{Z_n}{Z_A}\right) \frac{\frac{Z_n}{Z_A} - \frac{Y_A \cot\theta}{(\omega/\omega_0)(\omega_0 C_n^s)}}{\frac{Z_n}{Z_A}\cot\theta + \frac{Y_A}{(\omega/\omega_0)(\omega_0 C_n^s)}} \text{ ohms} \quad . \qquad \text{(VI G-4)}$$

Comparing the matrices with the parts of Fig. VI F-3, it can be seen that the first matrix in Eq. (VI G-1) represents the input reactance of the left-hand series stub, which has characteristic impedance Z_1 and is loaded at one end by capacitance C_1^s. The second matrix in Eq. (VI G-1) represents the left-hand transformer. The first matrix within the continued-product

sign in Eq. (VI G-1) represents the shunt stub of characteristic admittance Y_2 in parallel with the loading capacitance C_2'. The second matrix within the continued-product sign in Eq. (VI G-1) represents the connecting line of characteristic admittance $Y_{2,3}$, and so on throughout Eq. (VI G-1). The digital computer--a Burroughs 220--was programmed to carry out the matrix multiplication of Eq. (VI G-1) for $n \leq 15$.

Using the general-circuit parameters obtained from Eq. (VI G-1), the computer was also programmed to find the ratio of power available from the generator, P_{avail}, to the power P_2 actually delivered to the conductance Y_B when the filter is inserted between the generator and Y_B. This ratio is:

$$\frac{P_{avail}}{P_2} = \frac{Y_B}{4Y_A}\left[\left(A\frac{Y_A}{Y_B} + D\right)^2 + \left(bY_A + \frac{c}{Y_B}\right)^2\right] \qquad \text{(VI G-5)}$$

where use has been made of the fact that for a lossless network B and C are purely imaginary, by setting $B = jb$ and $C = jc$, $j = \sqrt{-1}$. (Also, A and D are purely real.) Finally, the transducer loss L_A was calculated by the computer using:

$$L_A = 10 \log_{10} \frac{P_{avail}}{P_2} \text{ decibels} \quad . \qquad \text{(VI G-6)}$$

REFERENCES

1. Leo Young and G. L. Matthaei, "Microwave Filters and Coupling Structures," Quarterly Progress Report 4, SRI Project 3527, Contract DA 36-039 SC-87398, Stanford Research Institute, Menlo Park, California (January 1962).

2. G. L. Matthaei, Leo Young, and P. S. Carter, Jr., "Microwave Filters and Coupling Structures," Quarterly Progress Report 5, SRI Project 3527, Contract DA 36-039 SC-87398, Stanford Research Institute, Menlo Park, California (May 1962).

3. L. Weinberg, "Additional Tables for Design of Optimum Ladder Networks," *J. Franklin Institute* 246, pp. 7-23 and 127-138 (July and August 1957).

4. G. L. Matthaei, *et al.*, "Design Criteria for Microwave Filters and Coupling Structures," Final Report, SRI Project 2326, Contract DA 36-039 SC-74862, Stanford Research Institute, Menlo Park, California (January 1961).

5. W. J. Getsinger, "Coupled Rectangular Bars Between Parallel Plates," *IRE Trans.* PGMTT-10, pp. 65-72 (January 1962).

6. S. B. Cohn, "Direct-Coupled-Resonator Filters," *Proc. IRE* 45, pp. 187-196 (February 1957).

7. J. R. Whinnery and H. W. Jamieson, "Equivalent Circuits for Discontinuities in Transmission Lines," *Proc. IRE* 32, pp. 98-114 (February 1944).

8. J. R. Whinnery, H. W. Jamieson, and T. E. Robbins, "Coaxial-Line Discontinuities," *Proc. IRE* 32, pp. 695-709 (November 1944).

9. N. Marcuvitz, *Waveguide Handbook*, MIT Rad. Lab. Series, Vol. 10 (McGraw-Hill Book Co., Inc., New York, N.Y., 1951).

10. H. M. Altshuler and A. A. Oliner, "Discontinuities in the Center Conductor of Symmetric Strip Transmission Line," *IRE Trans.* PGMTT-8, pp. 328-339 (May 1960).

11. J. F. Cline, *et al.*, "Design Data for Antenna-Multicoupler Systems," Final Report, SRI Project 2183, Contract AF 19(604)-2247, Stanford Research Institute, Menlo Park, California (September 1959).

12. E. M. T. Jones and J. T. Bolljahn, "Coupled-Strip-Transmission-Line Filters and Directional Couplers," *IRE Trans.* PGMTT-4, pp. 75-81 (April 1956).

13. G. L. Matthaei, "Design of Wide-Band (and Narrow-Band) Band-Pass Microwave Filters on the Insertion Loss Basis," *IRE Trans.* PGMTT-8, pp. 580-593 (November 1960).

VII CONCLUSIONS

A. MAGNETICALLY TUNABLE FILTERS

The new technique used in the two-resonator waveguide filter design for getting tighter coupling to a YIG sphere was demonstrated to be successful. Using this technique, it should be possible to use smaller spheres or spheres with lower saturation magnetization than would generally be practical otherwise. Using smaller spheres has the advantage of reducing the tendency towards the excitation of magnetostatic modes (which cause spurious responses). Using ferrimagnetic materials with lower saturation magnetization makes possible operation to lower frequencies.

B. BAND-STOP FILTERS

The procedure for the exact design of the basic shunt-stub type of band-stop filter that was described in Quarterly Progress Report 7 has been extended to cover two types of filters that employ parallel-coupled lines, with no loss of exactness in the designs. One of these types was shown to yield a practical filter where the basic shunt-stub type would have been impractical (namely, for the design of narrow-stop-band filters).

An advantage of the exact design procedure is that the filter response can be accurately determined over a very wide band (theoretically without limit) once the prototype response is known. The test filters that were constructed with parallel-coupled lines bore out this feature in general, even for frequencies in the second stop-band (three times the frequency of the first stop-band).

Certain additional parallel-coupled types of filter sections other than those investigated under this contract appear to be applicable to the exact design of band-stop filters and would therefore be suitable for further study along these lines.

C. MULTIPLEXERS

The measured performance of the three-channel comb-line multiplexer having contiguous channels compares well with the design prototype. Bandwidth spreading in the filters of the multiplexer caused the multiplexer

pass-band to be larger than the design prototype. It is recommended that in future designs the percentage bandwidth be understated to account for bandwidth spreading. Tuning of the multiplexer is facilitated by using an electronically swept frequency oscillator. Without the sweeper, tuning is difficult and tedious.

The design principles for multiplexers with contiguous channels may be extended to multiplexers with guard-bands between channels. However, cancelling the susceptance in the pass-bands of multiplexers with guard-bands by using a susceptance-annulling network in the form of an open- or short-circuited transmission line may be difficult to do very completely. However, susceptance cancellation can be obtained which is sufficiently good for most practical purposes.

D. INTERDIGITAL FILTERS WITH CAPACITIVE LOADING

Because of the complicated nature of capacitively loaded interdigital filters, the use of an approximate filter model was necessary in order to represent the filter structure in a form simple enough to permit practical design. That the model used is reasonably valid is demonstrated by the fact that an analogous model used for interdigital filters without capacitive loading gave good agreement between theory and experiment. By working out trial designs and computing the responses of the corresponding approximate models, it has been demonstrated that a practical design procedure for capacitively loaded interdigital filters with wide bandwidths has been obtained. The use of capacitive loading is seen to have the useful features of permitting an even smaller filter structure, and of causing the first spurious pass-band to be unusually far removed from the main pass-band. The capacitive loading feature may also be of interest with regard to the design of devices such as traveling-wave parametric amplifiers where the capacitive loading elements would consist of variable-capacitance diodes. An experimental model of capacitively loaded interdigital filter for laboratory tests is now being worked on.

ACKNOWLEDGMENTS

Mr. York Sato worked out many of the details of the mechanical design of the two magnetically tunable filters discussed in Sec. III, and made the laboratory tests on the filters.

Mr. R. B. Larrick and Mr. P. H. Reznek made the laboratory tests on the band-stop filters discussed in Sec. IV.

Mr. P. R. Reznek made the laboratory tests on the three-channel multiplexer discussed in Sec. V.

The programming of the Burroughs 220 computer for determining the responses of trial filter designs such as those discussed in Sec. VI was done by Mr. V. H. Sagherian.

IDENTIFICATION OF KEY TECHNICAL PERSONNEL

	HOURS CHARGED TO PROJECT DURING QUARTER
DR. P. S. CARTER, JR. *Senior Research Engineer*	30.5
DR. E. G. CRISTAL *Research Engineer*	172
DR. G. L. MATTHAEI *Manager, Electromagnetic Techniques Laboratory* *(Project Leader)*	386
MR. L. A. ROBINSON *Senior Research Engineer*	166
MR. B. M. SCHIFFMAN *Senior Research Engineer*	273
DR. LEO YOUNG *Senior Research Engineer*	164

In addition, Stanford Research Institute and the authors have contributed additional work time toward the microwave filter book being written on this project.

DISTRIBUTION LIST

ORGANIZATION	NO. OF COPIES
OASD (R&E) ATTN: Technical Library Room 3E1065 The Pentagon Washington 25, D.C.	1
Chief of Research and Development OCS, Department of the Army Washington 25, D.C.	1
Commanding General U.S. Army Materiel Command ATTN: R&D Directorate Washington 25, D.C.	1
Commanding General U.S. Army Electronics Command ATTN: AMSEL-AD Fort Monmouth, New Jersey	1
Director, U.S. Naval Research Laboratory ATTN: Code 2027 Washington 25, D.C.	1
Commander, Aeronautical Systems Division ATTN: ASAPRL Wright-Patterson Air Force Base, Ohio	1
Hq. Electronic Systems Division ATTN: ESAL L.G. Hanscom Field Bedford, Massachusetts	1
Commander, Air Force Cambridge Research Laboratories ATTN: CRO L.G. Hanscom Field Bedford, Massachusetts	1
Commander, Air Force Command & Control Development Division ATTN: CRZC L.G. Hanscom Field Bedford, Massachusetts	1
Commander, Rome Air Development Center ATTN: RAALD Griffiss Air Force Base, New York	1
Commander, Armed Services Technical Information Agency ATTN: TISIA Arlington Hall Station Arlington 12, Virginia	10
Chief, U.S. Army Security Agency Arlington Hall Station Arlington 12, Virginia	2
Deputy President U.S. Army Security Agency Board Arlington Hall Station Arlington 12, Virginia	1
Commanding Officer Harry Diamond Laboratories ATTN: Library, Room 211, Building 92 Washington 25, D.C.	1
Corps of Engineers Liaison Office U.S. Army Electronics Research and Development Laboratory Fort Monmouth, New Jersey	1
AFSC Scientific/Technical Liaison Office U.S. Naval Air Development Center Johnsville, Pennsylvania	1
USAELRDL Liaison Office Rome Air Development Center ATTN: RAOL Griffiss Air Force Base, New York	1
Commanding Officer U.S. Army Electronics Material Support Agency ATTN: SELMS-ADJ Fort Monmouth, New Jersey	1
Marine Corps Liaison Office U.S. Army Electronics Research and Development Laboratory ATTN: SELRA/LNR Fort Monmouth, New Jersey	1
Commanding Officer U.S. Army Electronics Research and Development Laboratory ATTN: Director of Research or Engineering Fort Monmouth, New Jersey	1
Commanding Officer U.S. Army Electronics Research and Development Laboratory ATTN: Technical Documents Center Fort Monmouth, New Jersey	1
Commanding Officer U.S. Army Electronics Research and Development Laboratory ATTN: SELRA/ADJ (FU No. 1) Fort Monmouth, New Jersey	1
Advisory Group on Electron Devices 346 Broadway New York 13, New York	2
Commanding Officer U.S. Army Electronics Research and Development Laboratory ATTN: SELRA/TNR Fort Monmouth, New Jersey (FOR RETRANSMITTAL TO ACCREDITED BRITISH AND CANADIAN GOVERNMENT REPRESENTATIVES)	3
Commanding General U.S. Army Combat Developments Command ATTN: CDCMR-E Fort Belvoir, Virginia	1
Commanding Officer U.S. Army Communications-Electronics Combat Development Agency Fort Huachuca, Arizona	1

DISTRIBUTION LIST

ORGANIZATION	NO. OF COPIES
Director, Fort Monmouth Office U.S. Army Communications-Electronics Combat Development Agency Building 410 Fort Monmouth, New Jersey	1
AFSC Scientific/Technical Liaison Office U.S. Army Electronics Research and Development Laboratory Fort Monmouth, New Jersey	1
Commanding Officer and Director U.S. Navy Electronics Laboratory San Diego 52, California	1
MELABS Library Stanford Industrial Park 3300 Hillview Avenue Palo Alto, California	1
Airborne Instruments Laboratory ATTN: Mr. R. Sleven Deer Park, Long Island, New York	1
Commanding Officer U.S. Army Signal Research Unit ATTN: SIGRU-3 Mountain View, California	1
Stanford Electronics Laboratory Stanford University ATTN: Applied Electronics Laboratory Stanford, California	1
Convair Pomona, California	1
Commander, Rome Air Development Center ATTN: RCLTM-2, Mr. Patsy A. Romanelli Griffiss Air Force Base Rome, New York	1
Rantec Corporation ATTN: S. B. Cohn, Technical Director Calabasas, California	1
U.S. Naval Ordnance Test Station ATTN: Code 4021, Mr. Robert Corsine China Lake, California	1
General Electric Microwave Laboratory ATTN: Technical Library 601 California Avenue Palo Alto, California	1
Dr. K. L. Kotzebue Watkins-Johnson Company 3333 Hillview Avenue Stanford Industrial Park Palo Alto, California	1
Dr. Griemmaman Polytechnic Institute of Brooklyn Route 110 Farmingdale, Long Island, New York	1
National Bureau of Standards Engineering Electronics Section ATTN: Mr. Gustave Shapiro, Chief Washington 25, D.C.	1
Chief Bureau of Ships ATTN: Mr. Gumina, Code 68182 Department of the Navy Washington 25, D.C.	1
Physical Electronics Laboratory ATTN: Philip Carter 2493 Pulgas Avenue E. Palo Alto, California	1
Loral Electronics Corporation ATTN: Mr. Magid 825 Bronx River Drive New York 72, New York	1
Commanding Officer U.S.A. Electronics Research & Development Laboratory Fort Monmouth, New Jersey	
ATTN: SELRA/SLM	1
ATTN: SELRA/PRM (Mr. Reingold)	1
ATTN: SELRA/SEA (B. Ellis)	1
ATTN: SELRA/PE (Dr. E. Both)	1
ATTN: SELRA/PE (Division Director)	1
ATTN: SELRA/PEM (Mr. W. Dattilo)	10